COMPOST DEGRADATION AND GROWTH OF *Agaricus bisporus*

Aurin M. Vos

The research described in this report was performed within the Microbiology group of Utrecht University, Padualaan 8, 3584 CH Utrecht, The Netherlands. It was supported by the Dutch Technology Foundation STW, which is part of the Netherlands Organisation for Scientific Research (NWO), and partly funded by the Ministry of Economic Affairs (Project number 11108).

ISBN/EAN 9789462956025

Cover photo
Soledad Ordonez and Aurin Vos

Printed by
Uitgeverij BOXpress, 's-Hertogenbosch

COMPOST DEGRADATION AND GROWTH OF *Agaricus bisporus*

Groei en compost afbraak door de champignon

(met een samenvatting in het Nederlands)

Proefschrift

ter verkrijging van de graad van doctor aan de Universiteit Utrecht op gezag van de rector magnificus, prof. dr. G.J. van der Zwaan, ingevolge het besluit van het college voor promoties in het openbaar te verdedigen op woensdag 21 juni 2017 des middags te 4.15 uur

door

Aurin Minnert VOS

geboren op 9 augustus 1986
te 's-Hertogenbosch

Promotor

Prof. dr. H.A.B. Wösten

Copromotor

Dr. L.G. Lugones

"Sometimes science is a lot more art, than science. A lot of people don't get that."
-Rick (from *Rick and Morty*)

CONTENTS

1

GENERAL INTRODUCTION

1

USE OF MUSHROOMS

Humans have used mushrooms throughout history. For instance, *Psilocybe* species were used by pre-colonial Indian cultures in shamanic rituals (Díaz 1977) and Vikings may have ingested the *Amanita muscaria* mushroom to induce a trance before going to war ("going Berserk", Fabing 1956). The mummified Iceman Ötzi carried material from *Piptoporus betulinus* and *Fomes fomentarius* mushrooms that were likely used for medicinal purposes and to start fire, respectively (Peintner et al. 1998). Ancient Egyptians believed that mushrooms were a source of immortality according to 4600-year-old hieroglyphics. Pharaohs brusquely decreed mushrooms were food for royalty (Daba 2006). Nowadays, mushrooms were and are still collected in forests and open fields throughout the world as a food source. The Chinese and Japanese were among the first to cultivate mushrooms. Cultivation of mushrooms was first mentioned in 1313 by Wang Zeng in his "Book of Agriculture". Mushroom growing in Europe started in the 17th century in France during the reign of Louis XIV. Mushrooms of *Agaricus* species were grown in the region of Paris in quarries. At that time, horse manure containing mycelium was used to re-inoculate newly prepared manure. The first pure culture spawn (based on spores) of *Agaricus bisporus* were developed in Europe at the end of the 19th century. The spawn was used to inoculate batches of horse manure. Several American spawn companies started up by using mycelium cultures produced from mushroom caps. This formed the basis for *A. bisporus* becoming the dominant cultivated mushroom in the world. Until 1927, all *A. bisporus* were brown or cream-colored. The white button mushrooms produced today find their origin in a cluster of white mushrooms within a bed of brown fruiting bodies in Pennsylvania (van Griensven 1988). Today, the production of the button mushrooms amounts one billion kilogram annually in the European Union. The Netherlands produces 25 % of this, representing a market value of € 400 million (Logatcheva et al. 2014). They are sold as fresh products or are conserved by canning.

COMMERCIAL PRODUCTION OF *Agaricus bisporus*

A. bisporus grows on litter in nature but compost is used for the commercial production of its mushrooms. In the Netherlands, composting consists of a phase I and phase II, *A. bisporus* is introduced in phase III, and in phase IV mushrooms are produced. In the past compost was produced outdoor but environmental regulations necessitated indoor production.

PHASE I

Wheat straw bedded horse manure, gypsum and water are mixed in phase I (PI) of compost production. Chicken manure and wheat straw may be added as additional or alternative nitrogen and carbon source, respectively. Wheat straw represents the major carbon source in compost. While gypsum has a stabilizing effect on the quality of the substrate and mushroom yield. Colloidal substances are flocculated by gypsum resulting in a less greasy compost with improved air circulation and structure. Furthermore, gypsum neutralizes negative effects of high ammonia content by decreasing pH. In tunnels, PI takes 3 - 6 days during which temperatures of up to 80 °C are reached due to microbial activity. The pH in compost is 8.4 and 8.9 at PI-end in the presence and absence of gypsum, respectively. At a higher compost pH more NH_3 is formed that has a negative effect on mushroom yield (Gerrits 1988). Some xylan and cellulose is consumed during PI, while lignin remains untouched (Jurak et al. 2014; 2015b; Jurak 2015). After PI, the compost is inoculated with a microflora contained in PII-end compost that went through phase II (PII) and is placed in large tunnels.

PHASE II

PII starts with a pasteurization process, after which the compost is conditioned by circulating air through the compost. During pasteurization, temperatures are first brought to 50 °C and then increased to 60 °C. This kills unwanted organisms such as insects but may also affect the microflora (Gerrits 1988; Straatsma et al. 1994). Pasteurization takes 2 days, after which conditioning is started by decreasing the temperature to 45 °C. The three days of conditioning allow a thermophilic fungal community to develop. The presence of *Scytalidium thermophilum* (also known as *Humicola insolens*, Straatsma and Samson 1993) is important for the growth of *A. bisporus* (Straatsma et al. 1989; Straatsma et al. 1994). *S. thermophilum* is associated with the removal of ammonia and suppression of competitors of *A. bisporus* (Ross and Harris 1983). After PII, 60 % and 50 % of xylan and cellulose has been degraded, respectively, as compared to the starting material, while lignin still remains largely unaffected (Jurak 2015; Jurak et al. 2015b). The pH has decreased from 8 to 7 - 7.5 and the compost is highly suitable for colonization by *A. bisporus*.

PHASE III

At the start of phase III (PIII) *A. bisporus* is introduced by mixing spawn through the compost. Spawn is usually prepared using rye, calcium carbonate, and calcium sulfate. The inoculated compost is transported to a new tunnel. The optimal growth temperature of *A. bisporus* of 25 °C is maintained by circulating air through the compost (Gerrits 1988). In PIII 15 % of xylan and 10 % of cellulose are removed

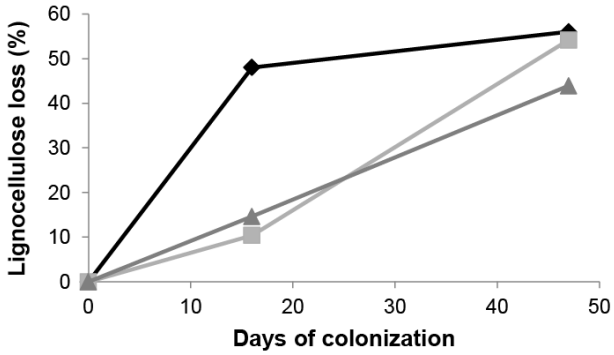

Figure 1.1: Loss of lignin (black), cellulose (light grey), and hemicellulose (dark grey) during the cultivation of *A. bisporus* after 0 days (end of PII), 16 days (PIII-16), and 47 days (2nd flush, days estimated from typical cutivation schedule). Values are based on Jurak (2015).

relative to the end of PII (Jurak 2015). The loss of cellulose is likely higher since the glucan in fungal material contributes to the glucose content on which the cellulose content is based. In contrast to PI and PII, lignin is removed efficiently during PIII (Jurak et al. 2015b). 48 % of lignin present at the start of PI is left after PIII (Jurak 2015). After 16 - 19 days the compost is fully colonized by *A. bisporus* and pH has declined to 6.5 - 7. To start phase IV the compost is transported to the mushroom growers. Mushroom yield and quality can be improved by supplementing the compost with formaldehyde treated, protein rich nutrients (Gerrits 1988).

PHASE IV

Phase IV (PIV) starts by placing the compost in large trays and topping it with casing layer. The casing layer consists of peat and lime and is essential for mushroom formation (Visscher 1988). It is nutrient poor and contains bacteria that assist in mushrooms formation, likely by removing volatiles produced by *A. bisporus*. During colonization of the casing layer the air temperature is kept at 22 °C to allow compost temperatures of 25 °C. In addition, CO_2 levels are high and relative humidity is 85 %. After 7 days, mushroom formation is induced by lowering the compost temperature to 18 - 22 °C, increasing relative humidity to 87 - 90 % and lowering CO_2 levels by venting (Visscher 1988). Mushrooms are harvested in 2 - 3 flushes with an interval of 7 - 8 days and a typical yield of 30 kg m^{-2} using 85 - 95 kg compost m^{-2}. Harvesting can be done manually, taking up to 6 days, or mechanically in which case all mushrooms of a flush are harvested simultaneously. The 1st flush provides 50 - 70 % of the total harvest. The contribution of each flush can be changed by varying climate conditions but total yield will remain similar.

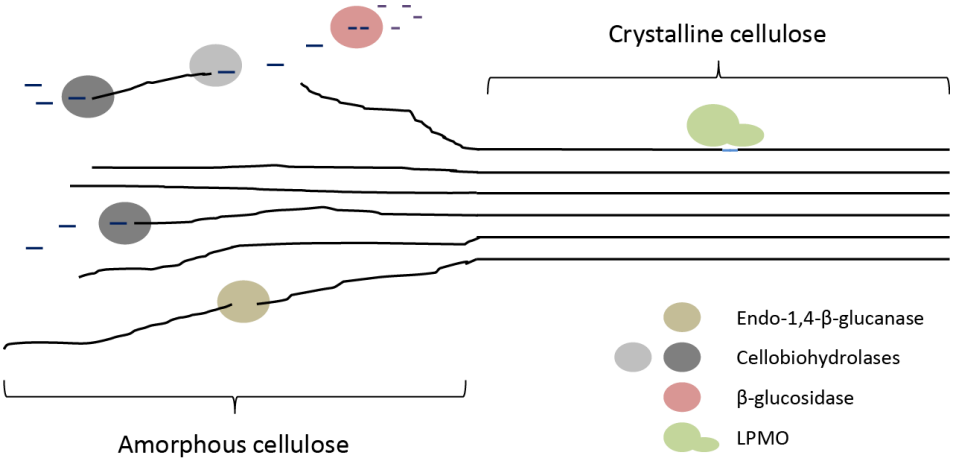

Figure 1.2: Schematic representation of cellulase activity on amorphous and crystalline cellulose.

Risk of pests and disease increases in time and therefore optimal harvest in flush I is preferred.

The amount of xylan and cellulose not consumed at PIV-end is 56 % and 46 % relative to the PII-end, respectively (Figure 1.1; Jurak 2015). The remaining cellulose may be an overestimation due to the glucose present in fungal material. Lignin is removed less efficiently during PIV as compared to PIII. Only, an additional 8 % of lignin is removed relative to the start of PI, bringing the total amount of remaining lignin to 44 % (Figure 1.1; Jurak 2015). Thus, a significant amount of carbohydrates and lignin remain in champost, the compost that remains after cultivation of button mushrooms (Iiyama et al. 1994; Chen et al. 2000, Jurak 2015). Space for mushrooms to develop is a limiting factor for mushrooms yield in the first flush but this is not the case in the 2nd and 3rd flush. This in combination with the sugar content in champost was the basis of the STW project leading to this PhD thesis.

Composition of wheat straw

Wheat straw is the primary carbon source of *A. bisporus*. It consists of 34 - 40 % cellulose, 24 - 35 % hemicellulose, and 14 - 24 % lignin (Lawther et al. 1995; Sun et al. 1995; Sun et al. 1998; Kirstensen et al. 2008). The primary cell wall contains mostly carbohydrates, while the secondary cell wall contains up to 20 % lignin (Vogel 2008). Cellulose is a polymer of β-(1⟶4)-D-linked glucose units with cellobiose as its repeating unit. It is the most abundant organic carbon in nature. Intra- and intermolecular hydrogen bonds produce rigid, insoluble microfibrils (Béguin and

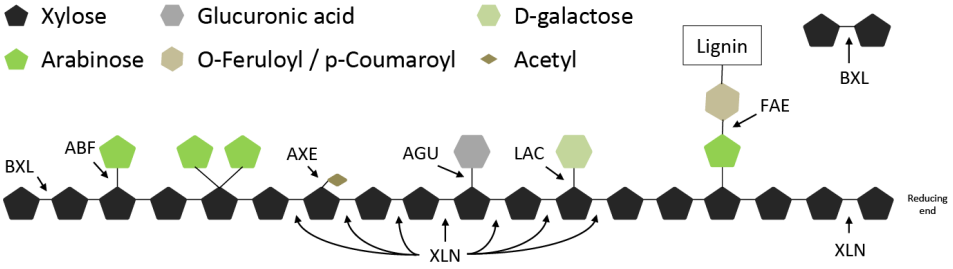

Figure 1.3: Schematic representation of xylan and enzymes involved in its degradation. XLN; endoxylanase, BXL; β-xylosidase, LAC; β-galactosidase, AGU; α-glucoronidase, FAE; feruloyl esterase, ABF; α-L-arabinofuranosidase and AXE; acetyl xylan esterase.

Aubert 1994). Cellulose microfibrils can be tightly packed in a crystalline structure or can be part of amorphous regions (Figure 1.2). Crystallinity of cellulose in wheat straw is approximately 40 % (Liu et al. 2005). Hemicellulose in wheat straw is more amorphous than cellulose and consists primarily of glucuronoarabinoxylan. This polymer consists of a β-(1⟶4)-linked D-xylose backbone that is decorated with L-arabinose, acetyl, and glucuronic acid residues (either or not methylated) (Figure 1.3). Glucuronic acid and arabinosyl decorations are most abundant (Sun et al. 1996) while D-galactosyl, rhamnose, and mannose are minor substituents (Sun et al. 1996; Sun et al. 2005). L-arabinose decorations occur as single or double substitutions on the xylan backbone at *O*3 and / or *O*2 of D-xylose (Fincher 2009). A portion of the glucuronic acid residues are suggested to be linked to lignin via ester bonds (Sun et al. 2005). Moreover, ferulic and coumaric acid link arabinose to lignin via ester or ether linkages (Sun et al. 2002; del Río et al. 2012).

Lignin is the second most abundant organic carbon in nature. It provides rigidity to the cell wall, and protects the plant cell wall from enzymatic attack. Lignin is a generic term for aromatic polymers that consist of *p*-coumaryl, coniferyl, and sinapyl alcohols (Boerjan et al. 2003; Vanholme et al. 2010). In the context of the cell wall these monomers form *p*-hydroxyphenyl (H), guaiacyl (G), and syringyl (S) phenylpropanoid units, respectively. Lignin is synthesized through a radical coupling reaction that may or may not be random (Davin et al. 2008). This reaction produces a heterogeneous and recalcitrant structure that is covalently linked to hemicellulose. Wheat straw lignin has a S : G : H ratio of 30 : 64 : 6. β-O-4 linkages are most abundant in wheat straw lignin, followed by phenylcoumarans with an abundance of roughly 75 % and 11 %, respectively (del Río et al. 2012). Typical lignin structures are presented in Figure 1.4. To utilize cellulose and hemicellulose in wheat straw as a carbon source, lignin needs to be removed and / or modified to increase accessibility of these carbohydrates.

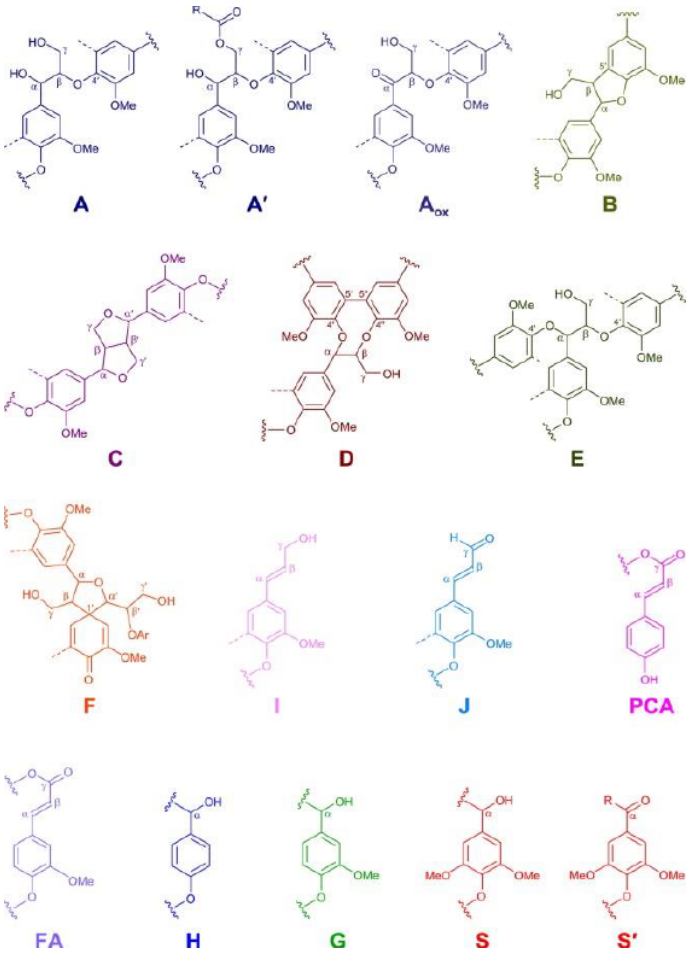

Figure 1.4: Main structures in wheat straw lignin. (A) β-*O*-4' alkyl-aryl ethers; (A') β-*O*-4' alkyl-aryl ethers with acylated γ-OH; (Aox) Cα-oxidized β-*O*-4' structures; (B) phenylcoumarans; (C) resinols; (D) dibenzodioxocins; (E) α,β-diaryl ethers; (F) spirodienones; (I) cinnamyl alcohol end-groups; (J) cinnamyl aldehyde end-groups; (PCA) *p*-coumarates; (FA) ferulates; (H) *p*-hydroxyphenyl units; (G) guaiacyl units; (S) syringyl units. Reprinted with permission from del Río J C, Rencoret J, Prinsen P, Martínez A T, Ralph J, Gutiérrez A (2012) J. Agric. Food Chem. 60:5922-5935. Copyright © 2012 American Chemical Society.

LIGNOCELLULOSE DEGRADATION

Enzymes can degrade lignocellulosic biomass by direct or indirect interaction with the substrate. Glycoside hydrolases (GHs), polysaccharide lyases (PLs), and carbohydrate esterases (CEs) (Lombard et al. 2014; http://www.cazy.org/) are enzymes that directly interact with the substrate. They act through hydrolysis and / or rearrangement of glycosidic bonds, non-hydrolytic cleavage of glycosidic bonds, and hydrolysis of carbohydrate esters, respectively. Lignocellulose is also degraded by oxidation through direct interaction with enzymes or indirectly by mediators. These enzymes are thought to support the GHs, PLs, and CEs in accessing their substrates. They are classified in the CAZy database as auxiliary activities (AAs) (Levasseur et al. 2013). Enzymes involved in generating co-factors for oxidative enzymes are also included in the AA class. Carbohydrate binding modules (CBM) are found in a variety of enzymes acting on carbohydrates. CBMs can bind strongly to the carbohydrate surface and support the specificity and activity of the enzymes (Gilbert et al. 2013).

CELLULOSE DEGRADATION

Several cellulases are involved in the synergistic degradation of cellulose (Figure 1.2; Baldrian and Valášková 2008; Glass et al. 2013). Endo-1,4-β-glucanases cleave internal bonds of the amorphous cellulose polymer. This creates new sites for the action of cellobiohydrolases that act on reducing or non-reducing ends of cellulose to release cellobiose, which is turn is hydrolyzed into glucose by β-glucosidases. There may be overlap in the substrates of cellulases and hemicellulases. For example, β-glucosidases can sometimes act on mannose, xylose or galactose units from hemicellulose with varying affinities. Copper-dependent lytic polysaccharide monooxygenases (LPMOs) can fulfill a function similar to endoglucanases by oxidatively cleaving cellulose chains. LPMOs are relevant in the degradation of crystalline cellulose but are also involved in the degradation of hemicellulose and chitin (Vaaje-Kolstad et al. 2010; Harris et al. 2010; Quinlan et al. 2011; Agger et al. 2014). Cellobiose dehydrogenase (CDH) may support LPMO activity by providing electrons through its action (Glass et al. 2013). Alternatively, CDH may contribute to cellulose and hemicellulose degradation by supporting the production of hydroxyl radicals in a Fenton-type reaction (Baldrian and Valášková 2008). In the Fenton reaction H_2O_2 oxidizes Fe^{2+} to Fe^{3+} which generates a hydroxyl radical capable of depolymerizing cellulose, hemicellulose and modifying lignin.

HEMICELLULOSE DEGRADATION

Hemicellulose is more heterogeneous than cellulose and requires a large set of enzymes for its degradation (Figure 1.3). Similar to cellulases, hemicellulases

degrade hemicellulose synergistically (Baldrian 2008; Dodd and Cann 2009; Glass et al. 2013). There are enzymes that make cleavage sites available for other enzymes, enzymes removing side chains and decorations, and enzymes that cleave shorter chains into sugar monomers. The xylan backbone of glucuronoarabinoxylan in wheat straw is attacked by endo- and exo-acting β-1,4-xylanases and β-xylosidases. Substituents are removed by enzymes like α-arabinofuranosidase, α-glucuronidase, and acetyl xylan esterase. Ferulic acid and *p*-coumaric esterases cleave the ester linkages between ferulic and coumaric acid decorating arabinose substituents of the xylan, while glucuronoyl esterases cleave the ester bonds between 4-*O*-methyl-D-glucuronic acid and lignin (Špániková and Biely 2006, Dodd and Cann 2009).

LIGNIN DEGRADATION

The efficient degradation of lignin requires an extracellular radical generating machinery. These radicals extract electrons from lignin resulting in lignin degradation through oxidation or "combustion" (Kirk and Farrell 1987). White rot fungi are thought to be efficient lignin degraders, while brown rot fungi only modify lignin (Hattaka 1994; Filley et al. 2002). Both brown and white rot fungi employ Fenton chemistry (Hammel et al. 2002), while white rots also produce ligninolytic enzymes. Brown rot fungi are polyphyletic. They may have arisen several times from white rots by losing genes encoding ligninolytic enzymes (Floudas et al. 2012; Riley et al. 2014).

Lignin peroxidase (LiP), manganese peroxidase (MnP), versatile peroxidase (VP) and laccase (LCC) are the main ligninolytic enzymes (Kirk and Farrell 1987; Hattaka 1994; ten Have and Teunissen 2001; Guillén et al. 2005). LiP, MnP, and VP contain a heme group and have a catalytic cycle similar to other peroxidases. Their heme group is oxidized by hydrogen peroxide (H_2O_2), resulting in the oxidation of small mediators like veratryl alcohol (for LiP and VP) and Mn^{2+} (for MnP and VP). These mediators oxidize lignin structures and are thought to be essential to reach lignin inaccessible to proteins. LiP can also oxidize lignin model compounds directly. VP acts as a hybrid of MnP and LiP since it may oxidize substrates of both LiP and MnP. At the protein level, VP may resemble a LiP containing a Mn^{2+} binding site or a MnP with a Trp residue normally present in a conserved region of LiP (Hammel and Cullen 2008). LCC is a copper containing oxidase that reduces oxygen to water resulting in the oxidation of a substrate. The relation of LCC to lignin degradation is less clear as compared to LiP, VP, and MnP. MnP and LCC activity are increased in the interaction zone of competing fungi (Hiscox et al. 2010) indicating that these enzymes have a role in fungal defense.

The *A. bisporus* genome does not contain genes encoding LiPs and VPs but

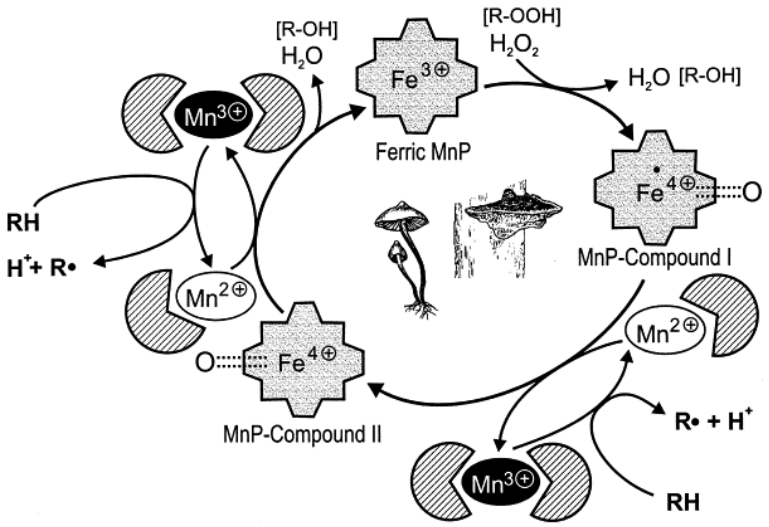

Figure 1.5: Catalytic cycle of MnP. Adapted from Hofrichter (2002).

contains two MnP genes (see below). The catalytic cycle of MnP is presented in more detail in Figure 1.5 (Hofrichter 2002). The Fe^{3+} in the heme of MnP binds H_2O_2 or an organic peroxide (R-OOH) thereby forming an iron-hydroxide complex. Next, two electrons are transferred from the heme group to the hydroxide group. This results in compound 1 that contains a Fe^{4+}-oxo-porphyrin-radical complex and the release of H_2O (or R-OH). Compound 1 is reduced to compound 2 by oxidizing Mn^{2+} to Mn^{3+}. In this step alternative substrates like phenolic compounds may be oxidized (Wariishi et al. 1988). Compound 2 preferentially oxidizes Mn^{2+} to Mn^{3+}. With an excess of H_2O_2 MnP can be reversibly inactivated to compound III. The Mn^{2+} ions used by MnP are thought to be chelated by an organic acid such as oxalic acid. Chelation by two oxalic acids stabilizes the Mn^{3+} ion and provides a more efficient release from MnP. The (chelated) Mn^{3+} serves as a redox mediator through which MnP is able to oxidize phenolic model lignin dimers. For the oxidation of non-phenolic model lignin structures additional mediators are required. For example, lipid peroxidation produces oxidants strong enough to cleave Cα-Cβ bonds and β-aryl ether bonds in non-phenolic lignin model dimers.

Enzymatic or non-enzymatic production of extracellular H_2O_2 is an essential co-factor for effective ligninolytic action. Extracellular oxidases like glyoxal oxidase produce H_2O_2 with glyoxal and methylglyoxal as substrate (Kersten and Kirk, 1987). Non-enzymatic reactions include quinone redox cycling which generates H_2O_2 and superoxide (Guillén et al. 2000; Gómez-Toribio et al. 2009). Quinones

may originate from lignin or are produced by the fungus. In addition, Mn^{3+} driven oxidation of fungal organic acids like oxalic acid can generate superoxide that may react with Mn^{2+} to generate Mn^{3+} and H_2O_2 (Urzúa et al. 1998; Schlosser and Höffer 2002). Quinone redox cycling and Mn^{3+} generation can be assisted by enzymes like (intracellular) benzoquinone reductase, LCC and MnP (Guillén et al. 1997; Gómez-Toribio et al. 2009).

COMPOST DEGRADATION BY *Agaricus bisporus*

The CAZymes found in the genome of *A. bisporus* reflect its capacity to degrade cellulose, hemicellulose, and lignin (Morin et al. 2012). The cellulose and hemicellulose degrading enzymes form a relatively complete set. The putative lignin degrading machinery of *A. bisporus* includes 12 LCCs and 2 MnPs but LiPs and VPs are absent. Calcium oxalate associated with the hyphae of *A. bisporus* may be a pool for oxalic acid to support MnP action (Whitney and Arnott 1987). Furthermore, predicted H_2O_2 producing oxidases and benzoquinone reductases would produce extracellular H_2O_2. Together, the MnPs of *A. bisporus*, either or not with the help of LCCs, and other AAs would provide a complete ligninolytic system. Enzyme families implicated in the detoxification of aromatic compounds like heme-thiolate peroxidases and glutathione-S-transferases were found to be expanded in the genome of *A. bisporus*. This suggests an adaptation to dealing with toxic aromatic structures in the humic rich compost that may originate from lignin or humic acids.

THE LIGNOCELLULOSE DEGRADING MACHINERY IN ACTION

A. bisporus preferentially degrades lignin during PIII illustrated by a 50 % loss of lignin as compared to 15 % xylan and 10 % cellulose (Figure 1.1). It was estimated that lignin removal by *A. bisporus* increases carbohydrate availability by 30 % (ten Have et al. 2003). The laccase genes *lcc1* and *lcc2* are highly expressed in compost during PIII, indicating a role in ligninolysis (Patyshakuliyeva et al. 2015). However, total LCC activity is lower in axenic compost cultures (Bonnen et al. 1994) supporting a role in fungal defense such as in the interaction of *A. bisporus* with *Trichoderma aggressivum* (Sjaarda et al. 2015). MnP activity increases during vegetative growth similarly to LCC (Bonnen et al. 1994). MnP1 is produced in compost and has been characterized (Bonnen et al. 1994; Lankinen et al. 2001). There is no evidence for expression of *mnp2* in transcriptome or proteomics data (Patyshakuliyeva et al. 2015) but transient production of its encoded enzyme cannot be excluded. Several oxidase genes putatively involved in H_2O_2 generation and a predicted quinone reductase gene were expressed in PIII (Patyshakuliyeva et al. 2015). In agreement with limited cellulose and hemicellulose degradation, *A. bisporus* produces only some cellulase and hemicellulase activity during PIII

(Wood and Goodenough 1977; Savoie 1998; Whiteford et al. 2000; Jurak et al. 2015a).

LCC and MnP activities decrease in PIV during mushroom production in the first flush (Wood and Goodenough 1977; Bonnen et al. 1994; Ohga et al. 1999). Interestingly, LCCs seem to be inactivated prior to degradation (Wood 1980ab). The mechanism for this remains unknown. Conversely, cellulase activity increases during mushroom production followed by a decrease (Wood and Goodenough 1977; Ohga et al. 1999). The relation of hemicellulase activity with mushroom formation is less clear. Transcriptome analysis at several time points during the first and second flush show increased production of cellulase and hemicellulase transcripts at the end of the 1st and 2nd flush (Whiteford et al. 2000; Patyshakuliyeva et al. 2015). Yet, xylanase activity does not correlate well with cellulase activity or fruiting (Wood and Goodenough 1977). Xylanase activities were similar in *A. bisporus* strains incapable and capable of fructification, while LCC and cellulase activities differ greatly in these strains. The discrepance between transcriptome analysis and enzyme activity assays may be due to post-transcriptional regulation and enzyme stability in compost. Production of cellulases and hemicellulases may be affected by catabolite repression and induction through compounds in the growth medium (Yagüe et al. 1997; de Groot et al. 1998). The increased activity and production of cellulases and hemicellulases during PIV fits well with the preferential removal of carbohydrates during this phase. As mentioned, a major part of the substrate is not degraded at the end of mushroom production. This is partly explained by selective degradation. Double substituted Ara / Xyl residues of hemicellulose accumulate during mushroom cultivation. The arabinofuranosidases predicted to act on this substrate are lacking from its genome (Jurak et al. 2015a; 2015b; 2015c). In addition, glucuronic acid substitutions accumulate in compost despite the presence of genes encoding α-glucuronidases in the genome of *A. bisporus* that have been shown to be produced and active on beechwood xylan (Puls et al. 1987). The encoding genes are lowly expressed during PIII and PIV but α-glucuronidase activity is absent at these stages (Jurak et al. 2015a; Patyshakuliyeva et al. 2015).

SCOPE OF THE THESIS

The aim of this thesis was to study *A. bisporus* growth and compost degradation which should ultimately result in reduced champost waste stream and increased mushroom production.

Fungal and bacterial biomass was quantified in PII-end and PIII compost in **Chapter 2**. Chitin content, indicative of total fungal biomass, increased during

PIII both in the absence (negative control) and presence of *A. bisporus*. The fungal phospholipid-derived fatty acid (PLFA) marker C18:2ω6, indicative of the living fraction of the fungal biomass, decreased in the negative PIII control. In contrast, it increased in the presence of *A. bisporus*. Bacterial PLFA markers remained constant during the negative control but decreased in the presence of *A. bisporus*. The latter was associated with a change in the ratio of Gram positive and Gram negative associated PLFA markers suggesting that Gram negative bacteria are more suppressed by *A. bisporus*. Together, these data indicate that fungal biomass can make up 6.8 % of the compost after *A. bisporus* colonization, 57 % of which being dead. Moreover, results strongly indicate that *A. bisporus* feeds on both bacteria and fungi that are preset in compost.

Double substituted arabinoxylan is part of the 40 % of wheat straw polysaccharides that is not degraded by *A. bisporus* during its growth and development. Genes encoding α-1,3-L-arabinofuranosidase (AXHd3) enzymes that act on double substituted arabinoxylan are absent in this mushroom forming fungus. In **Chapter 3**, the AXHd3 gene of *Humicola insolens* was expressed in *A. bisporus* under control of its actin promoter. Transformants secreted active AXHd3 as shown in an in vitro assay. However, carbohydrate composition and degree of arabinosyl substitution of arabinoxylans were not affected in compost showing that the production of AXHd3 is not sufficient to improve compost degradation by *A. bisporus*. The manganese peroxidase gene *mnp1* was over-expressed in *A. bisporus* with the aim to increase ligninolytic activity and thereby carbohydrate accessibility (**Chapter 4**). Over-expression neither impacted lignin degradation, carbohydrate composition, carbohydrate release by enzyme treatment, fungal biomass, nor mushroom yield. Notably, H_2O_2 consumption in compost extract was at least 4- to 8-fold higher than its de novo production. This indicates that H_2O_2 production limits MnP activity.

Codon optimized manganese peroxidase genes *mnp1* and *mnp2* of *A. bisporus* were introduced in *Schizophyllum commune* to assess their effect on ligninolytic activity (**Chapter 5**). In contrast to the wild-type, strains producing either or both MnPs decolorized Remazol Brilliant Blue R and coupled 3-methyl-2-benzothiazolinone hydrazone (MBTH) and (3-dimethylamino)benzoic acid (DMAB). Thermally assisted hydrolysis and methylation showed that birch wood lignin was not affected by *S. commune* wild-type or MnP-producing strains during a 119 day incubation. These data show that *mnp2* encodes an active enzyme. Yet, additional players apart from MnP1 and MnP2 are required for a minimal ligninolytic system in *S. commune*.

The inability to improve substrate degradation by the introduction and overex-

pression of enzymes involved in lignocellulose degradation suggests that compost degradation is not limiting mushroom production. Therefore, it was assessed whether expression of transcription factors involved in mushroom formation could be a bottleneck (**Chapter 6**). Over-expression of the transcription factor *c2h2* in *A. bisporus* strain A15 resulted in accelerated fruiting body formation by one day. This shows that white button mushroom production can be improved by modifying the regulatory network underlying mushroom development.

Chapter 7 describes respiratory rhythms during vegetative growth of *A. bisporus* in compost. The respiratory bursts were initially observed every 13 h but the interval increased up to 20 h and became more irregular in time. The bursts were accompanied by an up to 3.5 fold increase in CO_2 production and O_2 consumption and an increase in compost temperature of up to 3 °C. In addition, the respiratory quotient during a respiratory burst was up to 1.2 fold higher when compared to the pre-burst minimum. Respiratory bursts between parts of compost synchronized when they were in physical contact, showing that hyphal interactions and not volatiles or heat are necessary for synchronization. The potential role of the respiratory bursts in lignin degradation is discussed.

The results are summarized and jointly discussed in **Chapter 8**.

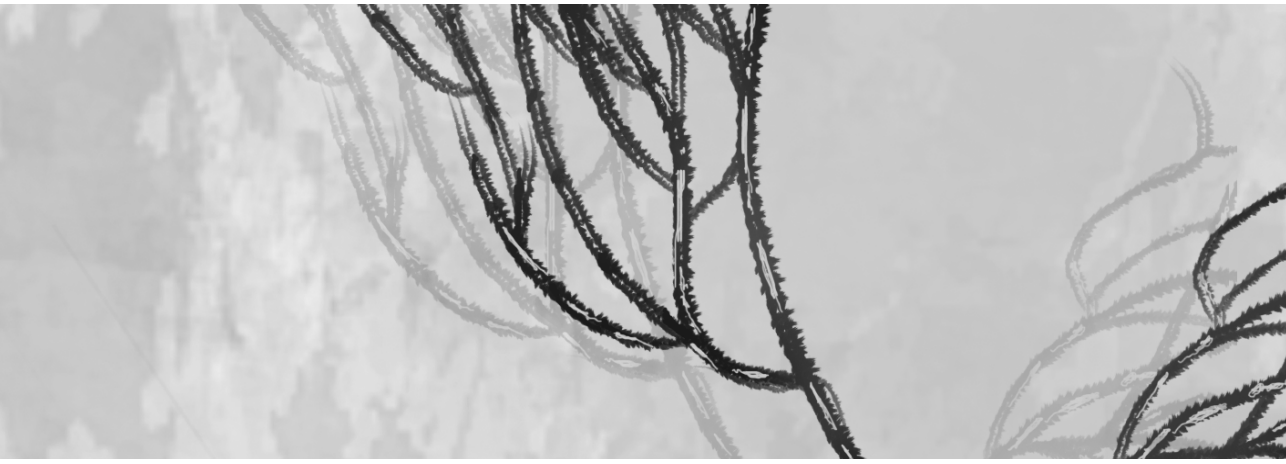

2

MICROBIAL BIOMASS IN COMPOST DURING COLONIZATION OF *Agaricus bisporus*

Aurin M. Vos, Amber Heijboer, Henricus T. S. Boschker, Barbara Bonnet, Luis G. Lugones, Han A. B. Wösten

This chapter has been published as: Vos AM, Heijboer A, Boschker HTS, Bonnet B, Lugones LG, Wösten HAB (2017) Microbial biomass in compost during colonization of *Agaricus bisporus*. AMB Express 7:12.

ABSTRACT

Agaricus bisporus mushrooms are commercially produced on a microbe rich compost. Here, fungal and bacterial biomass was quantified in compost with and without colonization by *A. bisporus*. Chitin content, indicative of total fungal biomass, increased during a 26-day period from 4.61 to 5.37 μmol N-acetylglucosamine g^{-1} compost in the absence of *A. bisporus* (negative control). A similar increase was found in the presence of this mushroom forming fungus. The fungal phospholipid-derived fatty acid (PLFA) marker C18:2ω6, indicative of the living fraction of the fungal biomass, decreased from 575 to 280 nmol g^{-1} compost in the negative control. In contrast, it increased to 1200 nmol g^{-1} compost in the presence of *A. bisporus*. Laccase activity was absent throughout culturing in the negative control, while it correlated with the fungal PLFA marker in the presence of *A. bisporus*. PLFA was also used to quantify living bacterial biomass. In the negative control, the bacterial markers remained constant at 3000 - 3200 nmol PLFA g^{-1} compost. In contrast, they decreased to 850 nmol g^{-1} compost during vegetative growth of *A. bisporus*, implying that bacterial biomass decreased from 17.7 to 4.7 mg g^{-1} compost. The relative amount of the Gram positive associated PLFA markers a15:0 and a17:0 and the Gram negative PLFA associated markers cy17:0 and cy19:0 increased and decreased, respectively, suggesting that Gram negative bacteria are more suppressed by *A. bisporus*. Together, these data indicate that fungal biomass can make up 6.8 % of the compost after *A. bisporus* colonization, 57 % of which being dead. Moreover, results show that *A. bisporus* impacts biomass and composition of bacteria in compost.

INTRODUCTION

Compost is used for the commercial production of the fruiting bodies of *Agaricus bisporus* known as button mushrooms. In the Netherlands, compost is produced from a mixture of wheat straw, horse manure, gypsum, and water, while chicken manure is either or not used as an additional nitrogen source (Gerrits 1988). Phase I (PI) of composting takes 3 - 6 days during which temperature increases to 80 °C due to microbial activity. Temperature of the compost during phase II (PII) is initially 50 °C, followed by a 2-day-period at 60 °C, and a 3-day-period at 45 °C (Gerrits 1988). The thermophilic fungus Scytalidium thermophilum (also known as Humicola insolens; Straatsma and Samson 1993) removes ammonia during PII and suppresses competitors of *A. bisporus* (Ross and Harris 1983; Straatsma et al. 1989; 1994). At the end of PII, 50 - 60 % of xylan and cellulose have been degraded as compared to the starting material, while lignin is still largely intact (Jurak 2015; Jurak et al. 2015). Introduction of *A. bisporus* spawn in PII-end compost initiates phase III (PIII). This phase takes 16 - 19 days, during

which the button mushroom colonizes the compost at 25 °C. This is accompanied by degradation of 50 % of the lignin, with an additional decomposition of 15 % of the xylan and 10 % of the cellulose (Jurak 2015; Jurak et al. 2015). PIII-end compost is either or not supplemented with formaldehyde treated, protein rich nutrients (Gerrits 1988), after which Phase IV (PIV) is initiated by topping the compost with a casing layer that consists of peat and lime. Casing is essential for mushroom formation (Visscher 1988), probably due to bacterial activity that removes suppressing volatiles produced by *A. bisporus* (Noble et al. 2009). CO_2 levels are high and relative humidity is 85 % during colonization of the casing layer. Mushroom formation is induced after 7 days by lowering the compost temperature to 18 - 22 °C, increasing relative humidity up to 90 %, and lowering CO_2 levels by venting (Visscher 1988). Mushrooms are harvested in 2 - 3 flushes with 7 - 8 day intervals with a typical yield of 30 kg m^{-2} and a bulk density of 85 - 95 kg m^{-2}. A total of 44 %, 29 %, and 8 % of cellulose, xylan, and lignin is degraded in PIV, respectively, when compared to PIII-end. Thus, a significant amount of the organic compounds remain unused in the compost after cultivation of button mushrooms (Iiyama et al. 1994; Chen et al. 2000; Jurak 2015). It should be noted that cellulose has been quantified based on glucose content in the compost. Since glucan in the fungal cell wall also consists of glucose, total cellulose degradation in PI - PIV will be higher than that reported.

Wheat straw represents the major carbon source for *A. bisporus* in compost but microbes may also represent an important part of its diet (Sparling et al. 1982). So far, dynamics of microbial biomass in compost have not been monitored. Here, we determined fungal and bacterial biomass in compost in time in the presence and absence of *A. bisporus* using chitin, laccase, and phospholipid-derived fatty acid (PLFA) analysis. Quantification of chitin determines both living and dead mycelium (Ekblad et al. 1998), while laccase activity can be used to monitor the linear vegetative growth phase (Wood 1979; Wood and Goodenough 1977). PLFA assays are used to determine the fraction of both living fungal and bacterial biomass (Frostegård et al. 2011). Experimental data indicate that *A. bisporus* can make up 6.8 % of the dry weight of compost, more than half of it being dead after 26 days of growth. In addition, experimental data indicate that *A. bisporus* feeds on bacterial and fungal biomass and that it impacts the bacterial composition.

Materials and Methods

Strains and growth conditions

The *A. bisporus* strain A15 (Sylvan, Horst, the Netherlands) was routinely grown at 25 °C on malt extract agar (MEA; 20 g l^{-1} malt extract agar [BD biosciences, Franklin Lakes, USA], 2.1 g l^{-1} MOPS, pH 7.0, and 1.5 % agar). Spawn was made

by mixing pieces of colonized MEA (0.5 by 0.5 cm) with a sterilized mixture of 50 g rye, 1.4 g $CaCO_3$, 1 g $CaSO_4$, and 50 ml demi water. The rye was colonized in 3 weeks at 25 °C and stored at 4 °C before use. PII-end compost (CNC Grondstoffen, Milsbeek, the Netherlands) was inoculated (5 spawn grains per 25 g of compost) in 250 ml bottles and incubated in the dark at 25 °C for up to 26 days. Compost not inoculated with *A. bisporus* served as a control. Samples of PII-end compost and PIII compost were stored at -20 °C.

Compost agar medium (CAM) was prepared by homogenizing 75 g phase III compost (CNC Grondstoffen) in 0.5 l water. The mixture was autoclaved 3 times at 120 °C for 20 min and mixed 1 : 1 with 3 % agar. To produce pure *A. bisporus* mycelium CAM was overlaid with a polycarbonate (PC) membrane (diameter, 76 mm; pore size, 0.1 µm; Profiltra, Almere, the Netherlands) and inoculated at the center of the plate. After 14 days at 25 °C mycelium was lyophilized, and ground to a powder.

Laccase activity

Compost extract was prepared by mixing 50 mg lyophilized and milled compost with 1 ml demi water and incubating head over tail for 1 h at 25 °C. Insolubles were removed by centrifugation at 4 °C and 15000 g for 15 min. Laccase activity was determined by mixing 20 µl 5 times diluted compost extract with 1 ml 1 mM ABTS in citric phosphate buffer, pH 4. Change in absorbance was followed at 420 nm for 30 sec. Activity in units (U) was calculated using the law of Lambert-Beer with an extinction factor of 36000 M^{-1} cm^{-1}.

Quantification of chitin

N-acetylglucosamine (GlcNAc) released from chitin was quantified in technical triplicates using a colorimetric assay (Reissig et al. 1955; François 2006). Compost (20 - 30 mg dry weight) was mixed with 1 ml 6 % KOH (w/v) and incubated at 80 °C for 90 min. The mixture was centrifuged at 10000 g at 4 °C for 10 min after adding 500 µl glacial acetic acid. Pellets were washed twice with water and once with 50 mM potassium phosphate buffer, pH 6.5. Chitin was digested overnight in 600 µl 50 mM potassium phosphate buffer pH 6.5 containing 0.42 U chitinase, 8.3 U lyticase, and 2 µl protease inhibitor (P8215, Sigma-Aldrich, St Louis, USA). Water was added to a final volume of 1.2 ml and 100 µl was used for colorimetric quantification of GlcNAc. To this end, 50 µl demi water and 150 µl 0.27 M tetraborate were added. After incubation at 100 °C for 15 min, 1.8 ml Reissig reagent (10 gram 4-(dimethylamino)benzaldehyde, 12.5 ml of 10 M HCl, and 87.5 ml glacial acetic acid) was added and incubated at 40 °C for 20 min. Liquid was transferred to a cuvette and the OD585 was measured. A standard curve of 0-90

nmol GlcNAc (with a detection limit of 2 nmol) was used to calculate the release of the aminosugar per gram compost after subtracting the signal obtained from the assay in the absence of chitinase. 0.5 to 8 mg of pure mycelium was used to determine the amount of GlcNAc release mg^{-1} mycelium. The average OD of the reaction mixture in the absence of compost was substracted from the OD of mixtures containing fungal colonized compost or pure mycelium. GlcNAc was not detected when using 3 x 10^9 dH5α Escherichia coli cells that contain a total amount of 174 nmol of the aminosugar (Wientjes et al. 1991). This shows that the GlcNAc in the assay does not orginate from bacterial biomass.

PHOSPHOLIPID FATTY ACID ANALYSIS

PLFAs were extracted from 300 mg compost as described (Frostegård et al. 1991; 1993; Hedlund, 2002) based on the methods of Bligh and Dyer (1959) and White et al. (1979). In short, PLFAs were extracted using 10 ml Bligh and Dyer solution (CHCl3 : MeOH : citrate buffer, 1 : 2 : 0.8, v / v / v). Phases were separated by addition of 4 ml $CHCl_3$ and 4 ml citrate buffer during overnight incubation at room temperature. An aliquot of 3 ml of the lipid extract was transferred to a glass tube. After evaporation of the solvent with a stream of N_2, samples were solubilized in $CHCl_3$ and applied on a silica column. Phospholipids were eluted with 1.5 ml MeOH after eluting the neutral and glycolipids with 1.5 ml $CHCl_3$ and 6 ml acetone, respectively. 5 µg of methyl nonadecanoate (C19:0, Sigma-Aldrich) was added to each sample as an internal standard. Samples were transesterified at 37 °C for 15 min by addition of 1 ml toluene : methanol (1 : 1) and 1 ml freshly made 0.2 M KOH in methanol. After cooling to room temperature for 20 min, 2 ml hexane : $CHCl_3$ (4 : 1 v / v), 0.3 ml 1 M HAc, and 2 ml H_2O were added. Samples were centrifuged for 5 min at 685 g and 5 µg of methyl dodecanoate (C12:0, Sigma Aldrich) was added as an internal control to the upper phase that contained the PLFAs. After evaporation of the solvent by a stream of N_2, lipids were taken up in 200 µl hexane for gas chromatography-flame ionization detector analysis. PLFAs were identified based on retention time and equivalent chain length as calculated using C12:0, C16:0, and C19:0. Abundance in nmol g^{-1} was calculated using spiked C19:0. The C18:2ω6 marker was used to estimate fungal biomass, while various PLFA markers (Table 2.3) were used as markers of bacterial biomass (Frostegård and Bååth 1996; Hedlund 2002; Ruess and Chamberlain 2010).

DATA ANALYSIS

Custom R (v3.03) scripts were used for annotation of PLFAs. Statistical analysis of chitin and PLFA biomass was done with T-tests in SPSS Statistics 22 software. Changes of laccase, chitin, and PLFA over time were analysed using ANOVA with Bonferroni or Dunnet T3 post-hoc correction (SPSS Statistics 22; $p < 0.05$).

Table 2.1: Fungal biomass in mg g^{-1} compost based on chitin (GlcNAc release) and PLFA C18:2ω6 content. Average biomass (μ) and standard deviation (σ) are shown. Significant differences between the biomass at each time point are indicated with letters ($p < 0.05$, T-test).

	Day 0*			Day 13			Day 19			Day 26		
Methods	**μ**	σ		**μ**	σ		**μ**	σ		**μ**	σ	
Chitin	58.1	2.3	A	64.2	0.3	A	65.6	3.2	A	67.6	1.5	A
C18:2ω6	14.2	2.8	B	23.0	4.4	B	30.2	1.5	B	28.9	8.1	B

*Based on conversion factor of *A. bisporus*.

RESULTS

FUNGAL BIOMASS IN COMPOST

A. bisporus strain A15 was grown in PII-end compost for 26 days. Fungal biomass was determined by laccase activity and by chitin and PLFA content. No laccase activity was found in the negative control (PII-end compost that had not been innoculated with *A. bisporus*) during the 26 days of incubation (Figure 2.1). In contrast, laccase activity increased to approximately 100 U g^{-1} compost after 19 - 26 days of colonization by *A. bisporus*. Fungal biomass based on chitin content increased during the first 19 days from 4.61 to 5.21 μmol GlcNAc g^{-1} in the absence of *A. bisporus*, after which it did not increase further (Figure 2.1). In the presence of *A. bisporus*, an increase in the released amino sugar was observed between day 0 and 19 from 4.61 to 6.03 μmol GlcNAc g^{-1} compost (Figure 2.1), after which no further increase was found. No significant differences in chitin content were observed in compost with or without *A. bisporus* throughout culturing. The amount of the fungal PLFA marker C18:2ω6 decreased during the 26-day-period from 575 to 280 nmol g^{-1} in the absence of *A. bisporus* (Figure 2.1). In contrast, it increased from 575 to 1200 nmol during the first 19 days in the presence of *A. bisporus*, after which it remained constant.

Pure *A. bisporus* mycelium grown on compost agar medium contained 40 nmol mg^{-1} C18:2ω6, and 80 nmol GlcNAc mg^{-1} (Figure 2.3). These amounts were used to calculate the fungal biomass in compost. The estimated biomass in PII-end compost based on chitin and PLFA was 58 and 14 mg g^{-1}, respectively (Table 2.1). These amounts had increased to 68 and 29 mg g^{-1} compost after 26 days of growth of *A. bisporus*.

BACTERIAL BIOMASS IN COMPOST

PLFA was used to quantify bacterial biomass in compost that had either or not been inoculated with *A. bisporus*. To this end, selected bacterial PLFA markers were used (Table 2.3). Bacterial biomass remained constant between day 0 and 26

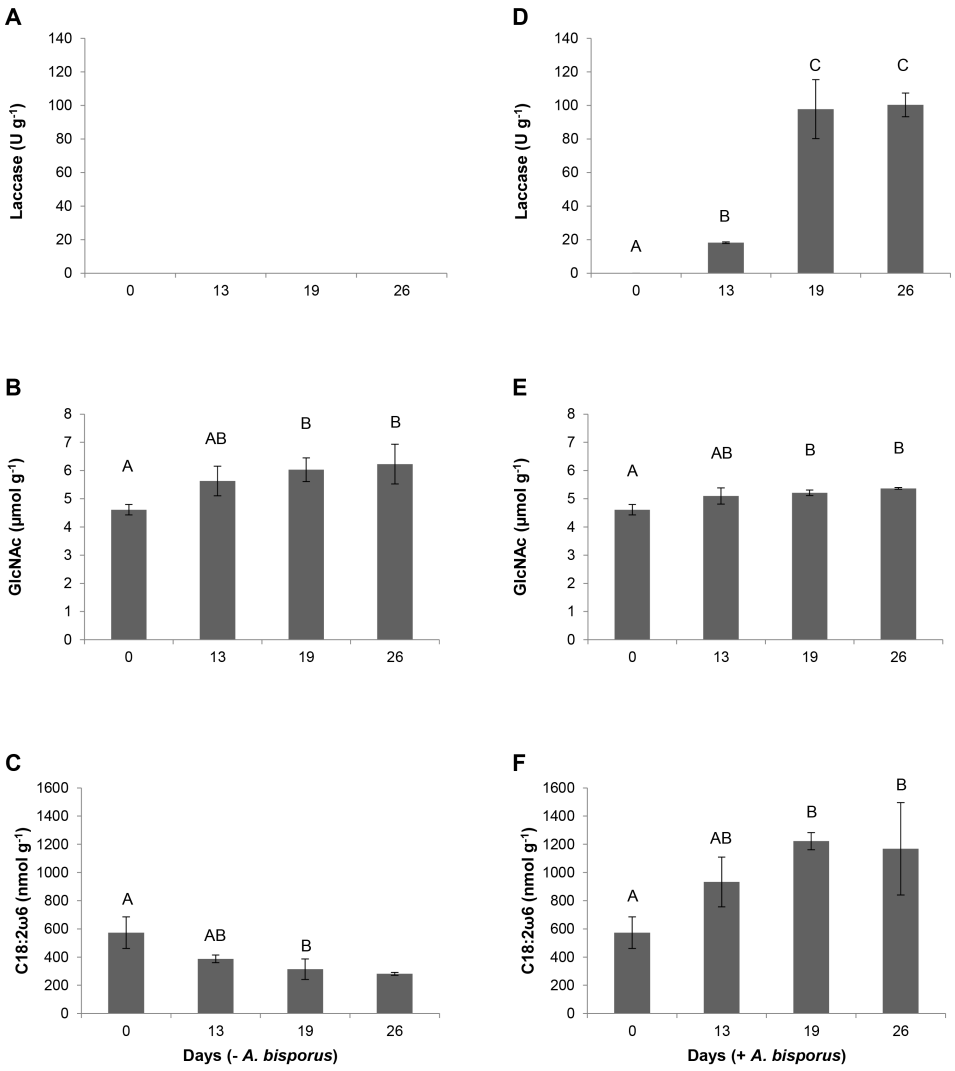

Figure 2.1: Fungal biomass in compost. Fungal biomass as determined by laccase activity (U g^{-1}) (A, D) and chitin (GlcNac, µmol g^{-1}) (B, E) and PLFA (C18:2ω6, nmol g^{-1}) (C, F) content in compost that had not (A, B, C) or had (D, E, F) been colonized with *A. bisporus*. Error bars indicate standard deviation. Significant differences are indicated with letters (ANOVA with Bonferonni or Dunnett T3 correction).

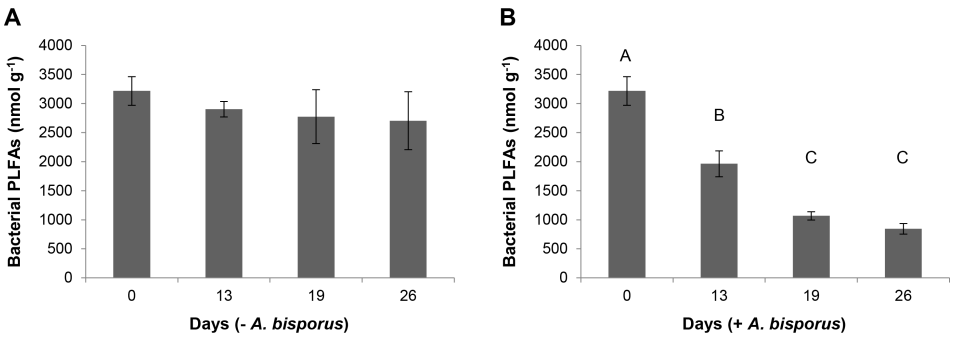

Figure 2.2: Bacterial biomass in compost based on PLFA. Sum of bacterial PLFAs in nmol g^{-1} compost in the absence (A) and presence (B) of *A. bisporus*. Error bars indicate standard deviation. Statistical differences are indicated with letters, absence of letters indicates no significant differences were found (ANOVA, Bonferroni correction).

in the absence of *A. bisporus* (Figure 2.2A). In contrast, bacterial PLFAs decreased from 3200 to 850 nmol g^{-1} in this time period in the presence of *A. bisporus* (Figure 2.2B). Only minor temporal changes in relative abundance of the bacterial markers were found in the absence of *A. bisporus*. In contrast, relative abundance of the bacterial markers a15:0, C15:0, and a17:0 increased 1.3, 2.8, and 1.2 fold, respectively, from day 13 onwards, while relative abundance of 16:1ω9, 10Me16:0, cy17:0, and cy19:0 decreased 5, 1.4, 2.5, and 1.8 fold, respectively (Table 2.2). The contribution of *A. bisporus* PLFAs to the pool of bacterial PLFAs was ≤ 5 % after 26 days of compost colonization. From these data and the assumptions that 363.6 nmol bacterial PLFA equals 1 mg C and bacterial biomass consists for 50 % of C (Bratbak and Dundas 1984; Tsiafouli et al. 2015) it is concluded that bacterial biomass decreased from 17.7 to 4.7 mg g^{-1} compost during the 26-day-colonization of compost by *A. bisporus*. In contrast, bacterial biomass was in the range of 14.9 to 17.7 mg g^{-1} compost in the absence of *A. bisporus*.

Discussion

Fungal and bacterial biomass was quantified during a 26-day-incubation of PII-end compost in the presence and absence of *A. bisporus*. Chitin was used to quantify total fungal biomass, laccase and C18:2ω6 for the living fraction of the fungal biomass, and bacterial PLFAs for living bacterial biomass. Laccase activity was absent in PII-end compost during the incubation period in the absence of *A. bisporus*, while chitin and C18:2ω6 content increased by 26 % and dropped by 50 %, respectively. In contrast, laccase activity and C18:2ω6 levels increased during the first 19 days of *A. bisporus* colonization, while chitin content already reached its maximum at day 13. These data confirm that laccase is a good marker

Table 2.2: Relative abundance of selected bacterial PLFAs in compost in the absence (-) and presence (+) of *A. bisporus*, and relative abundance of the selected bacterial PLFAs in pure *A. bisporus* mycelium (in mol %). Values are the average of 3 biological replicas.

		Selected bacterial PLFAs in mol %									
	Days	**i15:0**	**a15:0**	**C15:0**	**i16:0**	**16:1ω9**	**10Me16:0**	**a17:0**	**cy17:0**	**C18:1ω7**	**cy19:0**
- A. bisporus	0	17.3	14.7	2.4	23.2	0.8	4.5	9.2	8.6	9.2	10.2
	13	18.6	13.9	1.8	20.7	0.9	5.5	7.7	11.1	7.9	11.9
	19	19.6	14.7	1.8	20.4	0.9	5.5	7.5	10.9	7.5	11.3
	26*	18.8	15.0	1.9	20.4	0.9	5.0	7.3	10.6	8.4	11.6
+ A. bisporus	0	17.3	14.7	2.4	23.2	0.8	4.5	9.2	8.6	9.2	10.2
	13	17.4	15.5	2.8	22.1	0.5	4.9	10.1	10.2	5.8	10.8
	19	15.6	17.9	5.0	23.8	0.4	4.2	12.3	6.0	6.4	8.4
	26	16.2	19.6	7.8	24.3	0.1	3.4	12.3	4.0	6.3	6.1
Pure mycelium		11.4	11.2	39.8	14.6	2.4	1.1	0.0	3.6	14.3	1.5

*average of 2 replicates.

for vegetative growth of *A. bisporus* in compost as reported previously (Wood 1979). However, its activity (Wood and Goodenough 1977) and transcript levels (Ohga et al. 1999) drop during mushroom formation and therefore laccase can only be used as a biomarker during PIII.

Standard curves of chitin and PLFA content in pure mycelium of *A. bisporus* were used to estimate fungal biomass in compost. This approach assumes that chitin and PLFA content is identical between species and culture conditions, which is not necessarily the case. For instance, C18:2ω6 content ranges from 1.4 - 22.9 nmol mg^{-1} between fungal species with basidiomycetes containing 45 - 57 mol % and zygomycetes between 12 and 22 mol % (Klamer and Bååth 2004). Using these numbers, 25 and 400 mg g^{-1} represent the extremes of fungal biomass in PII-end compost. Notably, *A. bisporus* contains 40 nmol mg^{-1} C18:2ω6 and this number was used to estimate fungal biomass in this study. The use of the high C18:2ω6 content of *A. bisporus* to calculate fungal biomass does not impact relative changes found in this study but is expected to underestimate the fungal biomass in compost 2 - 4 fold in the absence of *A. bisporus*. Chitin levels can vary depending on culture age and growth conditions (Sharma et al. 1977). In the case of *A. bisporus*, however, chitin content did not change in time relative to fungal dry weight in malt extract (Matcham et al. 1985). Moreover, *A. bisporus* becomes the dominant fungal species after its inoculation. Fungal biomass in *A. bisporus* inoculated compost based on chitin and PLFA was calculated to amount 68 and 29 mg g^{-1} compost after 26 days. This indicates that more than half of the fungal biomass is dead. The 50 % decrease in living fungal biomass in the absence of *A. bisporus* shows that the applied growth conditions negatively impact the established fungal community in PII compost. At the same time, the increase in chitin content under this condition suggests that part of the fungal community continues to grow, albeit slower than the death rate.

Relative abundance of bacterial PLFAs changed during the 26-day-period. This shows that the bacterial community is influenced by the vegetative growth of *A. bisporus* and that (selected) bacteria divide and thus produce biomass. The relative increase of the Gram positive associated markers a15:0 and a17:0 and the relative decrease of Gram negative associated markers cy17:0 and cy19:0 indicates that Gram negative bacteria are more suppressed by *A. bisporus* than Gram positive bacteria. Previously, it was caculated that the microbial biomass consumption would contribute < 10 % of the mushroom dry weight biomass (Sparling et al. 1982). This was based on colony forming units in PII-end compost extracts and by direct counting. It did not include bacterial biomass formation in PIII and therefore bacterial consumption could be much higher. The fact that bacterial biomass was relatively stable in the absence of *A. bisporus*, while

it decreased about 4-fold in the 26-day-period in the presence of *A. bisporus* supports the hypothesis that this mushroom forming fungus feeds on bacteria. This is also suggested from the fact that growth of *A. bisporus* is strongly reduced when it is exposed to sterilized compost (not shown). Based on a conversion factor from the literature the PII-end compost contained 8.9 mg C bacterial biomass g^{-1} compost (Frostegård and Bååth 1996; Tsiafouli et al. 2015). When assuming a C content of 50 % in dry material of bacteria (Bratbak and Dundas 1984) a decrease in living bacterial biomass from 17.7 to 4.7 mg g^{-1} compost occurred during the 26 day period of compost colonization by *A. bisporus*. The increase in fungal biomass from 14 to 30 mg g^{-1} in the same period and the fact that bacterial biomass production in PIII is not taken into account suggests that the *A. bisporus* diet may contain bacteria as its main course. In this view, *A. bisporus* would secrete the enzymes that degrade lignocellulose. The bacteria would use the degradation products as nutrients, after which *A. bisporus* feeds on the bacterial biomass. This strategy would alleviate the deficiency of *A. bisporus* to produce molecules such as vitamins.

SUPPLEMENTARY MATERIALS

Table 2.3: Bacterial PLFA markers used in this study (Hedlund 2002; table adapted from Ruess and Chamberlain 2010; Heijboer et al. 2016).

PLFA markers	Fatty acid type	Predominant origin	References
i15:0, a15:0, i16:0, a17:0	Ise/anteiso methyl-branched	G+ bacteria	Zelles (1997, 1999)
cy17:0, cy19:0	Cyclopropyl ring	G- bacteria	Zelles (1997, 1999)
15:0	Straight-chain saturated < 19	Non-specific	
10Me16:0	10-methyl-branched	Sulphate reducing bacteria and/or Actinomycetes	Dowling et al. (1986) & Kerger et al. (1986)
18:1ω7	Double bond C7	Bacteria	Zelles (1999)
16:1ω9	Double bond C9	Non-specific	
18:2ω6	Poly-unsaturated ω6 family	Sapotrophic fungi	Frostegård and Bååth (1996) & Zelles (1999)

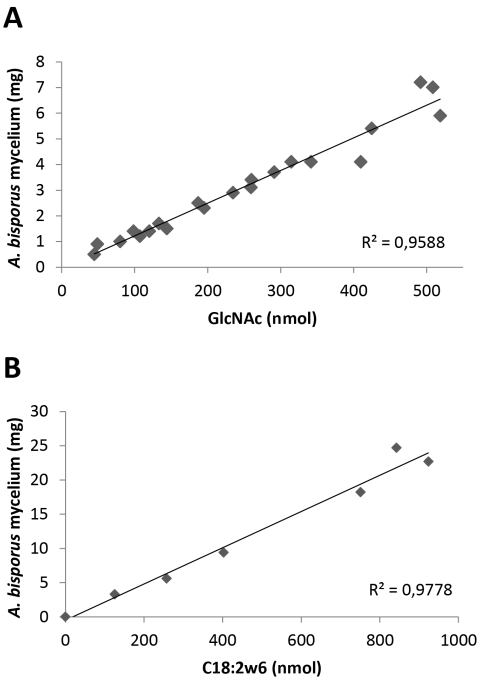

Figure 2.3: N-acetylglucosamine (GlcNAc) (A) and PLFA marker C18:2ω6 (B) content in pure *A. bisporus* mycelium.

3

PRODUCTION OF α-1,3-L-ARABINOFURANOSIDASE (AXHD3) ACTIVE ON SUBSTITUTED XYLAN DOES NOT IMPROVE COMPOST DEGRADATION BY *Agaricus bisporus*

Aurin M. Vos, Edita Jurak, Peter de Gijsel, Robin A. Ohm, Bernard Henrissat, Luis G. Lugones, Mirjam A. Kabel, Han A. B. Wösten

ABSTRACT

Agaricus bisporus consumes wheat straw carbohydrates contained in compost used for commercial mushroom production. Double substituted arabinoxylan is part of the 40 % of the wheat straw polysaccharides that is not degraded by *A. bisporus* during its growth and development. Genes encoding α-1,3-L-arabinofuranosidase (AXHd3) enzymes that act on xylosyl residues doubly substituted with arabinosyl residues are absent in this mushroom forming fungus. Here, the AXHd3 gene of *Humicola insolens* was expressed in *A. bisporus* under control of its actin promoter. Transformants secreted active AXHd3 as shown by the degradation of doubly substituted arabinoxylan oligomers in an in vitro assay. However, carbohydrate composition and degree of arabinosyl substitution of arabinoxylans were not affected in compost showing that the production of AXHd3 is not sufficient to improve compost degradation by *A. bisporus*.

INTRODUCTION

Agaricus bisporus mushrooms are produced in the Netherlands using a wheat straw based compost. Wheat straw consists of 34 - 40 % cellulose, 24 - 35 % hemicellulose, and 14 - 24 % lignin (Lawther et al. 1995; Sun et al. 1995; Sun et al. 1998; Kristensen et al. 2008). The hemicellulose fraction consists for a large part of glucuronoarabinoxylan. Its β-(1$\longrightarrow$4)-linked D-xylosyl backbone is decorated with L-arabinosyl, acetyl, and / or glucuronic acid residues that are either or not methylated and with D-galactosyl, rhamnose, and mannose as minor substituents (Sun et al. 1996; Sun et al. 2005; Figure 1.3). Acetyl, glucuronic acid, and arabinosyl residues have a degree of substitution (based on xylosyl) of 0.1, 0.038, and 0.077, respectively (Sun et al. 1996; Sun et al. 2005). Some of the glucuronic acid is suggested to be linked to lignin via ester bonds (Sun et al. 2005), while the arabinosyl substituents can be covalently linked to lignin via ester or ether bonds with ferulic and coumaric acid (Sun et al. 2002; Fincher 2009; del Río et al. 2012).

Compost used by the Dutch *A. bisporus* industry is prepared in three phases. At the start of phase I (PI), wheat straw, horse manure, gypsum, and water, either or not supplemented with chicken manure as an additional nitrogen source, are mixed in a tunnel (Gerrits 1988). The temperature of the compost reaches up to 80 °C and ammonia is produced during the 3 - 6 days PI period. As a consequence, the mesophilic microbiota is replaced by a thermophilic microbiota (Gerrits 1988). Lignin remains, while some xylan and cellulose is consumed (Jurak et al. 2014; Jurak 2015; Jurak et al. 2015c). The PI-material is transported to a new tunnel at the start of phase II (PII). Temperature is decreased to 50 °C and then increased to 60 °C, while ammonia is removed from the compost, affecting

the composition of the microflora (Gerrits 1988; Straatsma et al. 1994). After 2 days, the temperature is decreased to 45 °C to start a conditioning process. During this 3-day period remaining ammonia is sequestered by thermophilic fungi like *Scytalidium thermophilum* (also named *Humicola insolens*; Straatsma and Samson 1993). These fungi also suppress competitors of *A. bisporus* (Ross and Harris 1983; Straatsma et al. 1989; Straatsma et al. 1994). Lignin is still unaffected after PII, while 50 % and 60 % of cellulose and xylan have been removed, respectively (Jurak 2015). Spawn of *A. bisporus* is introduced in PII-end compost, after which the mixture is transferred to a new tunnel to start Phase III (PIII). The compost is colonized by *A. bisporus* during a 16 - 19 day period at 25 °C. Lignin is preferentially removed during this phase with a loss of 50 %, while only 15 % and 10 % of xylan and cellulose are degraded, respectively (Jurak 2015). Formaldehyde treated, protein rich supplements can be mixed through the compost after PIII to improve mushroom yield and quality (Gerrits 1988), after which the compost is transported to mushroom growers to start Phase IV (PIV). To this end, the compost is topped with a casing layer and mushrooms are produced in 2 - 3 flushes with 7 - 8 day intervals and a typical yield of 30 kg m^{-2} when using 85 - 95 kg compost m^{-2}. Bacterial activity in the casing layer likely removes *A. bisporus* volatiles that suppress mushroom formation (Visscher 1988; Noble et al. 2009). High CO_2 levels are required for optimal colonization of the casing layer. After 7 days, mushroom formation is induced by lowering CO_2 levels through venting, increasing relative humidity from 85 % up to 90 %, and lowering the compost temperature to 18 - 22 °C (Visscher 1988). An additional 44 %, 29 %, and 8 % of cellulose, xylan, and lignin are degraded during PIV, respectively (Jurak 2015). It should be noted that the loss of cellulose in PI - PIV is underestimated since glucose from cellulose cannot be distinguished from fungal glucan. Still, this leaves a significant proportion of the carbohydrates unutilized for mushroom production.

Recalcitrant hemicellulose accumulates as xylan substituted with (4-*O*-methyl) glucuronic acid and single and double substitutions of arabinosyl residues (Jurak et al. 2015a; Jurak et al. 2015c). The arabinosyl and glucuronoyl substitution ratio of xylose increases during PIV but not during PIII of mushroom cultivation (Jurak et al. 2014; Jurak et al. 2015a). The genome of *A. bisporus* encodes GH115 α-glucuronidase genes (geneID 121649 and 121650; Morin et al. 2012). Based on characterization of other GH115 proteins it is expected that those of *A. bisporus* act on (4-*O*-methyl) glucuronic acid substituted xylan (Martínez et al. 2016). The encoded proteins are actively produced in beech wood xylan (Puls et al. 1987), but their activity could not be found in compost (Jurak et al. 2015a; Patyshakuliyeva et al. 2015). Arabinofuranosidases (GH43) predicted to act on the *O*3 position of doubly substituted xylosyl residues (AXHd3) are absent in the genome of *A. bisporus*

(Jurak et al. 2015c), which would explain why arabinose substituents accumulates in compost. Here, the AXHd3 gene from *Humicola insolens* was introduced in *A. bisporus* to assess whether this activity increases substrate utilization by this basidiomycete. Although transformants produced active enzyme, no effect on carbohydrate composition or xylan substitution was found during PIII and PIV. This indicates that expression of AXHd3 by *A. bisporus* is not the bottleneck to improve compost degradation.

Material and Methods

Strains and substrate

Agaricus bisporus strain A15 (Sylvan, Netherlands) was routinely grown at 25 °C on malt extract agar medium (MEA; 20 gr l^{-1} malt extract [BD biosciences, Franklin Lakes, USA], 1.5 % agar, 2.1 gr l^{-1} MOPS, pH 7.0). Mycelium for RNA isolation was grown for 16 days from 4 mycelial plugs (5 x 5 mm) on a polycarbonate (PC) membrane (diameter, 76 mm; pore size, 0.1 µm) overlaying MEA.

Spawn was made by inoculating a sterilized mixture of 50 g rye, 1.4 g $CaCO_3$, 1 g $CaSO_4$, and 50 ml demi water with 0.5 by 0.5 cm pieces of colonized MEA. After 3 weeks of growth, spawn was stored at 4 °C. For small scale cultivation of *A. bisporus* 20 g spawn was mixed with 2.5 kg PII compost (CNC Grondstoffen, Milsbeek, the Netherlands) in a box (30 x 20 x 22 cm) overlaid with plastic foil containing 20 evenly distributed holes of 2 - 3 mm. After 16 days of growth at 24 °C, the compost was topped with 1 kg casing layer (CNC Grondstoffen, Milsbeek, the Netherlands) and growth was prolonged for 7 days. Plastic foil containing 20 evenly distributed holes of 2 - 3 mm prevented water evaporation. Mushroom formation was induced by removing the foil and lowering the air temperature to 20 °C. Mushrooms were harvested in two flushes during a 2 week period.

Plasmid construction

The coding sequence of *H. insolens hgh43* (GenBank: CAL81199.1) was codon optimized using the OptimumGeneTM algorithm (Genscript USA Inc). To this end, a codon usage table of coding sequences of *A. bisporus* (strain H97, genome version 2.0) was used combined with that of the 1000 most highly expressed genes on compost (Morin et al. 2012). The codon tables were produced using a custom Python script that discarded coding sequences that did not start with ATG or ended with an in frame stop codon. The codon optimized arabinofuranosidase genes were ordered at Genscript (New Jersey, United States). The gene contained intron 4 of *gpdII* (gene ID 138631) including 6 upstream and 8 downstream nucleotides after its stop codon. To create the expression vector, the actin promoter and terminator of *A. bisporus* were amplified with primers 1 & 2 and 3 & 4 (Table

S1). Fragments were cloned in pGEMt and reamplified with primers 5 & 6 and 7 & 8 (Table S1). They were cloned in PacI / AscI digested pBHg-PA (Pelkmans et al. 2016) using InFusion cloning, resulting in pBHg-ActPT. Primers 9 & 10 were used to amplify codon optimized *hgh43* with the intron following the stop codon using Phusion polymerase (Table S1). InFusion cloning (Takara Bio USA, Inc) was used to introduce the amplified fragment in between the 5' and 3' actin regulatory elements in PacI / AscI digested pBHg-ActPT resulting in plasmid pBHg-HGH43.

Transformation of Agaricus bisporus

Plasmid pBHg-HGH43 was transformed to *A. bisporus* A15 gills using *Agrobacterium tumefaciens* mediated transformation (Chen et al. 2000; Romaine and Chen 2005). For selection, gills were placed on MEA containing 25 μg ml^{-1} hygromycin, 200 μM cefotaxime, and 100 μg ml^{-1} chloramphenicol. Resistant mycelium originating from gills was transferred to a second selection plate containing 40 μg ml^{-1} hygromycin.

RNA isolation and qPCR

Mycelium was homogenized for 1 min with 2 metal balls at 25 Hz in a 2 ml tube that was placed in a holder cooled to -80 °C. RNA was extracted with 500 μl Trizol reagent (Chomczynski and Sacchi 1987). After a 5 min incubation at room temperature, 200 μl chloroform was added and phases were separated through centrifugation at 15000 g for 15 min. RNA in the aqueous phase was precipitated by addition of 0.5 volume isopropanol and centrifugation at 15000 g for 15 min. RNA was washed with 70 % ethanol and dissolved in water. cDNA was prepared from 1 μg of RNA using the Quantitect® reverse transcription kit (QIAGEN).

An optical 96 wells plate (Applied Biosystems) and a ViiA™ 7 Real-Time PCR System (Thermo Fisher Scientific) were used for qPCR with SYBR® Green to monitor DNA synthesis. Primers 11 & 12, 13 & 14, and 15 & 16 (Table S1) were used to detect *gpdII*, *18S*, and *hgh43*, respectively. Reactions were performed using 40 cycles of 15 s at 95 °C and 1 min at 60 °C preceded with an incubation for 2 min at 50 °C and 10 min at 95 °C. RNA levels of *hgh43* were calculated relative to *gpdII* and *18S* using the $2^{-\Delta\Delta Ct}$ method (Livak and Schmittgen 2001; Schmittgen and Livak 2008).

Arabinofuranosidase assay

An aliquot of 10 g compost harvested after the 2nd flush was mixed with 100 ml water and shaken for 1 h at 250 rpm. Compost particles were removed by centrifugation for 15 min at 4500 g, after which the extract was filter sterilized (Minisart® syringe filter, 0.45 μm), concentrated, and washed with 4 ml ultra-

pure water using Amicon Ultra-4 centrifugal filters (Merck Millipore, Billerica, USA) with a pore size of 10 kDa. Concentrated extract (150 µl) was supplemented with wheat arabinoxylan (WAX) oligomers (45 µl, 2.5 mg ml^{-1} in 20 mM NaOAc, pH 4.5) and 0.1 % azide (5 µl, 8 mg ml^{-1}). The WAX oligomers were prepared by treating WAX (medium viscosity wheat arabinoxylan, Megazyme, Ireland) with endo-xylanase (Kormelink et al. 1993). High performance anion exchange chromatography (HPAEC) was performed to analyze reaction mixtures. To this end, a Dionex ICS-5000 unit (Dionex, Sunnyvale, USA) equipped with a CarboPac PA-1 column (2 mm x 250 mm ID) was used in combination with a Carbopac guard column (2mm x 50 mm ID) and pulsed amperometric detection (PAD). Chromelion software (Thermo scientific, Sunnyvale, USA) was used to control the system. Flow rate during the 35-min elution was 0.3 ml min^{-1} using a linear gradient from 0 - 38 % 1 M NaOAc in 0.1 M NaOH. A 3 min cleaning step with 100 % 1 M NaOAc in 0.1 M NaOH and a 12 min equilibration step with 0.1 M NaOH were used in between runs. Identification and quantification of degradation products was not affected by the high baseline resulting from the presence of mono- and oligosaccharides in the compost extracts.

Analysis of neutral sugars and uronic acids

Samples were incubated for 1 h at 30 °C in 72 % (w / w) H_2SO_4, after which samples were hydrolyzed for 3 h in 1 M H_2SO_4 at 100 °C. Alditol acetate derivatives of the sugars were produced and analyzed using gas chromatography (FocusGC, Thermo Scientific, Waltham, USA) using inositol as internal standard (Englyst and Cummings 1984).

Uronic acid content was measured as anhydro-uronic acid using an automated m-hydroxydiphenyl assay (Thibault 1979) with addition of sodium tetraborate using an autoanalyzer (Skalar Analytical, Breda, The Netherlands). Glucuronic acid (12.4 to 200 µg ml^{-1} (Fluka AG, Busch, Switzerland) was used as a reference. The sum of neutral sugars and uronic acids was defined as the total carbohydrate content.

Phylogenetic analysis of arabinofuranosidases

Members of the GH43_36 subfamily (Mewis et al. 2016) were identified in 145 fungal genomes of which an evolutionary tree had been constructed based on 71 highly conserved fungal genes (Sabotič et al. 2016).

RESULTS

PHYLOGENY OF AXHD3 MEMBERS

The GH43 subfamily 36 represents fungal AXHd3 members that act on double substituted arabinoxylan (Mewis et al. 2016). The distribution of genes of this subfamily was assessed in 145 fungal genomes (Sabotič et al. 2016), of which the clade with 69 basidiomycetes is presented in Figure 3.1. The GH43_36 subfamily appears to be present in two clusters of basidiomycetes and is absent in the order Agaricales that includes *A. bisporus*. The GH43 proteins of *A. bisporus* were previously identified as GH43_5 arabinases (protein ID 224152 and 119499), GH43_13 bifunctional xylosidase / arabinofuranosidase (protein ID 211524), and a protein that is part of the uncharacterized GH43_23 subfamily (protein ID 208425) (Jurak et al. 2015c; Mewis et al. 2016).

INTRODUCTION OF AN AXHD3 GENE IN *A. bisporus*

The coding sequence of the AXHd3 gene *hgh43* of *H. insolens* was codon optimized for expression in *A. bisporus* and introduced in this basidiomycete under control of *A. bisporus* actin regulatory sequences. Expression of this gene was assessed by qPCR in MEA grown cultures of 6 transformants. As expected no *hgh43* expression was found in wild-type A15 (not shown). Transformants HGH43-1 and HGH43-2 expressed *hgh43* most highly with a 4- and 10-fold higher expression as compared to HGH43-13 when normalized to *gpdII* and *18S* (Figure 2). Strain HGH43-1 and HGH43-2 were selected for a small scale cultivation to assess carbohydrate degradation and GH43 activity in compost.

SMALL SCALE CULTIVATION OF *A. bisporus* EXPRESSING *hgh43*

A small scale *A. bisporus* cultivation was performed to assess the effect of HGH43 production in compost. To this end, PII compost was mixed with spawn of A15 wild type or strains HGH43-1 and HGH43-2. After 16 days of compost colonization, PIV was initiated by topping the compost with casing layer. Mushrooms were harvested in two flushes. Total fresh weight of mushrooms of strain A15 was 293 g kg^{-1} compost. The mushroom yield of the transformants was 80 - 100 % of that of A15.

Oligomers of wheat arabinoxylan (WAX) substituted with arabinosyl residues were incubated with compost extracts and analyzed by HPAEC (Figure 3.3 and Figure S1). Compost extract from PII-end compost (i.e. before inoculation with *A. bisporus*) completely degraded both single and double substituted WAX oligomers (Figure 3.3A, A'). Single substituted arabinoxylan oligomers (Figure 3.3, Figure S1; structure 3.2 and 4.1) were also degraded when WAX-oligomeric substrate was incubated with PIV compost extracts of A15 and its transformants (Figure 3.3B' -

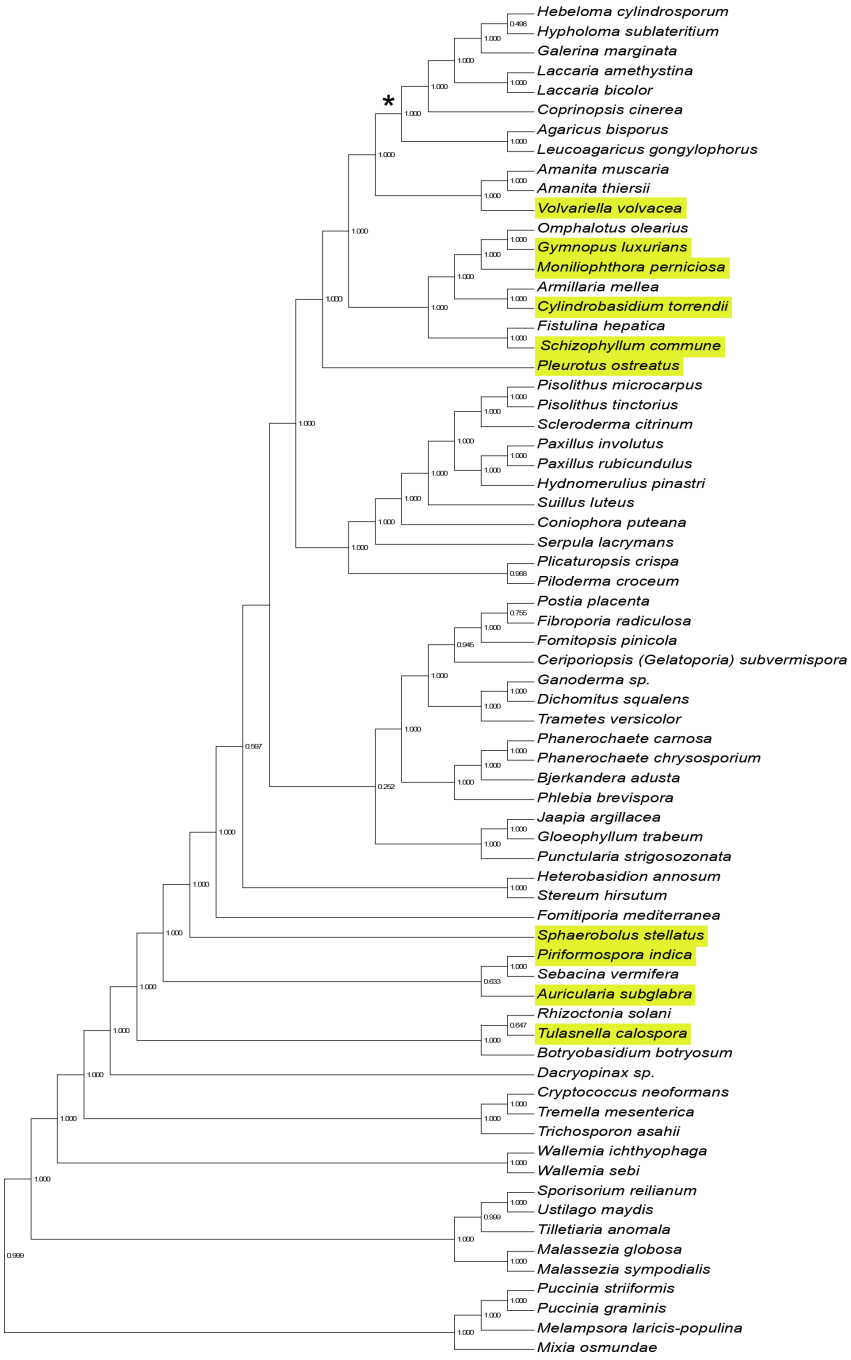

Figure 3.1: Basidiomycota branch from a phylogenetic tree of 145 fungi based on 71 highly conserved fungal genes (Sabotič et al. 2016). Presence of genes of the GH43_36 subfamily is indicated in yellow. Loss of GH43_36 in the ancestor of *A. bisporus* is indicated with an asterisk.

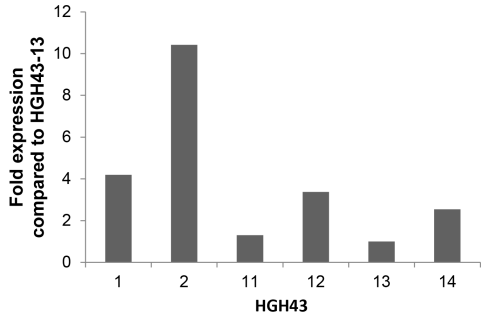

Figure 3.2: Expression of *hgh43* in *A. bisporus* transformants relative to transformant HGH43-13.

D', 13.15 and 13.30 min). In addition, these extracts degraded the multiple substituted oligomers (Figure S1; structures 6.2, 5.2, 8.1, 7.1, 10.1, 6.3, and 9.1) almost completely (Figure 3.3B - D, 18 - 24 min). The doubly substituted oligomer 5.1 decreased in abundance in WAX-oligomeric substrate treated with A15 compost extract (Figure 3.3B' - D', 15.45 min). Conversely, the double substituted oligomer 6.1 increased in abundance (Figure 3.3B', 15.15 min). In addition, an unknown oligomer with a slightly lower retention than 6.1 had accumulated (Figure 3.3B', shoulder of the 6.1 peak). Compost extract from the *hgh43* transformants was more active on the 5.1 oligomer as compared to compost extract from A15 (Figure 3.3C' - D ', 15.45 min). Furthermore, the abundance of the 6.1 oligomer and the unknown oligomer that eluted between 14.45 and 15.30 min was up to 73 % lower in the transformants as compared to A15 (Figure 3.3C'-D'; T-test, $p < 0.05$). The average area of A15, GH43-1, and HGH43-2 was 11.2, 4.5, and 3.0 nC*min, respectively, with standard deviations of 1.6, 1.7, and 0.4, respectively. Together, this shows that arabinofuranosidase active on doubly substituted xylosyl residues was produced by *hgh43* transformants and was lower or absent in the extracts of A15.

Carbohydrate compositions of PII-end compost and PIV compost were analyzed (Table 1) to assess the impact of *hgh43* expression during cultivation of *A. bisporus*. The relative abundance of glucosyl, xylosyl, and arabinosyl residues in the PII-end compost was 56.1, 30.3, and 4.3 % (mol / mol), respectively. Relative abundance of glucosyl and xylosyl (Xyl) residues had decreased to 51.3 and 26.6 % (mol / mol), respectively, while the arabinosyl (Ara) abundance had increased to 4.8 % (mol / mol) after 2 flushes of A15 mushroom production. As a consequence, the Ara / Xyl ratio had increased from 14 to 18 (mol / 100 mol) in PII-end compost and after the 2nd flush, respectively. No differences in carbohydrate composition (mol / mol %) or Ara / Xyl ratio were observed between A15 and the strains producing active AXHd3.

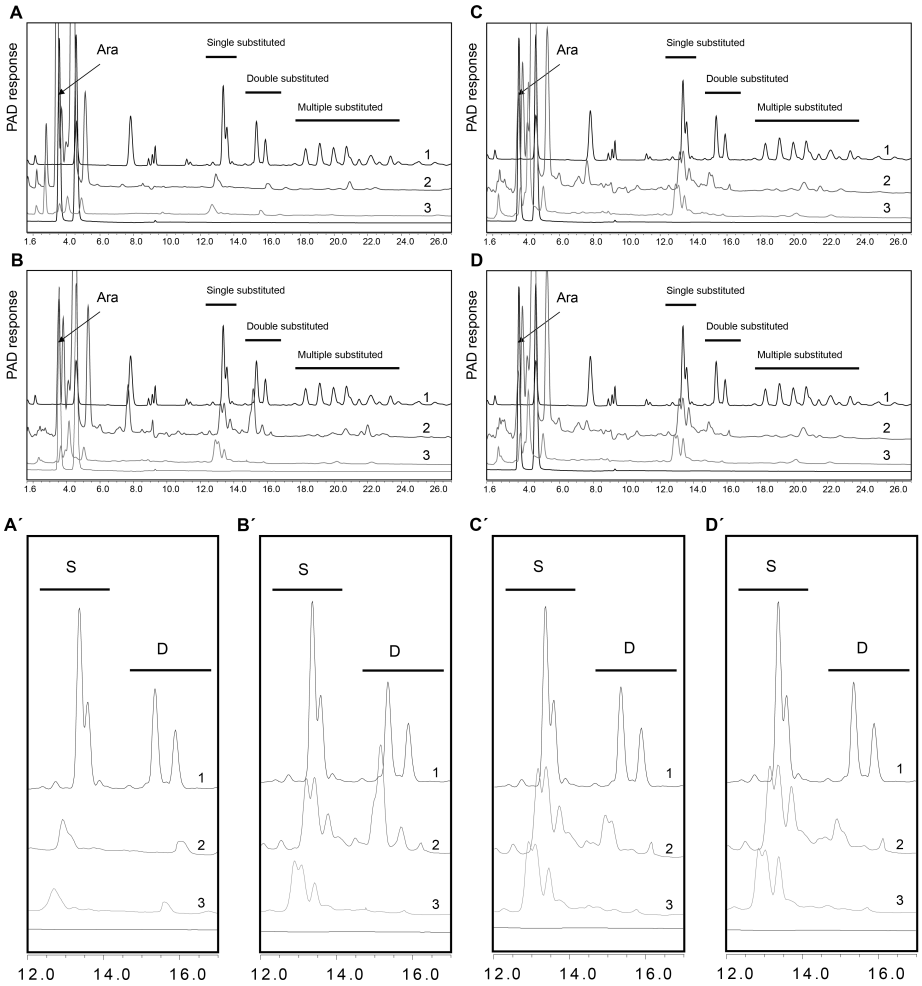

Figure 3.3: HPAEC chromatogram of endoxylanase predigested WAX incubated with concentrated compost extract of PII (A) and extract of compost colonized by A15 (B), HGH43-1 (C), and HGH43-2 (D). Endoxylanase predigested WAX without compost extracts (1), with concentrated compost extract (2), and compost extract without WAX-oligomers added (3) are shown in each panel. The line closest to the x-axis shows the retention time of arabinose and xylose at 3.5 and 4.5 min, respectively. Each sample is representative for a biological triplicate. The chromatogram is magnified from retention time 12 - 16.5 min (A', B', C', and D') for each sample where single and double substituted arabinoxylan oligomers are indicated with S and D, respectively. Chromatograms of compost extract or compost extract incubated with WAX were shifted 10 - 30 sec to the left as compared to endoxylanase predigested WAX.

Table 3.1: Carbohydrate composition (mol / mol %) of PII compost and PIV compost colonized by strains A15, HGH43-1, and HGH43-2. Averages and standard deviation (in parentheses) of biological triplicates are shown.

Compost	Rha	Man	Gal	Glc	Uronic acid	Ara	Xyl	Ara/Xyl (mol / 100 mol)
PII	0.7 (0.07)	1.6 (0.22)	1.5 (0.14)	56.1 (0.14)	5.3 (0.28)	4.3 (0.19)	30.3 (0.77)	14.1 (1.01)
PIV A15	1.1 (0.13)	6 (0.66)	2.2 (0.09)	51.3 (1.51)	7.7 (0.65)	4.8 (0.39)	26.6 (0.98)	18.1 (1.19)
PIV HGH43-1	1.2 (0.1)	6.3 (0.81)	2.5 (0.27)	50.2 (0.37)	8 (0.41)	4.9 (0.29)	26.5 (1.45)	18.8 (2.02)
PIV HGH43-2	1.2 (0.16)	6.3 (0.48)	2.3 (0.08)	51.6 (1.15)	8 (0.54)	4.9 (0.21)	25.5 (0.73)	19.2 (0.35)

DISCUSSION

Compost colonization and subsequent mushroom production by *A. bisporus* may be limited by its inability to degrade recalcitrant polysaccharides such as doubly substituted arabinoxylan (Jurak et al. 2015a; Jurak et al. 2015c). AXHd3 removes the *O*3 linked arabinosyl decorations from the xylan backbone. Phylogenetic analysis revealed that 59 out of 69 basidiomycetes did not have a predicted AXHd3 gene, among which mushroom forming basidiomycetes such as *A. bisporus*, *Coprinopsis cinerea*, and *Laccaria bicolor*. The absence of AXHd3 genes in *A. bisporus* would explain why arabinoxylan accumulates during cultivation of this mushroom forming fungus.

H. insolens colonizes compost during PII before the introduction of *A. bisporus* (Straatsma et al. 1989). The GH43 AXHd3 of *H. insolens* acts specifically on the *O*3 position of doubly substituted xylosyl residues (Sørensen et al. 2006) and would thereby be involved in removing doubly substituted arabinoxylan during this stage of composting. Indeed, arabinofuranosidase contained in PII compost extract degraded both single and double substituted arabinoxylo-oligosaccharides. Previously it was shown that double substitutions were not removed by compost extract of PIII and PIV compost (Jurak et al. 2015a). As a solution, the AXHd3 gene *hgh43* of *H. insolens* was introduced in *A. bisporus* controlled by actin regulatory elements. The pH optimum of the encoding enzyme, pH 6.7 (Sørensen et al. 2006), is close to that found in PIII and PIV compost (being 7 and 6.5, respectively). AXHd3 activity was found in PIV compost colonized by *hgh43* transformants and was low or even absent in A15 extract. Enzyme activities in compost extract from A15 were able to degrade multiple substituted arabinoxylo-oligomers. This is explained by xylanases that cleave the large oligomers into smaller single and double substituted arabinoxylo-oligomers. The small single substituted arabinoxylan oligomers were also completely degraded but not the doubly substituted oligomers. Part of the double substituted 5.1 structure disappeared by the action of A15 compost extract. This may be explained by GH51 arabinofuranosidase activity that acts on xylan with double substituted arabinose residues at the non-

reducing terminal xylose (Ferré et al. 2000; Lagaert et al. 2010; Borsenberger et al. 2014; Koutaniemi and Tenkanen 2016). *A. bisporus* contains one GH51 that is highly expressed during its vegetative growth but less active during mushroom formation (Patyshakuliyeva et al. 2015). This would agree with the lack of arabinosyl accumulation during PIII (Jurak et al. 2015a). Alternatively, structure 5.1 may (partly) disappear due to the action of a xylanase that removes the terminal non-substituted xylose from this oligomer that consists of a backbone of 3 xylose residues. This may explain the appearance of an unknown oligomer eluting slightly faster than structure 6.1 and that was formed when arabinoxylo-oligomers were incubated with compost extract from A15. Together, it is clear that compost extracts from the *hgh43* transformants are much more active in removing doubly substituted arabinoxylo-oligomers when compared to A15.

The production of AXHd3 by *A. bisporus* was expected to result in a reduction of the degree of substitution (DS) of xylan in colonized compost by removal of arabinose from double substituted arabinoxylan. Consequently, a reduction in the Ara / Xyl ratio was expected. However, no difference in carbohydrate composition or Ara DS was found in compost colonized by the HGH43 producing transformants as compared to compost colonized by A15. This may be explained by the production of too low amounts of AXHd3 or by inaccessibility of the double substituted arabinoxylan due to covalent interactions with lignin through ferulic acid. These ferulate crosslinks can protect hemicellulose from enzymatic degradation (Grabber et al. 1998; Grabber et al. 2009). Improved ligninolysis may therefore be required to benefit from AXHd3 production.

SUPPLEMENTARY DATA

Table 3.2: Primers used in this study.

Number	Name	Sequence (5' - 3')
1	Actin prmtr F	AAGCTTAGCCGAGAGAAGATGCCCC
2	Actin prmtr R	CCATGGTTTGTTATTCGTGTGTTCG
3	Actin trmntr F	GGATCCGCTGATGGTGCTTTATGATAAATAAAGTCCTTGGG
4	Actin trmntr R	GAATTCTACTACTACCCCCAAAACCGACATCATCC
5	Act-Pr_F	CCAGGGGGATCGTTAAAGCTTAGCCGAGAGAAG
6	pBHg_ActP_R	AATTAAGAATTCAGATCTCAATTGGGCGCGCCTTTGTTATTC GTGTGTTCG
7	pBHg_ActT_F	TCTGAATTCTTAATTAAGGATCCGCTGATGGTGCTTTATG
8	Act-Ter_R	CGCCGAATTGGCGCGGAATTCTACTACTACCCCC
9	HiGH43_F	AATAACAAAGGCGCGATGCTCGGACTTAAAGTTTTG
10	HiGH43_R	ATCAGCGGATCCTTAGATTGAACGGGCTGCCATG
11	APqGPD_F	TCGATCTTGTTGTTCGTCTTGAG
12	APqGPD_R	GCGCATGACCTCCTTGATTT
13	q18S_F	TCGCCGCTCCCTTGGT
14	q18S_R	GCATCGCCGGCACAA
15	qPCR_HiGH43_F	ATCGGCATGGAATTGGCAAC
16	qPCR_HiGH43_R	AGAGTTGCGCAACGTTGATG

4

H_2O_2 AS A CANDIDATE BOTTLENECK FOR MnP ACTION DURING CULTIVATION OF *Agaricus bisporus* IN COMPOST

Aurin M. Vos, Edita Jurak, Jordi F. Pelkmans, Koen Herman, Gill Pels, Johan J. Baars, Ed Hendrikx, Mirjam A. Kabel, Luis G. Lugones, Han A. B. Wösten

ABSTRACT

Degradation of lignin by fungi enhances availability of cellulose and hemicellulose in plant waste and thereby increases the amount of carbon source available to these microorganisms. The button mushroom *Agaricus bisporus* degrades only around 58 % of the total lignin in compost and a significant part of the carbohydrates remain unutilized during mushroom cultivation. Here it was assessed whether over-expression of the manganese peroxidase gene *mnp1* improves lignin degradation and, as a consequence, carbohydrate breakdown by *A. bisporus*. Transformants expressing *mnp1* under control of actin regulatory sequences produced MnP activity in malt extract medium, while the parental strain A15 did not. MnP activity was increased 0.3- and 3-fold at casing and after the 2nd flush of a semi-commercial cultivation, respectively, when compared to strain A15. Pyrolysis-GC-MS showed that overexpression of MnP decreased phenylmethane and phenylethane type lignin relative to the phenylpropane type (Ph-C1,2 / Ph-C3) after the 2nd flush. However, it neither affected the S / G ratio nor the ratio of oxidized to non-oxidized lignin residues. Moreover, the carbohydrate content and accessibility was not affected in compost. Notably, the capacity of compost extract to consume the MnP co-factor H_2O_2 was 4- to 8-fold higher than its producing capacity. This may well explain why over-expression of *mnp1* did not improve carbohydrate degradation in compost. In fact, availability of H_2O_2 may limit lignin degradation by wild-type *A. bisporus*.

INTRODUCTION

The button mushroom *Agaricus bisporus* is cultivated worldwide on straw based compost. The commercial substrate of *A. bisporus* used in the Netherlands is produced in two phases of composting. Phase I (PI) comprises a 3 - 6 day incubation of a mixture of wheat straw, horse manure, gypsum, and water, either or not supplemented with chicken manure (Gerrits 1988). Temperature increases up to 80 °C during this phase, replacing a mesophilic with a thermophilic microbiota (Gerrits 1988). Phase II starts after the microflora of a previous phase II is introduced into PI compost. The temperature is decreased to 50 °C and then increased to 60 °C in a 2-day-period changing the microflora and killing unwanted organisms like insects (Gerrits 1988; Straatsma et al. 1994). This is followed by a 3-day-period at 45 °C during which thermophilic fungi like *Scytalidium thermophilum* (also named *Humicola insolens*; Straatsma and Samson 1993) colonize the compost sequestering ammonia and suppressing competitors of *A. bisporus* (Ross and Harris 1983; Straatsma et al. 1989; Straatsma et al. 1994). During phase I and II 50 - 60 % of the carbohydrates in the compost is consumed, while lignin remains intact (Jurak 2015). The end product of phase II is relatively selective for

growth of *A. bisporus*. PII-end compost is colonized by *A. bisporus* during 16 - 19 days at 25 °C. As a result, 15 %, 10 %, and around 50 % of xylan, cellulose, and lignin is consumed, respectively in phase III (PIII) when compared to PII-end (Jurak 2015). PIII-end compost, either or not supplemented with formaldehyde-treated protein rich substrates, is topped with a casing layer. *A. bisporus* mycelium colonizes this casing layer during phase IV (PIV) under high CO_2 conditions with a relative humidity of 85 %. Mushroom formation is induced by reducing CO_2 levels, lowering the temperature to 18 - 22 °C, and increasing relative humidity to 87 - 90 % (Visscher 1988). Mushrooms are produced in 2 - 3 flushes with 7 - 8 day intervals, resulting in a typical yield of 30 kg m^{-2} per 85 - 95 kg compost m^{-2}. An additional 44 %, 29 %, and around 8 % of cellulose, xylan, and lignin is degraded, respectively, during PIV (Jurak 2015). Thus, about 20 % and 40 % of the carbohydrates are not consumed when compared to the starting material and PII-end, respectively (Iiyama et al. 1994; Chen et al. 2000a; Jurak 2015).

Lignin is a cohesive of cellulose microfibrils and forms covalent interactions with hemicellulose (Boerjan et al. 2003). Consequently, enzymatic degradation of these carbohydrates is hampered. It has been estimated that lignin removal makes 30 % of the carbohydrates available for consumption by *A. bisporus* (ten Have et al. 2003). Lignin consists of the monolignol monomers *p*-coumaryl alcohol, coniferyl alcohol, and sinapyl alcohol (Boerjan et al. 2003; Vanholme et al. 2010) that form *p*-hydroxyphenyl (H), guaiacyl (G), and syringyl (S) phenylpropanoid units within lignin, respectively. Lignin has a heterogeneous and recalcitrant structure that, unlike cellulose and hemicellulose, cannot be degraded by enzymes directly. Therefore, fungi produce lignin peroxidase (LiP), manganese peroxidase (MnP), and versatile peroxidase (VP) that generate extracellular radicals (Kirk and Farrell 1987; Hatakka 1994; ten Have and Teunissen 2001; Guillén et al. 2005). Laccase (Lac) has also been implicated in ligninolysis but its role is less clear (Eggert et al. 1996; 1997; Li et al. 2001).

A. bisporus contains two *mnp* genes and 13 *lac* genes in its genome (Morin et al. 2012). MnP acts on lignin using Mn^{2+} and (organic) hydrogen peroxide (H_2O_2 or R-OOH) as cofactors (Hofrichter 2002). H_2O_2 oxidizes the heme group in MnP to form compound I. Compound I oxidizes Mn^{2+} or a phenolic compound to generate compound II that subsequently oxidizes another Mn^{2+} to return the MnP to its original oxidation state. Oxalic acid chelates the generated Mn^{3+}, which stimulates its release from MnP and increases its stability. MnP is able to oxidize both phenolic and non-phenolic lignin model structures. For the latter, other mediators like unsaturated lipids are required to initiate extracellular lipid peroxidation that results in highly reactive compounds. MnP and Lac are highly produced during the vegetative colonization of compost but are downregulated

upon mushroom formation (Wood and Goodenough 1977; Bonnen et al. 1994). Manganese peroxidase MnP1 but not MnP2 has been characterized (Bonnen et al. 1994; Lankinen et al. 2001).

Xylan substituted with arabinose and glucuronic acid accumulates in compost (Jurak et al. 2015a; Jurak et al. 2015c). Expression of arabinofuranosidase from *H. insolens* in *A. bisporus* did not result in increased degradation of arabinose substituents (Chapter 3). This may be due to linkage of this pentose to lignin through ester bonds with ferulic acid. Here, *mnp1* of *A. bisporus* was overexpressed with the aim to improve ligninolytic activity, thereby increasing degradation of hemicellulose and cellulose in compost. Overexpression of *mnp1* increased MnP activity in compost but neither affected lignin content nor carbohydrate content and accessibility. Experimental evidence indicates that this is due to a limiting availability of H_2O_2 as a cofactor.

Material and Methods

Culture conditions and strains

A. bisporus strains were grown at 25 °C on malt extract agar medium (MEA; 20 g l^{-1} malt extract [BD biosciences, Franklin Lakes, USA], 2.1 g l^{-1} MOPS, pH 7.0, and 1.5 % agar), wheat bran (WB; 4 % wheat bran (w / w) in water), or PII-end compost (CNC Grondstoffen, Milsbeek, the Netherlands). Spawn was produced using a mixture of 24 g kg^{-1} $CaSO_4$, 6.87 g kg^{-1} $CaCO_3$, and 75 g *Sorghum* seeds. The seeds had been heated in water at 100 °C for 20 min followed by sterilization for 20 min at 121 °C. The mixture was colonized for 3 weeks at 25 °C using 2 1-week-old MEA-grown *A. bisporus* colonies as inoculum. End phase II compost was colonized in 18 boxes per strain (40 cm width x 60 cm length x 22 cm height) containing 16 kg phase 2 compost (CNC, Milsbeek, The Netherlands) each inoculated with 75 g of spawn. Temperature was maintained at 25 °C using an air temperature of 22 °C. Relative humidity in the growth cell was kept at 95 % with 1500-2000 ppm CO_2. Boxes that had been randomly distributed in the growth cell (Unifarm, Wageningen) were overlaid with 7 kg casing layer (CNC, Milsbeek, The Netherlands) after 16 days, after which growth was prolonged for 14 days. The casing was manually broken and mixed to create fast regenerative growth and a more equal distribution of *A. bisporus* in the casing layer 4 days prior to venting (i.e. 10 days after casing). Venting resulted in a gradual decrease of compost and air temperature to 19 and 18 °C, respectively, while relative humidity and CO_2 levels decreased to 85 % and 1200 ppm. The first buttons were removed from the bed 9 days after venting. Compost from 4 boxes of each strain was collected at casing (day 15), venting (day 30), and after the 2^{nd} flush (day 56). After removing the casing, compost was mixed manually for 3 min, after which samples were

frozen in liquid nitrogen and stored at -20 °C.

TRANSFORMATION OF *A. bisporus*

The coding sequence of *mnp1* (gene ID 221245) was synthesized at Genscript (Nanjing, China) with its ApaI, BsaI, MfeI, BclI, NcoI, EcoRI, and BclI restriction sites removed (Table 4.5) without altering the amino acid sequence (Table 4.6). The actin promoter and terminator were amplified from genomic DNA of *A. bisporus* A15 using Taq polymerase and primers 1 & 2 and 3 & 4, respectively (Table 4.3). Fragments were cloned in pUC20 using HindIII / NcoI, and BamHI / EcoRI, respectively. The *mnp1* coding sequence was cloned in between the actin regulatory elements using NcoI and BamHI. The *mnp1* coding sequence flanked by the actin regulatory elements was amplified using Phusion Hot Start II High-Fidelity DNA polymerase (Thermo Fisher Scientific, Waltham, USA) and primers 5 & 6 (Table 4.3). The PCR product was cloned in pBHgPA digested with PacI and SgsI using InFusion cloning (Pelkmans et al. 2016). The resulting plasmid pBHg-221245-ActPT was introduced in *A. bisporus* A15 gills using *Agrobacterium tumefaciens* strain AGL-1 (Chen et al. 2000b). Transformants were screened on MEA plates containing 25 μg ml^{-1} hygromycin, 200 µM cefotaxime, and 100 µg ml^{-1} chloramphenicol, and transferred to a second selection plate containing 40 µg ml^{-1} hygromycin.

LACCASE AND MANGANESE PEROXIDASE ACTIVITY

Compost samples were taken up in 10 volumes demi water and shaken at 250 rpm at 25 °C for 1 h. The extract was separated from insoluble particles at 15000 g for 15 min. Lac activity was determined by mixing 10 - 100 µl 5 times diluted compost extract with 1 mM ABTS in 1 ml citric phosphate buffer pH 4. Change in absorbance at 420 nm was followed for 30 sec. MnP activity was measured via the oxidative coupling of 3-methyl-2-benzothiazolinone hydrazone (MBTH) and (3-dimethylamino)benzoic acid (DMAB) (Castillo et al. 1994). The reaction mix contained 0.07 mM MBTH, 0.99 mM DMAB, 0.1 mM $MnSO_4$, 0.05 mM H_2O_2, and 100 mM succunic-lactate buffer pH 5. The reaction was followed for 30 sec at 590 nm. Compost extract was diluted to obtain changes in OD < 0.3 (usually 5 times diluted extract was used). The Mn^{2+} independent activity was obtained by adding 1 mM EDTA. MnP activity was defined as the difference in OD change over time in the presence and absence of EDTA. Lac and MnP activities were expressed in units (U) using the law of Lambert-Beer with an extinction coefficient of 36000 M^{-1} cm^{-1} and 53000 M^{-1} cm^{-1}, respectively.

CHITIN ASSAY

N-acetylglucosamine (GlcNAc) release from chitin was determined as described (Chapter 2). In short, homogenized lyophilized compost (see below) was treated with KOH, followed by an incubation with chitinase and lyticase. OD585 was converted to [GlcNAc] using a reference line of 0 - 300 μM GlcNAc.

LIGNIN ANALYSIS WITH PYROLYSIS-GC-MS

Lyophilized compost (15 g) was ground using a mortar and homogenized using a Tissuelyser at 30 Hz for 1 min (Qiagen Tissuelyser II and grinding jar). Technical triplicates of 60 - 70 μg and 100 - 107 μg compost were used for pyrolysis of wheat straw and PII, and PIII and PIV samples, respectively. Samples were pyrolyzed at 500 °C for 1 min with helium as carrier gas using a 2020 microfurnace pyrolyzer (Frontier Laboratories, New Ulm, MN, USA) with an AS 1020E Autoshot GC-MS, using a Trace GC with a DB1701 fused-silica capillary column coupled to a DSQ-II (El at 70 eV). Amdis software was used to characterize peaks in the GC-MS chromatogram. Molar areas were calculated by dividing areas by the molecular weight of the corresponding molecule (Jurak et al. 2015c).

TOTAL CARBOHYDRATE CONTENT AND COMPOSITION

Composition and content of neutral carbohydrates in homogenized compost samples (see above) was determined in technical duplicates using gas chromatography with inositol as an internal standard (Englyst et al. 1982). Glucose, arabinose, rhamnose, xylose, galactose and mannose were used as standards (1 mg). Samples were hydrolyzed with 1M H_2SO_4 for 3 h at 100 °C after treatment with 72 % (w / w) H_2SO_4 for 1 h at 30 °C. Sugar monomers were derivatized to their alditol acetates by reducing the sugars with sodium borohydride followed by acetylation of the formed alditols and analysed using a Focus-GC (Thermo Scientific, Waltham, MA, USA). Uronic acid content was determined as the anhydro-uronic acid content using a m-hydroxydiphenyl assay in which $Na_2B_4O_7$ was added. Analysis was performed using an autoanalyser (Skalar Analytical, Breda, The Netherlands) with 12.5 - 100 μg ml^{-1} glucuronic acid as a standard (Thibault 1979). Total carbohydrate content was calculated as the sum of the neutral carbohydrate and uronic acid content.

SACCHARIFICATION AND MONOSACCHARIDE QUANTIFICATION

Technical duplicates of 250 mg homogenized compost samples (see above) were wetted using a vortex mixer in 9.75 ml 50 mM NaOAc buffer (pH 5) containing 0.25 mg ml^{-1} NaN_3. Samples were heated at 100 °C for 10 min, followed by addition of 0.25 ml of a mix of cellulases and hemicellulases (Cellic Ctec2, 2.7 % w / w of DM and Cellic Htec, 0.3 % w / w of DM). The enzyme preparations were kindly

provided by Novozymes (Bagsvaerd, Denmark). After rotation head over tail for 24 h at 50 °C, samples were heated at 100 °C for 10 min. Insoluble particles were removed by centrifugation at 20 °C for 10 min at 10000 g. As a control, samples were incubated without enzymes. Content of monosaccharides was analysed by high performance anion exchange chromatography (HPAEC) using a Dionex ICS-5000 unit (Dionex, Sunnyvale, CA, USA) equipped with a CarboPac PA-1 column (2 mm x 250 mm ID) in combination with a Carbopac guard column (2 mm x 50 mm ID) and pulsed amperometric detection (PAD). Chromelion software (Thermo scientific, Sunnyvale, CA, USA) was used to control the system. Elution was performed with a flow rate of 0.4 ml^{-1} min as follows: 40 min 100 % H_2O; 5 min from 100 % 1 M NaOH to 100 % 1 M NaOAc; 5 min 100 % 1M NaOAc; 8 min with 100 % H_2O; followed by elution for 15 min at 0.1 ml min^{-1} using 0.5 M NaOH. Monosaccharides were detected and quantified during the first 40 min and the last 15 min of elution. Calibration curves of 12.5 - 100 μg ml^{-1} rhamnose, galactose, glucose, xylose and mannose were used as a reference.

Hydrogen peroxide consumption and production

The H_2O_2 consuming and producing capacity were measured in compost extract using a Hydrogen Peroxide Assay Kit (BioVision Inc.). The de novo H_2O_2 production in compost extract was calculated using measurements 8, 13, 18, 23, and 28 min after addition of HRP and OxiRed. In order to determine H_2O_2 consumption in compost the compost extract was supplemented with 10 µM H_2O_2. The H_2O_2 consumption was calculated based on the remaining H_2O_2 in compost extract after incubation at room temperature for 10, 20, 30 and 40 min and corrected for H_2O_2 production. One reaction of 100 µl contained 25 µl compost extract, 25 µl 40 µM H_2O_2 and 50 µl reaction mix containing 0.4 µl HRP and 0.2 µl OxiRed. A standard curve of 0 - 12.8 µM H_2O_2 was used to calculate the H_2O_2 producing and consuming capacity in nmol min^{-1} g^{-1} compost.

Data analysis

Differences between strains and temporal changes in the H_2O_2 producing and consuming capacity were assessed with a T-test using SPSS 22. Temporal changes in other variables were assessed using ANOVA followed by a Bonferroni or Dunnett's T3 post hoc correction. Ratios of S / G, Ox / non-Ox, and Ph-1,2 / Ph-3 were log transformed prior to testing. Statistical significance is indicated with * ($p < 0.05$), ** ($p < 0.01$), and *** ($p < 0.001$).

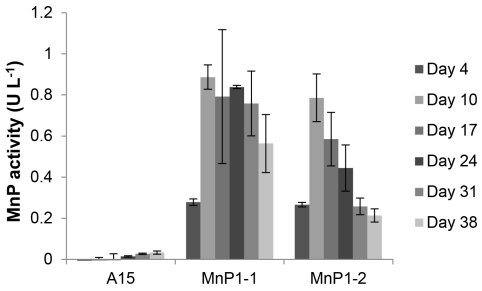

Figure 4.1: MnP activity of A15, MnP1-1, and MnP1-2 in malt extract. Error bars indicate standard deviation of biological triplicates.

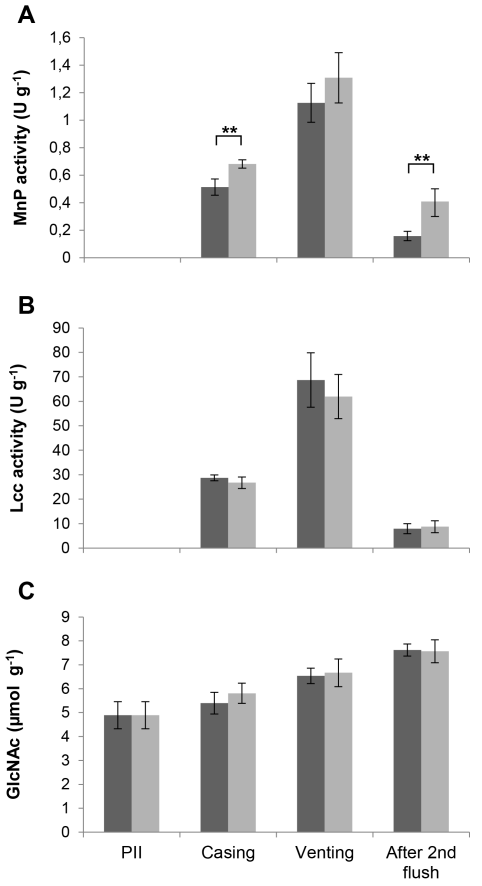

Figure 4.2: MnP (A) and Lcc (B) activity and GlcNAc release (C) in a semi-commercial cultivation of A15 (dark grey shading) and the MnP overexpressor MnP1-1 (light grey shading). Significant differences between A15 and MnP1-1 at each time point are indicated. Significant differences between time points are presented in Table 4.4. Error bars represent standard deviation of biological quadruplicates.

RESULTS

Manganese peroxidase gene *mnp1* of *A. bisporus* that was cloned in between the actin regulatory sequences was introduced in *A. bisporus*. No MnP activity was detected after growth of the wild type strain A15 in ME. In contrast, transformants MnP1-1 and MnP1-2 produced 0.9 and 0.8 U l^{-1} MnP activity after 17 days of growth, respectively (Figure 4.1). A semi-commercial cultivation was performed with strain A15 and MnP1-1. MnP activity g^{-1} wet compost was increased 0.30- and 3-fold at casing (day 15) and the 2nd flush (day 56), respectively (Figure 4.2A). Lac activity (Figure 4.2B) and chitin content (Figure 4.2C) of strain A15 and MnP1-1 was similar throughout the cultivation. Moreover, MnP overexpression did neither affect flush pattern nor mushroom yield (not shown). Pyrolysis-GC/MS showed that the ratio of syringyl to guaiacyl derived residues (S / G) had increased from 0.38 (PII-end) to 0.47 and 0.48 (venting) in compost colonized by A15 and MnP1-1 until venting, respectively (Table 4.1, Figure 4.3). After the 2nd flush the S / G ratio had dropped to 0.43 in compost colonized by A15 or MnP1-1. The relative abundance of oxidized to non-oxidized lignin derived residues (Ox / non-Ox) in compost colonized by A15 was 0.28, 0.47, 0.72, and 0.93 at PII, casing, venting, and after the 2nd flush, respectively. These ratios were similar in compost colonized by MnP1-1. The relative abundance of lignin derived residues of the phenylmethane and phenylethane type relative to those of the phenylpropane type (Ph-C1,2 / Ph-C3, Del Rió et al. 2001) decreased in compost colonized by A15 from 5.46 (PII-end compost) to 4.17 (venting). After the 2nd flush, Ph-C1,2 / Ph-C3 had increased to 4.53, a similar value to casing. In compost colonized by MnP1-1, Ph-C1,2 / Ph-C3 decreased similarly to A15. However, after the 2nd flush Ph-C1,2 / Ph-C3 of compost colonized by MnP1-1 had not increased and differed significantly from the Ph-C1,2 / Ph-C3 after the 2nd flush of A15 (T-test after log transformation, $p < 0.05$ after Bonferroni correction). A total of 30 - 35 % of the lignin was removed after the 2nd flush based on the pyrolysis area and Klason lignin content. No differences in lignin content were found between A15 and MnP1-1 throughout the cultivation (not shown). Moreover, carbohydrate accessibility and composition were similar. Hydrolysis of the carbohydrates in the compost showed that total carbohydrate content (w / w %) decreased by about 50 % from PII-end to the 2nd flush in case of A15 and MnP1-1 (Table 4.2). Moreover, glucose and xylose release after incubating compost with cellulases and hemicellulases was similar between A15 and MnP1-1 (Figure 4.4).

The consuming and producing capacity of the MnP co-factor H_2O_2 in compost extract was monitored during cultivation of A15 and MnP1-1 (Figure 4.5). The H_2O_2 consuming capacity in compost extract of A15 was 32 and 8 nmol min^{-1} g^{-1} wet compost at casing and after the 2nd flush, respectively. The H_2O_2 consuming

Table 4.1: S/G, Ox/non-Ox, and Ph-C1,2/Ph-C3 ratios in compost colonized by strain A15 or MnP1-1. Each value represents the average of 4 biological replicas except for PII-end which represents 3 replicas and standard deviations are shown in brackets. Means of each ratio that share a letter (A, B or C) are not significantly different (ANOVA after log transformation). Differences between A15 and MnP1-1 are indicated with an asterisk (T-test, Bonferroni correction, $p < 0.01$).

	A15			MnP1-1		
	S / G[a]	Ox / Non-ox[b]	Ph1,2 / Ph3[b]	S / G[b]	Ox / Non-ox[b]	Ph1,2 / Ph3[b]
PII-end	0.38 (0.028) AB	0.29 (0.01) A	5.46 (0.153) A	0.38 (0.028) A	0.29 (0.01) A	5.46 (0.153) A
Casing	0.45 (0.024) AB	0.47 (0.038) B	4.68 (0.074) B	0.46 (0.019) BC	0.49 (0.033) B	4.59 (0.202) B
Venting	0.48 (0.002) A	0.73 (0.013) C	4.17 (0.04) C	0.48 (0.013) B	0.73 (0.023) C	4.15 (0.088) C
2nd flush	0.44 (0.005) B	0.94 (0.023) D	4.53 (0.046) B*	0.43 (0.017) C	0.97 (0.026) D	4.35 (0.053) BC*

a: ANOVA with Dunnett's T3 post hoc test; b: ANOVA with Bonferroni post hoc test.

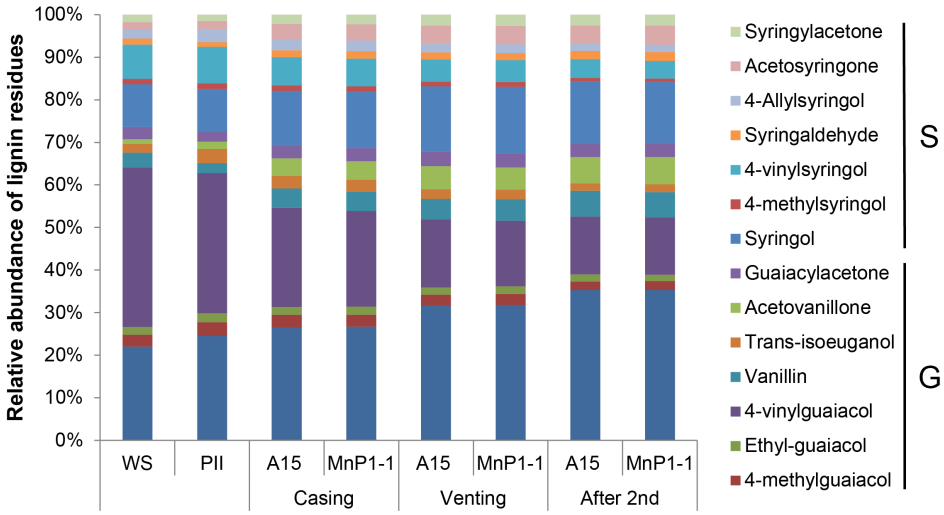

Figure 4.3: Relative abundance of lignin derived residues as measured by pyrolysis-GC/MS in compost samples of a semi-commercial cultivation of A15 and the MnP overexpressor MnP1-1. Each compost sample represents the average of biological quadruplicates. Error bars have been left out for clarity, all values are available in Table 4.7. WS = wheat straw, PII = compost from end of phase II.

capacity in compost extract of MnP1-1 was similar at casing but was 2-fold higher with 17.5 nmol min^{-1} g^{-1} wet compost after the 2nd flush. The H_2O_2 producing capacity in compost extract at casing and after the 2nd flush was 3.6 and 1.85 nmol min^{-1} g^{-1} wet compost, respectively, for A15. After the 2nd flush the H_2O_2 producing capacity in extract from MnP1-1 was higher with 1.99 nmol min^{-1} g^{-1} wet compost. The H_2O_2 consuming capacity in compost extract was always 4 - 8 times higher than the capacity for H_2O_2 production. Together, this strongly indicates that co-factor H_2O_2 is limiting MnP activity in compost of both A15 and the over-expression strain MnP1-1.

DISCUSSION

A significant fraction of carbohydrates is not utilized by *A. bisporus* during colonization and mushroom production (Iiyama et al. 1994; Chen et al. 2000a; Jurak 2015). This may in part be explained by limited degradation of lignin that makes the carbohydrates inaccessible to enzymatic degradation (ten Have et al. 2003). *A. bisporus* removes around 50 % of the lignin originally present in compost in PIII, while an additional 8 % is removed during PIV (Jurak 2015). This correlates with a decreased MnP activity during mushroom production when compared to vegetative growth in PIII (Bonnen et al. 1994). Here, the *mnp1* gene was over-expressed using actin regulatory sequences with the aim to increase MnP activity during vegetative growth and mushroom production thus increasing lignin degradation, and, as a consequence, carbohydrate utilization by *A. bisporus*. Transformants MnP1-1 and MnP1-2 produced MnP activity in malt extract, while strain A15 did not. Moreover, MnP was overproduced 3 - 4 fold in wheat bran (data not shown) and a 40 % increase in compost was observed in transformants MnP1-1 and MnP1-2 relative to A15 in a small scale cultivation (data not shown).

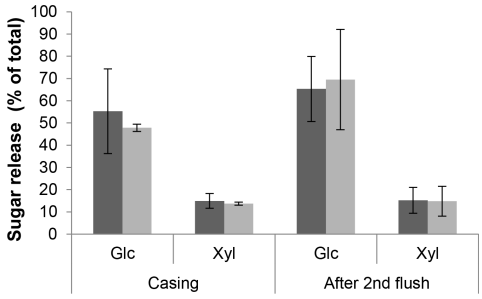

Figure 4.4: Glucose (Glc) and xylose (Xyl) release after treating compost at casing and after the 2nd flush with cellulases and hemicellulases. Monosaccharide release is expressed as a percentage of the total corresponding carbohydrate. Error bars represent standard deviations based on four biological replicas.

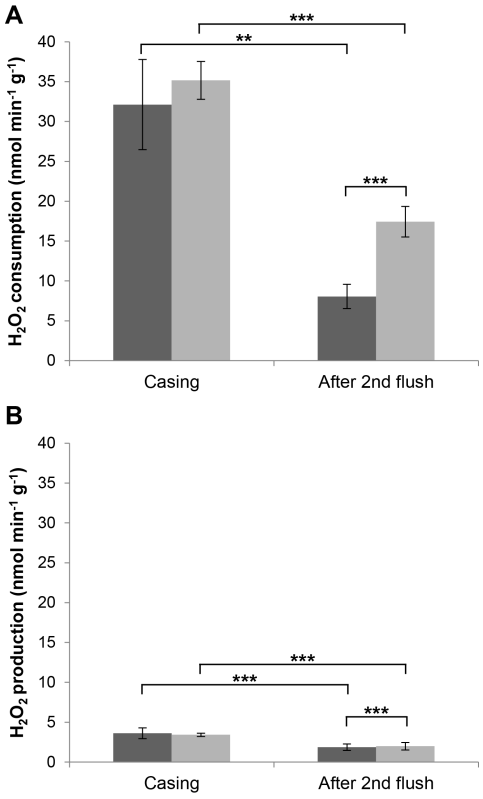

Figure 4.5: H_2O_2 consuming and producing capacity in compost extract from a semi-commercial cultivation of A15 (dark shading) and MnP1-1 (light shading). Statistical difference between the time points and between A15 and MnP1-1 are indicated. Error bars represent standard deviations based on biological quadruplicates.

MnP activity was increased 0.3- and 3-fold at casing and 2nd flush, respectively, in a large scale cultivation of A15 and MnP1-1, respectively. However, no major changes in lignin content and composition were observed during cultivation of these two strains. The S / G ratio increased from 0.38 in PII-end compost to 0.47 at venting where after it decreased to 0.43 at the end of the 2nd flush. This pattern agrees with previous reports (Zeng et al. 2011; Jurak et al. 2015b; Patyshakuliyeva et al. 2015). However, ligninolytic activity in other systems has been associated uniquely with a decrease of the S / G ratio (Camarero et al. 2001; Martınez et al. 2001; Vane et al. 2001a; Vane et al. 2001b; Del Rio et al. 2002; Geib et al. 2008). It is assumed that a higher redox potential and condensation degree makes G lignin more recalcitrant than S lignin. From this perspective, ligninolytic action should result in a decrease of the S / G ratio. In the case of *A. bisporus* the increase in the S / G ratio during casing and venting may relate to a part of the G lignin that is solubilized during PI, PII and / or PIII. This is supported by the observation that the S / G ratio of lignin in water insoluble compost particles at the end of PIII is similar to that of PI, i.e. lower than the S / G ratio in the total PIII sample (Jurak et al. 2015b). The Ox / non-Ox ratio increased throughout the cultivation from 0.28 in PII-end compost to 0.93 at the end of the 2nd flush and the Ph-C1,2 / Ph-C3 ratio decreased from 5.46 in PII-end compost to 4.17 at venting. The changes in S / G, increase in Ox / non-Ox, and decrease in Ph-C1,2 / Ph-C3 after venting show that lignin is modified during PIV. The direction of change of the S / G and Ph-C1,2 / Ph-C3 ratio reverted after venting (i.e. a decrease in S / G after venting as compared to an increase during PIII and an increase in Ph-C1,2 / Ph-C3 as compared to a decrease during PIII). From this it is concluded that A. bisporus affects lignin differently in PIV as compared to PIII, specifically during mushroom formation. This fits with the induction of cellulases and hemicellulases and downregulation of the ligninolytic machinery during fruiting (Wood and Goodenough 1977; Bonnen et al. 1994; Patyshakuliyeva et al. 2015). Notably, the Ph-C1,2 / Ph-C3 ratio had increased after the 2nd flush for compost colonized by A15 but not for compost colonized by MnP1-1. This may be explained by an increased loss of Ph-C1 and Ph-C2 residues as compared to A15 or a higher turnover of Ph-C3 to Ph-C1 and Ph-C2. However, this did not result in detectable differences in carbohydrate composition or accessibility. In contrast, overexpression of a VP in *P. ostreatus* increased the mineralization of lignin and carbohydrate digestibility in cotton stalk (Salame et al. 2012). This illustrates that in other systems ligninolytic action can be improved by overexpression of lignin-modifying enzymes.

The most important co-factors of MnPs are H_2O_2 and Mn^{2+}. High Mn^{2+} concentration in PIV compost has a positive effect on mushroom yield (Weil et al. 2006). However, Mn^{2+} is not considered a limiting micronutrient in Dutch com-

Table 4.2: Carbohydrate composition, degree of substitution, and total carbohydrate content of compost colonized by A15 or strain MnP1-1. Standard deviation is shown in parentheses.

Strain	Sample	Carbohydrates (mol %)[b]							Degree of substitution		w / w %[c]
		Rha[a]	Ara	Xyl	Man[d]	Gal	Glc[e]	UA	Ara/Xyl	UA/Xyl	Total
	WS	0.5 (0.3)	5.2 (0.2)	38.2 (1)	0.6 (0.1)	1.4 (0.1)	50.0 (1)	3.9 (0.6)	13.7 (0.3)	10.2 (1.7)	60.2 (1.4)
	PII-end	0.6 (0.2)	4.4 (0.1)	32.7 (1.7)	1.7 (0)	1.5 (0.1)	53.8 (3.4)	5.3 (2.2)	13.5 (0.6)	15.9 (6.1)	30.9 (3.6)
A15	**Casing**	0.7 (0.2)	4.4 (0.3)	32.3 (2.4)	3.1 (0.3)	1.7 (0.2)	50.9 (4.1)	6.9 (1.3)	13.7 (0.7)	21.1 (2.7)	21.8 (4.1)
	Venting	0.5 (0.1)	4.7 (0.5)	30.1 (3)	10.5 (9.3)	1.8 (0.5)	44.3 (9.5)	8.1 (2)	15.6 (2.8)	27.4 (8.2)	21.3 (4)
	After 2nd flush	0.9 (0.2)	6.3 (0.3)	26.4 (1.6)	10.1 (5.6)	2.5 (1.3)	41.7 (4.9)	12.0 (2)	24.1 (2.4)	45.8 (9.4)	12.0 (1.1)
MnP1-1	**Casing**	0.6 (0.1)	4.3 (0.2)	31.5 (1.2)	3.1 (0.6)	1.6 (0.1)	52.4 (1.4)	6.5 (1.1)	13.7 (1.1)	20.7 (2.9)	24.1 (1.5)
	Venting	0.7 (0.3)	4.4 (0.6)	28.6 (5.5)	13.6 (12)	1.6 (0.2)	43.7 (10.3)	7.4 (1.5)	15.7 (3.4)	27.2 (10.6)	25.2 (4.6)
	After 2nd flush	1.1 (0.3)	5.8 (0.1)	24.5 (2)	10.9 (6.2)	2.6 (0.7)	44.0 (5.6)	11.1 (1.9)	23.9 (1.9)	45.8 (11.1)	13.0 (0.7)

a: Rha = rhamnosyl, Ara= arabinosyl, Xyl= xylosyl, Man= mannosyl, Gal= galactosyl, Glc= glucosyl, UA= uronyl residues
b: Ratio mol/100 mol
c: Based on dry matter
d: Not corrected for mannitol
e: Not corrected for sorbitol and trehalose

post (CNC Grondstoffen and Walkro Compost, personal communication; Burton 2016). Furthermore, MnP overexpressor MnP1-1 did not affect lignin differently during its vegetative growth compared to A15 in compost supplemented with Mn^{2+} (data not shown). We did show that H_2O_2 consumption in compost extract of A15 and Mnp1-1 was 4 - 8 fold larger than its production, implying that this co-factor is limiting for MnP activity and thus explaining why over-expression of *mnp1* does not impact lignin and carbohydrate utilization. H_2O_2 as a limiting factor for ligninolytic activity has also been found in *Phanerochaete chrysosporium* (Buswell et al. 1984; Kirk et al. 1986). This makes H_2O_2 generation a target for optimizing lignin removal from compost in *A. bisporus* and, consequently, improving carbohydrate consumption of this mushroom forming fungus.

SUPPLEMENTAL MATERIAL

Table 4.3: Primers used in this study.

Primer	Primer name	Sequence
1	Actin prmtr F	AAGCTTAGCCGAGAGAAGATGCCCC
2	Actin prmtr R	CCATGGTTTGTTATTCGTGTGTTCG
3	Actin trmntr F	GGATCCGCTGATGGTGCTTTATGATAAATAAAGTCCTTGGG
4	Actin trmntr R	GAATTCTACTACTACCCCCAAAACCGACATCATCC
5	Act-Pr_F_infu	CCAGGGGGATCGTTAAAGCTTAGCCGAGAGAAG
6	Act-Ter_R_infu	CGCCGAATTGGCGCGGAATTCTACTACTACCCCC

Table 4.4: Statistical differences over time in MnP and Lcc activity and chitin content in compost as presented in Figure 4.2. Time points sharing a letter are not significantly different (ANOVA with Bonferroni post hoc test, $p < 0.05$).

	A15			MnP1-1		
	MnP	**Lcc**	**Chitin**	**MnP**	**Lcc**	**Chitin**
PII	-	-	A	-	-	A
Casing	A	A	AB	A	A	AB
Venting	B	B	BC	B	B	BC
After 2nd flush	C	C	C	C	C	C

Table 4.5: Supplemental sequence 1

CCATGGCTTTCAAAATTCTTCTCAGCCTTATTTTGGCTTTGAACGCCGTCCAATTTATTGCTGGTACGCACTTTACTC
ATATCCTCATATTATTTGCCGACAAGTCAACGATGTAGCTGTTCCTACCAGGAGGGCGCAATGTGCCGATGGCACCAC
TGTTTCTAATGAGGCCTGTTGCGTTCTGCTCCCCATTATAGCAGATATCCAGCCGAACTTGTTCGAAAACGAGTGCGG
TGAAGAGGTAATGATTTAATTTTTTGATAGAGTTACGATATTCAACAGCATATTTATACTTTAGGTCCATGAAACCTTGC
GGGCATCATTTCATGATGCTATCGGATTCTCCAGAGCAGCTGGGTAGGTTCTGACTGTCTGTGGCGGCAGCTAGTATC
GCTAAAATGATTTCCAGTGGTGGTGGTGCTGATGGTTCTCTCGTCACTTTCGGCGATGTGGAGACGACATTTGCCGC
TAACGCAGGAATCGACGAGATTGTAGAGACATTACGACCTTTTATAAACAGCCACAACATCAGTGCCGGCGATTTGTG
AGCCTGGACTCATAATCTGTGTTGCATCCTGTTAACGCTCTTCCTAGCATCCAGTTTGCAACCGTTGTTGGATTGACC
AACTGCCCCGGCGCACCTCGCATACCCTTTTTCTTAGGCCGCCCAGACGCTACCGCCGCTTCCCCCGATGGTCTTGT
CCCTGAGCCCTTCGGTCAGTCTCTCATCAGCCTTTCCGGTATAATCTACAACCCAAGTTGATAATCAACAGATTCCGT
CACGAAAATTCTTGAACGCTTCGATGATGCTGGTTTTACCCCCACTGAAGTTGTTGCATTGCTTGCATCGTGAGTCTC
TAGAACAAGATCGAGAAATATGTGTCCAATCCCCCCGTAGTCATACTGTCGCAGCTTCGGACACTATTGAGCCCGGTG
TAAGTTTATTTCTTCGTCAGTATGCATTCTCATCTCATGAGCACCTTATTCCAGCTCGAAGGGTAAGACATTCCCTATC
AATAAGAAACGTCTCAGTATCCAACGCAACCTCTAGTGTCCCCTTCGACTCGACTCCCGGAGAATTTGACAGGCAGT
TCTTTATCGAGACTATGCTTAAAGGCACTTCCTTCCCAGGGTAAGTAGTTCGTTGACATTCGTTACGCATCCTAATTT
TGGCAAAGCACTGGGGGGAACCAAGGTGAAGCCTTATCTCCCTTGCCGGGAGAACTTCGTCTCGAATCCGATGGACT
TGTACGTATACAGTCTTTTGTTGTCTGAATTTGTGATTGTTAACATTATTTATCATTAGTTGGCTCGAGGTCTGTCTTG
CTAACAAAAGGCATCTGATAACATTGAAGGACTAACTTCATCATAGATGAACGAACCGCATGTGACTGGCAACTCTTC
GCTAGTAAGAATGTTTGCCAACCAAGAAGAATAGCTCACCTAAAATTCCACGATAGCAGATCAACAAAAAATGGCATC
GGCATTTAGCGACGCGATGGTCAAACTGTCTCTCGTCGGGCAAGATAAGAGCCAGTTGATTGATTGTTCAGACGTCAT
TCCGCGAACGATCCCTTTGACAAATGAACCATACTTCCCTGCCGACTTGACCAAAGATGATCTTGAGCAGACCGTGAG
TCCAATAGACATTCACAATACGATTTCCACTCTGAGCCTGCTTGTTTTTGATACAGTGCCCGGATGAATTTCCTGATT
ACCCTTCCAACCCCAGTGTCACTTCGGTCGCGCCAGTGTAAGTTTATGAACAGCTCCAGACGTCTGCTCTTATTCAC
TCTGCGCAAATATCTAGTCCCACCTCGTAAGGATCC

Table 4.7: Relative abundance of lignin residues as percentage of total molar area as presented in Figure 4.3. Standard deviations are indicated between brackets.

		G-residues							
		Guaiacol	**4-methylguaiacol**	**Ethyl-guaiacol**	**4-vinylguaiacol**	**Vanillin**	**Trans-isoeuganol**	**Acetovanillone**	**Guaiacylacetone**
	WS	22 (4)	2.8 (0.5)	1.9 (0.5)	37.4 (6.4)	3.5 (0.7)	2 (0.5)	1.2 (0.3)	2.8 (0.6)
	PII	24.5 (1.4)	3.3 (0.3)	2.1 (0.4)	32.9 (2.9)	2.3 (0.2)	3.4 (0.2)	1.7 (0.2)	2.3 (0.2)
Casing	**A15**	26.6 (5.4)	2.9 (0.8)	1.9 (0.6)	23.2 (6.2)	4.6 (1)	2.9 (1)	4.2 (0.7)	3.1 (0.8)
	MnP1-1	26.7 (5.6)	2.8 (0.7)	1.9 (0.4)	22.4 (5)	4.6 (0.9)	2.8 (0.6)	4.3 (0.9)	3.1 (0.6)
Venting	**A15**	31.7 (3.6)	2.5 (0.4)	1.7 (0.3)	15.9 (1.9)	4.9 (0.6)	2.2 (0.3)	5.4 (0.5)	3.3 (0.4)
	MnP1-1	31.9 (1.6)	2.5 (0.2)	1.8 (0.2)	15.5 (1)	5 (0.4)	2.2 (0.2)	5.3 (0.3)	3.3 (0.2)
After 2nd	**A15**	35.3 (2.9)	2 (0.2)	1.7 (0.2)	13.6 (1.1)	6 (0.4)	1.7 (0.1)	6.2 (0.3)	3.1 (0.2)
	MnP1-1	35.3 (2.8)	2 (0.2)	1.6 (0.2)	13.4 (1.5)	6 (0.8)	1.8 (0.3)	6.4 (0.8)	3.3 (0.4)

		S-residues						
		Syringol	**4-methylsyringol**	**4-vinylsyringol**	**Syringaldehyde**	**4-Allylsyringol**	**Acetosyringone**	**Syringylacetone**
	WS	10 (1.8)	1.3 (0.3)	8.1 (1.5)	1.4 (0.2)	2.1 (0.4)	1.8 (0.4)	1.8 (0.3)
	PII	10.2 (1.5)	1.3 (0.1)	8.5 (1.5)	1.2 (0.2)	3 (0.3)	2 (0.1)	1.5 (0.2)
Casing	**A15**	12.8 (2.6)	1.2 (0.3)	6.6 (1.3)	1.6 (0.3)	2.6 (0.5)	3.7 (0.7)	2.1 (0.4)
	MnP1-1	13.2 (2.8)	1.3 (0.3)	6.5 (1.3)	1.7 (0.3)	2.6 (0.5)	3.8 (0.7)	2.3 (0.4)
Venting	**A15**	15.4 (1.9)	1.1 (0.2)	5.2 (0.6)	1.7 (0.2)	2 (0.2)	4.3 (0.4)	2.6 (0.3)
	MnP1-1	15.6 (1.1)	1.2 (0.1)	5.1 (0.5)	1.6 (0.1)	2 (0.1)	4.4 (0.3)	2.6 (0.2)
After 2nd	**A15**	14.8 (1.4)	0.8 (0.1)	4.4 (0.2)	2 (0.2)	1.7 (0.1)	4.2 (0.3)	2.6 (0.2)
	MnP1-1	14.3 (1.7)	0.8 (0.1)	4.2 (0.6)	2.1 (0.2)	1.7 (0.2)	4.5 (0.5)	2.6 (0.3)

Table 4.6: Supplemental sequence 1

MAFKILLSLILALNAVQFIAAVPTRRAQCADGTTVSNEACCVLLPIIADIQPNLFENECGEEVH
ETLRASFHDAIGFSRAAGGGGADGSLVTFGDVETTFAANAGIDEIVETLRPFINSHNISAGDF
IQFATVVGLTNCPGAPRIPFFLGRPDATAASPDGLVPEPFDSVTKILERFDDAGFTPTEVVALL
ASHTVAASDTIEPGLEGVPFDSTPGEFDRQFFIETMLKGTSFPGTGGNQGEALSPLPGELRLE
SDGLLARDERTACDWQLFATDQQKMASAFSDAMVKLSLVGQDKSQLIDCSDVIPRTIPLTNE
PYFPADLTKDDLEQTCPDEFPDYPSNPSVTSVAPVPTS

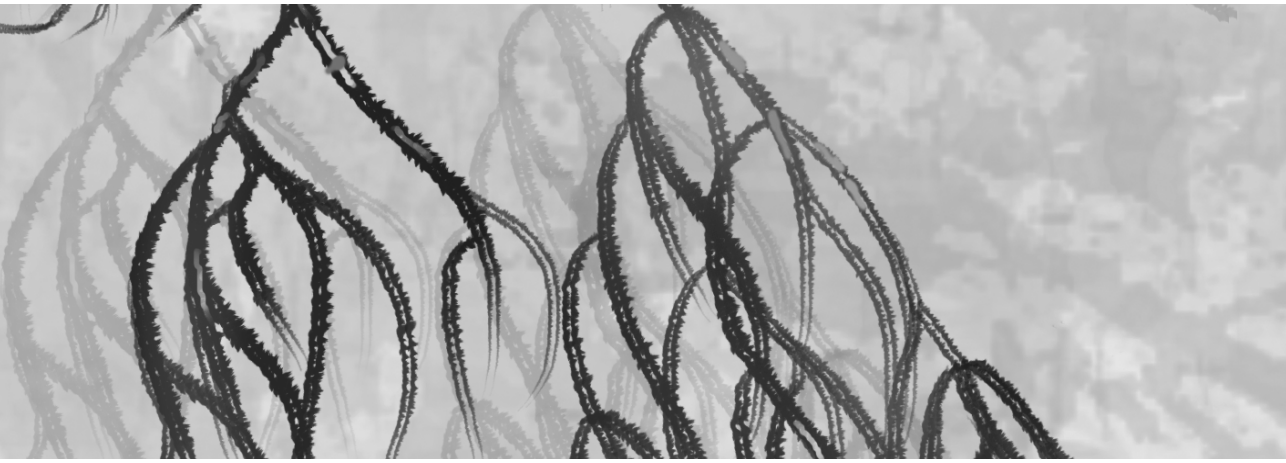

5

INTRODUCTION OF MnP ACTIVITY IN *Schizophyllum commune*; TOWARDS A MINIMAL LIGNINOLYTIC MACHINERY

Aurin M. Vos, Klaas G. J. Nierop, Koen Herman, Tom van den Brule, Thomaz Bastiaanssen, Maarten Punt, Luis G. Lugones, Han A. B. Wösten

ABSTRACT

The mushroom forming basidiomycete *Schizophyllum commune* has been classified to be intermediate between white and brown rot fungi. It deviates from the white rot fungi by lacking lignin degrading peroxidases such as manganese peroxidase, while it deviates from the brown rot fungi by possessing a variety of enzymes acting on crystalline cellulose. Here, the codon optimized manganese peroxidase genes *mnp1* and *mnp2* from *Agaricus bisporus* were introduced in *S. commune* to assess their effect on ligninolytic activity. In contrast to the wild-type, strains producing either or both MnPs decolorized Remazol Brilliant Blue R and coupled 3-methyl-2-benzothiazolinone hydrazone (MBTH) and (3-dimethylamino)benzoic acid (DMAB). Thermally assisted Hydrolysis and Methylation showed that birch wood lignin was not affected by *S. commune* wild-type or MnP-producing strains during a 119 day incubation. These data indicate that additional players are required for a minimal ligninolytic system in *S. commune*.

INTRODUCTION

Fungi play a major role in nature by recycling plant waste material. Basidiomycetes are well known for their capacity to mineralize wood that is rich in lignin. These fungi are classified as white or brown rots based on the color and macrostructure of their substrate after degradation. Recently, the dichotomy of brown and white rots was challenged based on the analysis of genes encoding carbohydrate active enzymes (CAZyme) and microscopical analysis of wood decay (Riley et al. 2014; Floudas et al. 2015). Brown rots have a reduced number of CAZymes active on (hemi)cellulose and lignin. They use Fenton chemistry to efficiently depolymerize (hemi)cellulose and to modify, but not effectively degrade, lignin (Yelle et al. 2008; Yelle et al. 2011; Arantes et al. 2012). White rots typically contain a reservoir of CAZymes for the degradation of (hemi)cellulose. Furthermore, they produce peroxidases such as lignin peroxidase (LiP), versatile peroxidase (VP), and manganese peroxidase (MnP) to degrade lignin (Kirk and Farrell 1987; Hatakka 1994; ten Have and Teunissen 2001; Hofrichter 2002; Guillén et al., 2005; Gómez-Toribio et al. 2009), while they may use Fenton chemistry as well. Ligninolytic peroxidases produce small highly reactive intermediates like oxidized veratryl alcohol (LiP and VP) and Mn^{3+} (VP and MnP) that effectively penetrate the plant cell wall to oxidize and depolymerize the lignin within this matrix.

Schizophyllum commune has classically been classified as a white rot but it does not degrade lignin efficiently (Schmidt and Liese 1980). In agreement, it was shown to cause weak wood decay while leaving the middle lamella intact (Floudas et al., 2015). Genome analysis revealed that *S. commune* lacks the typical lignin

degrading peroxidases present in white rot fungi but it does have lytic polysaccharide monooxygenases acting on crystalline cellulose that are absent or reduced in number in the brown rots (Ohm et al., 2010; Riley et al., 2014). *S. commune* was therefore classified as an organism that is intermediate between white and brown rot fungi (Riley et al., 2014). Here, *S. commune* was used as a model organism to study the minimal requirements of an in vivo ligninolytic system. Introduction of MnP genes of *A. bisporus* resulted in Remazol Brilliant Blue R degradation and oxidative coupling of 3-methyl-2-benzothiazolinone hydrazone (MBTH) and (3-dimethylamino)benzoic acid (DMAB) but did not impact lignin degradation in birch wood. This shows that additional players in lignin degradation have to be introduced to equip *S. commune* with an efficient lignin degrading machinery.

MATERIAL AND METHODS

STRAINS AND CULTURE CONDITIONS

Isogenic mono- and dikaryons of *S. commune* strain H4.8 (Ohm et al. 2010; 2011) and their derivatives were routinely grown at 30 °C on minimal medium (MM) with 2 % glucose and 1.5 % agar (van Peer et al. 2009). Strains were crossed by growing mycelial plugs on MM plates that had been sealed with Parafilm. After 3 days growth in the dark, the sealing was removed and cultures were placed upside down in the light at 25 °C to allow development of fruiting bodies. Spores were harvested from the lid of the Petri dish and spread on MM supplemented with 0.5 % activated charcoal. Germlings were transferred after 1 day to MnP screening plates (see below).

Mycelial homogenates were used to inoculate static liquid cultures and birch wood (BW) cultures. To this end, a quarter of a 7-day-old colony (including the underlying agar medium) was homogenized 3 times 20 s at high speed in 50 ml MM in a Waring blender (Waring Product, Torington, CT). For static liquid cultures, 6 ml homogenate was transferred to a Petri dish. After 2 days incubation, 10 ml MM either or not supplemented with 0.05 mM NaOH that either or not contained 0.5 mg ml^{-1} hemin was introduced underneath the mycelium. For BW cultures, 90 ml MM supplemented with 35 μg ml^{-1} chloramphenicol and 50 μg ml^{-1} ampicillin was added in polypropylene containers (182 x 120 x 92 mm; Eco2 NV, Netherlands) and inoculated with 10 ml mycelial homogenate. After 6 days of growth, cultures were overlaid with a mixture of 30 g birch wood chips (1 - 5 mm) and 40 ml MM in the absence of glucose but presence of 250 mg l^{-1} hemin and 1 mM NaOH and culturing was prolonged for 119 days.

PLASMID CONSTRUCTION

Manganese peroxidase genes *mnp1* (GeneID 221245) and *mnp2* (GeneID 118334) of *A. bisporus* (genome version 2) were codon optimized (Scholtmeijer et al. 2014) and synthesized by Genscript (New Jersey, USA). Primers 1 & 2 (Table 5.1) were used to amplify the *mnp* genes with Phusion polymerase (Thermo Fisher Scientific, Massachusetts, USA). The protocol included a 5 min incubation at 98 °C, followed by 35 cycles of 10 sec at 98 °C, 20 sec at 55 °C, and 1.5 min at 72 °C, and was completed with a 10 min incubation at 72 °C. Reactions contained 6 % DMSO (v / v). Amplified fragments were digested with NcoI / BamHI and cloned in pESCT (Scholtmeijer et al. 2014) bringing the *mnp* genes under control of the promoter of the tubulin gene *tub1* and the *sc3* terminator. The nourseothricin resistance cassettes in the resulting expression vectors pESCT-Nour-mnp1 and pESCT-Nour-mnp2 were replaced with a phleomycin resistance cassette using EcoRI (Schuren and Wessels 1994) resulting in plasmids pESCT-Phleo-mnp1 and pESCT-Phleo-mnp2.

TRANSFORMATION

Transformation of *S. commune* was performed as described (van Peer et al. 2009). 10^7 protoplasts were incubated with 10 μg plasmid DNA and transformants were selected on 20 μg ml^{-1} phleomycin or 8 μg ml^{-1} nourseothricin after overnight regeneration. Transformants were transferred to a second selection plate after 4 days.

MNP ASSAY

For MnP plate assays, MM was supplemented with 200 μg ml^{-1} Remazol Brilliant Blue R (RBBR; Sigma-Aldrich, USA) and 0.3 mM $MnSO_4$. Oxidative coupling of 3-methyl-2-benzothiazolinone hydrazone (MBTH) and (3-dimethylamino)benzoic acid (DMAB) was used to measure MnP activity in liquid (Castillo et al. 1994). Medium from static liquid cultures was centrifuged for 10 min at 12000 g to remove mycelium. Birch wood extract was prepared by mixing homogenized birch wood (see below) with miliQ water in a 1 : 5 (w / v) ratio. After shaking at 25 °C for 1 h at 225 rpm extract was separated from the wood particles by centrifugation for 20 min at 5500 g. MnP activity was measured by mixing 100 - 200 μl culture medium or birch wood extract with 0.07 mM MBTH, 0.99 mM DMAB, 0.1 mM $MnSO_4$, 0.05 mM H_2O_2, and 100 mM succinic-lactate buffer pH 5 using a final volume of 1 ml. Changes in OD590 were followed for 30 sec. Unless otherwise stated MnP activity was obtained by subtracting the activity in a reaction containing 1 mM EDTA. MnP activity was expressed in units (U) using the law of Lambert-Beer and an extinction coefficient 53000 M_{-1} cm_{-1}.

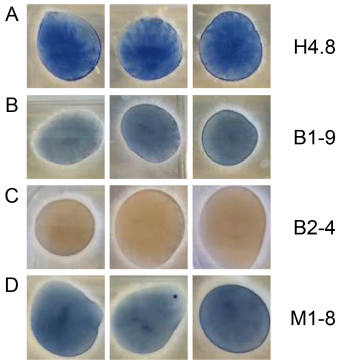

Figure 5.1: RBBR decoloration in Mn^{2+} supplemented MM by wild type strain H4.8 (A), *mnp1* transformant B1-9 (B), *mnp2* transformant B2-4 (C), and by strain M1-8 containing both *mnp1* and *mnp2* (D).

qPCR

S. commune was grown for 3 days on MM overlaid with a polycarbonate (PC) membrane (diameter, 76 mm; pore size, 0.1 μm; Maine Manufacturing, LCC, Sanford, USA). Mycelium was frozen in liquid nitrogen and homogenized for 1 min at 25 Hz using a TissueLyser II (Qiagen, Düsseldorf, Germany). RNA was isolated from the homogenized mycelium using 1 ml TRIzol reagent (Chomczynski and Sacchi 1987). Chloroform (200 μl) was added and shaken for 15 sec. After 3 min at rt, the suspension was centrifuged at 4 °C for 15 min at 12000 g. RNA in the aqueous phase was precipitated with 0.8 volume isopropanol, washed with 75 % ethanol, and resuspended in RNAse-free water. 1 μg RNA was used for cDNA preparation using a Quantiscript Reverse Transcriptase kit (Qiagen Inc., Netherlands) according to the manufacturer's instructions. A ViiA™ 7 Real-Time PCR System (Thermo Fisher Scientific, Massachusetts, USA) and an optical 96 wells plate (Applied Biosystems, California, USA) were used for qPCR with SYBR® Green (Thermo Fisher Scientific, Massachusetts, USA). Transcripts of *mnp1* and *mnp2* were amplified using primers 3 & 4 and 5 & 6, respectively (Table 5.1), starting with a 2-min incubation at 50 °C and a 10-min incubation at 95 °C and followed by 40 cycles of 15 s at 95 °C and 1 min at 60 °C.

Thermally assisted Hydrolysis and Methylation (THM)

Birch frozen in liquid nitrogen was milled at 30 Hz for 1 min using a tissuelyser (Qiagen Tissuelyser II and grinding jar). Samples (2 mg) were treated with a droplet of 25 % tetramethylammonium hydroxide (TMAH) and dried under a 100 W halogen lamp, after which they were pyrolyzed at 600 °C for 5 s in a Horizon Instruments Curie-point pyrolyzer (Heathfield, UK). THM products were transferred

into a Carlo Erba GC8060 gas chromatograph (Milano, Italy) using helium and separated onto a silica column (25 m, 0.32 mm i.d.; Varian, Palo Alto, USA) coated in CP-Sil5 (film thickness 0.40 μm). The oven was heated to 320 °C with 7 °C min-1 and kept at peak temperature for 15 min. A Fisons MD800 mass spectrometer (Loughborough, UK; mass range m / z 40 - 650, ionization energy 70 ev, cycle time 0.7 s) was used to analyze the THM products that were identified based on their mass spectrum and relative retention times. The peak area was based on the two dominant fragment ions of each identified compound.

RESULTS

The *A. bisporus mnp1* (Agabi Gene ID 221245) and *mnp2* (Agabi Gene ID 118334) coding sequences were codon optimized for *S. commune* and placed in between the *tub1* promoter and *sc3* terminator. The expression vectors that contained an artificial intron directly after the stop codon of the *mnp* genes (Lugones et al. 1999; Scholtmeijer et al. 2014) as well as a nourseothricin or phleomycin resistance cassette were introduced in the compatible strains H4.8 (phleomycin resistance cassetes) and H4.8b (nourseothricin resistance cassettes). About 25 % of the *mnp1* and *mnp2* transformants were capable of decolorizing RBBR in medium supplemented with Mn^{2+}. Based on the decoloration of RBBR, one nourseothricin resistant transformant of *mnp1* (B1-9), one nourseothricin resistant transformant of *mnp2* (B2-4), one phleomycin resistant transformant of *mnp1* (A1-15), and one phleomycin resistant transformant of *mnp2* (A2-11) were selected. Expression of the introduced MnP genes was verified in B1-9 and B2-4 using qPCR. Transcripts of *mnp1* and *mnp2* were detected at Ct values of 15.6 ± 0.2 and 18.8 ± 0.2, respectively, while actin was detected at a Ct value of 19.5 ± 0.2. The wild type strain H4.8 did not produce transcripts of *mnp1* and *mnp2* as expected.

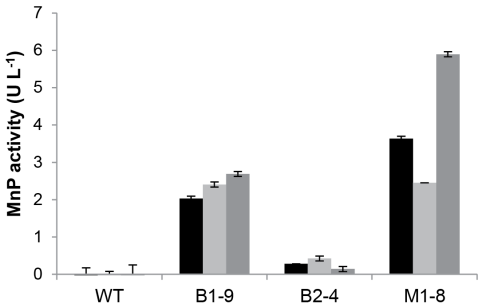

Figure 5.2: MnP activity in culture medium of strain H4.8, B1-9, B2-4, and M1-8 without supplements (black shading), or culture medium that had been supplemented with 0.05 mM NaOH (light grey shading), or 0.05 mM NaOH and 500 mg l^{-1} hemin (dark grey shading). Values are based on two biological replicas.

Strain M1-8 was created using three crossing events. First, strain A1-15 and A2-11 were each crossed with B1-9. Progeny of these two crosses was plated on phleomycin and nourseothricin containing medium and compatible strains were again crossed. Progeny of this cross was again plated on phleomycin and nourseothricin containing medium resulting in strain M1-8 that contained both *mnp1* and *mnp2* (Figure 5.1). Strains H4.8, B1-9, B2-4, and M1-8 were grown on plates containing RBBR. Strain B2-4 decolorized the dye most actively, B1-9 and M1-8 showed intermediate activity, while H4.8 hardly decolorized RBBR. In the next step, activity of MnP was measured in liquid cultures using the MBTH/DMAB assay. This assay was performed in the absence or presence of hemin being an essential cofactor of MnP (Stewart et al. 1996; Conesa et al. 2002). The MnP activity of cultures of H4.8 and the transformants was assessed in the culture medium that had either or not been supplemented with the co-factor hemin. As a control, cultures were supplemented with NaOH. Strain M1-8 produced a 2-fold higher MnP activity as compared to B1-9, while MnP activity of B2-4 was just above background levels in cultures that had not been supplemented with hemin (Figure 5.2). Supplementation of this co-factor during growth increased MnP activity of B1-9 and M1-8 by 0.1- and 2.4-fold, respectively. The pH optima of MnP activity in standing cultures of M1-8 and compost extract of *A. bisporus* strain A15 were assessed by the MBTH/DMAB assay after supplementation with H_2O_2 and Mn^{2+}. A pH optimum of 5.4 was observed for culture medium of M1-8 and compost extract of A15 (Figure 5.3). The pH dependent MnP activity in compost extract of *A. bisporus* followed a similar pattern as compared to M1-8 (R^2 of 0.95). MnP activity was at background levels in the presence of H_2O_2 alone (not shown) but upon addition of Mn^{2+} alone some activity was measured that increased linearly with increasing pH (Figure 5.3).

Strains H4.8 and M1-8 were grown for 119 days on birch wood to study the effect of MnP production on the degradation of lignin. Wood extract from M1-8 cultures contained MnP activity, while wood extract of H4.8 did not (Figure 5.4C). Both the Ac / Al ratio and Γ proxy (Filley et al. 2006) of the untreated birch wood (0.42 and 0.24, respectively) were not affected by colonization of H4.8 or M1-8 (Figure 5.4A and B).

Discussion

The lack of class II peroxidases in the genome of *S. commune*, its poor performance in wood decay, and genetic accessibility make this basidiomycete an interesting model to study the minimal requirements for efficient ligninolytic action. Codon optimized *mnp1* and *mnp2* genes of *A. bisporus* were successfully expressed by *S. commune* as shown by qPCR and RBBR discoloration. Crossing

mnp1 and *mnp2* transformants resulted in strain M1-8 that produced 2-fold and 13-fold more MnP activity in the MBTH/DMAB assay as compared to strain B1-9 and B2-4, respectively. The pH spectrum of MnP activity in compost extract of *A. bisporus* was similar to that in standing cultures of M1-8. The pH optimum of 5.4 was similar as reported previously but the decrease in MnP activity at pH > 5.5 was not as steep (Bonnen et al. 1994). This may be caused by the guaiacol substrate used by Bonnen et al. (1994). Notably, activity was also observed, albeit lower, when H_2O_2 was not supplemented in the assay. This activity increased with increasing pH and may be caused by de novo production of H_2O_2 (Chapter 4).

MnP2 has not been isolated from compost and expression of its encoding gene has not been observed (Lankinen et al. 2001; Patyshakuliyeva et al. 2015). This suggested that it is a pseudogene. However, we here showed that transformants expressing *mnp2* did decolorize RBBR. In fact, *mnp2* transformant B2-4 showed higher RBBR decoloration when compared to *mnp1* transformant B1-9 while mRNA production was higher in B1-9. In contrast, activity of the *mnp1* transformants was higher when using the MBTH/DMAB assay. This difference may be due to differences in the interaction of MnP1 and MnP2 with their substrates.

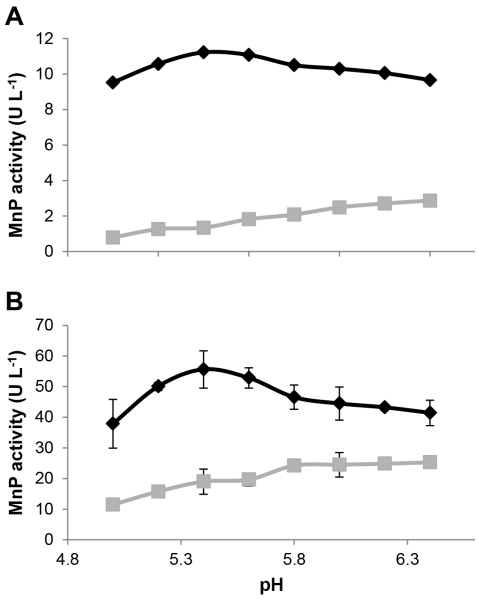

Figure 5.3: pH spectrum of MnP activity in culture medium of transformant M1-8 (A) and compost extract of *A. bisporus* strain A15 (B). MnP activity measured after supplementing the assay with H_2O_2 and Mn^{2+} (black line) and H_2O_2-independent but Mn^{2+} dependent activity (grey line). Data for M1-8 represents 1 biological replica, while A15 represents a biological triplicate with standard deviations as error bars.

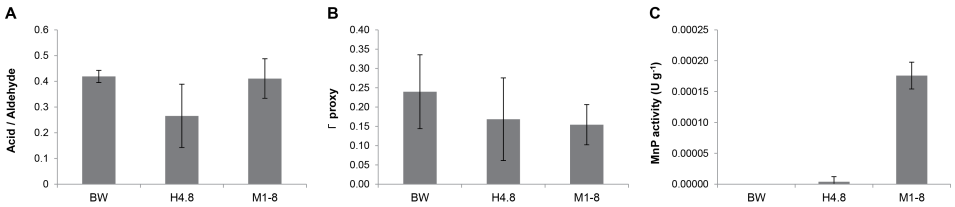

Figure 5.4: Thermally assisted Hydrolysis and Methylation of birch wood (BW) and birch wood colonized by wild type H4.8 or M1-8. Data is represented as the acid / aldehyde ratio (A), and the Γ proxy (B). MnP activity (C) was measured in BW colonized by H4.8 and M1-8. BW, H4.8, and M1.8 represent 3, 4, and 4 replicas, respectively. Error bars represent standard deviations.

Some genes involved in lignin degradation have been identified. This was done by random mutagenesis, by targeted knockouts, and by using in vitro assays (Boominathan et al. 1990; Addleman et al. 1995; Eggert et al. 1997; Salame et al. 2014). However, a bottom up approach of introducing a (minimal) ligninolytic system in a fungus has not been attempted yet. The introduction of MnP in *S. commune* was a first step in this approach. THM of wood colonized by *S. commune* did not show any effect on the oxidation of propenyl chains as indicated by both the Γ proxy and the acid / aldehyde ratio. This suggests that introduction of MnP alone is not sufficient to adapt the life style of *S. commune* to a ligninolytic white rot. Based on the results of Chapter 4 it is tempting to speculate that introduction of a H_2O_2 generating enzyme may stimulate ligninolysis in MnP producing transformants of *S. commune*.

SUPPLEMENTAL MATERIAL

Table 5.1: Primers used in this study.

Primer	Sequence
1	CGCCATGGCCTTCAAGATCCTCCTCTC
2	GCGGATCCTCAGGACGTGGGACCGGG
3	AGGACAAGTCGCAGCTCATC
4	AAGTACGGCTCGTTCGTCAG
5	ACCACTTCGAGAACGTCTGC
6	ATGTCCGAGAAGGTGACGATG

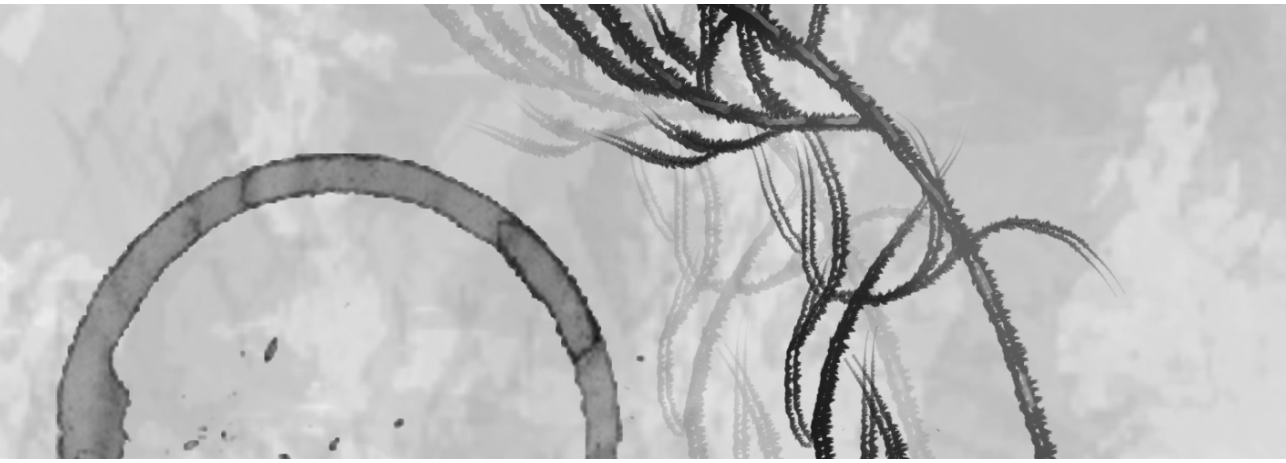

6

THE TRANSCRIPTIONAL REGULATOR *c2h2* ACCELERATES MUSHROOM FORMATION IN *Agaricus bisporus*

Jordi F. Pelkmans, Aurin M. Vos, Karin Scholtmeijer, Ed Hendrix, Johan J.P. Baars, Thies Gehrmann, Marcel J. T. Reinders, Luis G. Lugones, Han A.B. Wösten

This chapter has been published as: Pelkmans JF, Vos AM, Scholtmeijer K, Hendrix E, Baars JJP, Gehrmann T, Reinders MJT, Lugones LG, Wösten HAB (2016) The transcriptional regulator *c2h2* accelerates mushroom formation in *Agaricus bisporus*. Appl Microbiol Biotechnol 100:7151–7159.

ABSTRACT

The Cys2His2 zinc finger protein gene *c2h2* of *Schizophyllum commune* is involved in mushroom formation. Its inactivation results in a strain that is arrested at the stage of aggregate formation. In this study, the *c2h2* orthologue of *Agaricus bisporus* was over-expressed in this white button mushroom forming basidiomycete using *Agrobacterium*-mediated transformation. Morphology, cap expansion rate, and total number and biomass of mushrooms was not affected by over-expression of *c2h2*. However, yield-per-day of the *c2h2* over-expression strains peaked one day earlier. These data and expression analysis indicate that C2H2 impacts timing of mushroom formation at an early stage of development, making its encoding gene a target for breeding of commercial mushroom strains.

INTRODUCTION

The basidiomycete *Agaricus bisporus* is cultivated globally for the production of white button mushrooms. These fruiting bodies have a relative high protein content and contain fibers, vitamins, minerals, and bioactive compounds. *A. bisporus* is grown on compost formed from wheat straw, horse or chicken manure, and gypsum. During colonization, the compost is topped with a casing layer needed for moisture and microbial flora (Bels-Koning 1950; Flegg 1956; Kalberer 1987). Induction of mushroom formation depends on environmental signals. The volatile 1-octen-3-ol represses early development, while high temperature (i.e. 25 °C instead of 18 °C) inhibits development from smooth to elongated primordia. On the other hand, CO_2 impacts the number of fruiting bodies that are formed (Noble et al. 2009; Eastwood et al. 2013). Development of *A. bisporus* is a complex process (Kües and Navarro-González 2015). It starts with aggregation of hyphae into hyphal knots (Umar and van Griensven 1997). These structures develop into 1 - 2 mm initials, also called primordia, that differentiate by forming cap and stem tissues (Umar and van Griensven 1997). Up to 10 % of differentiated primordia develop into mushrooms (Noble et al. 2003). Breaking of the veil of these fruiting bodies enables airborne dispersal of basidiospores that had been formed in the gill tissue within the cap.

Production conditions of white button mushrooms have been optimized with respect to yield and quality of fruiting bodies (Straatsma et al. 2013). However, molecular mechanisms underlying mushroom formation are poorly understood. For instance, transcription factors (TFs) involved in white button development have not been identified so far. Such regulatory proteins have been identified in the model organism *Schizophyllum commune* (Ohm et al. 2010; 2011; 2013). Formation of its fruiting bodies is induced by blue light and is repressed by high CO_2 (Perkins and Gordon 1969; Niederpruem1963; Raudaskoski and Viitanen

1982; Ohm et al. 2013). The blue light receptor complex consists of the sensor WC-1 and TF WC-2. Inactivation of *wc-1* and / or *wc-2* results in a blind strain not able to produce aggregates, primordia, and fruiting bodies (Ohm et al. 2013). Strains in which the homeodomain gene *hom2* or the zinc finger TF gene *fst4* have been inactivated are also not able to produce aggregates (Ohm et al. 2010; 2011). In contrast, inactivation of the gene encoding the Cys2His2 zinc finger protein C2H2 results in a strain that does form aggregates but primordia and fruiting bodies are not formed (Ohm et al. 2011). Strains in which genes are inactivated that encode the zinc finger protein Fst3, the GATA type zinc finger protein Gat1, or the homeodomain protein Hom1 form smaller fruiting bodies but in higher numbers (Ohm et al. 2011). These proteins were proposed to play a role in repression of outgrowth of primordia into fruiting bodies or to play a role in expansion of the fruiting body.

Homologues of the *S. commune* TFs involved in fruiting body development have been identified in other mushroom forming fungi. Expression analysis in *A. bisporus*, *Laccaria bicolor*, and *Coprinopsis cinerea* suggest that mushroom development in the Basidiomycota follows a core regulatory program with species specific variations that explain differences in morphology and sensitivity to environmental signals (Ohm et al. 2010; Morin et al. 2012; Plaza et al. 2014; Muraguchi et al. 2015). In this study, the *A. bisporus c2h2* homologue was over-expressed in the commercial A15 strain of this mushroom forming fungus. This resulted in an accelerated rate of mushroom production. Experimental data indicate that C2H2 functions both early and late in mushroom development and that it is an interesting target for breeding of commercial strains.

MATERIAL AND METHODS

CULTURE CONDITIONS AND STRAINS

The heterokaryotic *A. bisporus* strain A15 (obtained from the fungal collection of Plant Breeding Wageningen UR, the Netherlands) and its derivatives AT273-1 and AT273-5 that over-express *c2h2* were routinely grown at 25 °C on malt extract agar medium (MEA; 20 g l^{-1} malt extract agar [BD biosciences, Franklin Lakes, USA], 2.1 g l^{-1} MOPS, pH 7.0). Spawn was produced using a mixture of 24 g kg^{-1} $CaSO_4$, 6.87 g kg^{-1} $CaCO_3$, and 75 g *Sorghum* seeds. The seeds had been heated in water at 100 °C for 20 min followed by sterilization for 20 min at 121 °C. Spawn was colonized for 3 weeks at 25 °C using 2 1-week-old *A. bisporus* colonies as inoculum. Mushrooms were produced by inoculating boxes (40 cm width x 60 cm length x 22 cm height) containing 16 kg phase 2 compost (CNC, Milsbeek, The Netherlands) with 75 g of spawn. Compost temperature was maintained at 25 °C with an air temperature of 22 °C. Relative humidity in growth cells was kept at 95

%, while CO_2 levels fluctuated between 1500 ppm and 2000 ppm. 10 boxes were inoculated per strain and were randomly distributed in the growth cell. After 16 days, the compost in each box was topped with 7 kg casing layer (CNC, Milsbeek, The Netherlands). Growth was prolonged for 14 days before venting. The casing was manually broken 4 days prior to venting and mixed to create fast regenerative growth and a more equal distribution of *A. bisporus* in the casing layer. Venting resulted in a gradual decrease of compost and air temperature to 19 and 18 °C, respectively. Relative humidity and CO_2 levels decreased gradually to 85 % and 1200 ppm, respectively. The first buttons were removed from the bed 9 days after venting.

Analysis of mushroom formation

Photos of casing layer surfaces were taken in a fixed rig at 24 h intervals from venting until the start of the first flush. Emergence of mushrooms and growth rate of the caps was monitored using ImageJ (http://imagej.nih.gov/ij/). Harvesting of mushrooms was done by a professional picker as performed in commercial production. Prior to the flushes some buttons were removed to open up the space between developing buttons. Fruiting bodies with a diameter between 40 and 60 mm were always harvested, while fruiting bodies with a diameter of ≤ 40 mm were picked from densely populated areas to provide more space, water, and nutrients to the remaining mushrooms, thereby ensuring optimal yield. Mushrooms were classified as size 40 (mushrooms with a cap ≤ 40 mm) and size 60 (mushrooms with a cap between 40 - 60 mm). Mushrooms were harvested in two flushes. All mushrooms had reached a size ≥ 40 mm during the second flush at day 22 and all fruiting bodies were therefore harvested, thus completing the experiment. Yield per box was expressed as the biomass and the number of harvested mushrooms. Height and width of cap and stem were determined of 10 randomly selected mushrooms per box during the peak day of the first flush. Dry weight of the mushrooms was assessed by drying 200 g wet weight fruiting bodies at 100 °C. Relative dry weight is defined as the dry weight compared to the original wet weight.

Over-expression of *c2h2*

Primers GATCGTTAATTAAGAATTCAGATCTCAATTGGGCGCGCC and GGCGCGCCCAATTGAGATCTGAATTCTTAATTAAC were used to introduce PacI and AscI sites into pBHg (Chen et al. 2000), creating pBHgPA. Gene *c2h2* of *A. bisporus* (ProteinID 230069, http://genome.jgi.doe.gov/ Agabi_varbisH97_2) encompassing its coding region with 750 bp up- and downstream sequences was amplified by PCR using genomic DNA of *A. bisporus* A15, primers CGCTTAATTAACCTGGCAAAAAAGTGAAC and ATATGGCGCGCCACTACGTCGATGATCATG and Phusion

Hot Start II High-Fidelity DNA polymerase (Thermo Fisher Scientific, Waltham, USA). The amplicon contained PacI and AscI linkers at its 5' and 3' ends, respectively, enabling its introduction in pBHgPA that had been cut with PacI and AscI. The resulting plasmid pKS273 was introduced in *Agrobacterium tumefaciens* AGL-1 (Chen et al. 2000). Transformation of *A. bisporus* A15 gills was performed as described (Romaine and Chen 2005). Transformants were screened on MEA plates containing 25 μg ml^{-1} hygromycin, 200 μM cefotaxime, and 100 μg ml^{-1} moxalactum. Transformants were transferred to a second selection plate containing 40 μg ml^{-1} hygromycin, 200 μM cefotaxime, and 17 μg ml^{-1} tetracycline.

Whole genome expression analysis

Mycelium in the casing layer, initials, stage I and stage II buttons, and young fruiting bodies of *A. bisporus* strain A15 were harvested 9 days after venting from two distinct places of the casing bed (thereby creating biological duplo's). Due to the method of cultivation at the commercial hand-picking grower Maatschap van den Heuvel, de Rips, The Netherlands, all developmental stages were present on the casing bed at this time point. Casing mycelium was harvested with casing soil. The initials were pooled to obtain sufficient material for RNA isolation. A single stage I button was divided in cap and stipe using a scalpel. A stage II button and a young fruiting body were divided into components of the stipe (skin, underlying tissue and center) and cap (skin, underlying tissue, gill tissue and veil). Samples were immediately frozen in liquid nitrogen. The casing mycelium sample was broken in pieces and kept frozen with liquid nitrogen while harvesting mycelium using cooled tweezers. Samples were homogenized using the TissueLyser II (Qiagen, Düsseldorf, Germany) and RNA was purified using the NucleoSpin RNA kit (Macherey-Nagel, Düren, Germany). Quality was assessed by gel electrophoresis and sent to ServiceXS (Leiden, the Netherlands) for Illumina Next Generation Sequencing. RNA sequencing data have been deposited at NCBI under accession PRJNA309475.

Sequencing revealed between 20,002,387 and 38,840,092 reads. The RNA-Seq pipeline used the TRIMMOMATIC read trimmer version 0.32 (Bolger et al. 2014) to remove low quality regions and the ILLUMINA adapters from the 125 bp paired end reads. These filtered reads that made up 79 - 86 % of the initial reads were aligned to the *A. bisporus* v3.0 genome (Sonnenberg, unpublished data) using STAR aligner version 2.4.0f1 (Dobin et al. 2013). The size of the introns was limited to 1500 bp based on the largest intron sizes in the genome annotation provided by the Joint Genome Institute of the Department of Energy (JGI DOE). This resulted in an alignment of 80 - 93 % of the filtered reads. Abundance estimation was calculated with Cufflinks version 2.1.1 (Trapnell et al. 2012), and differential

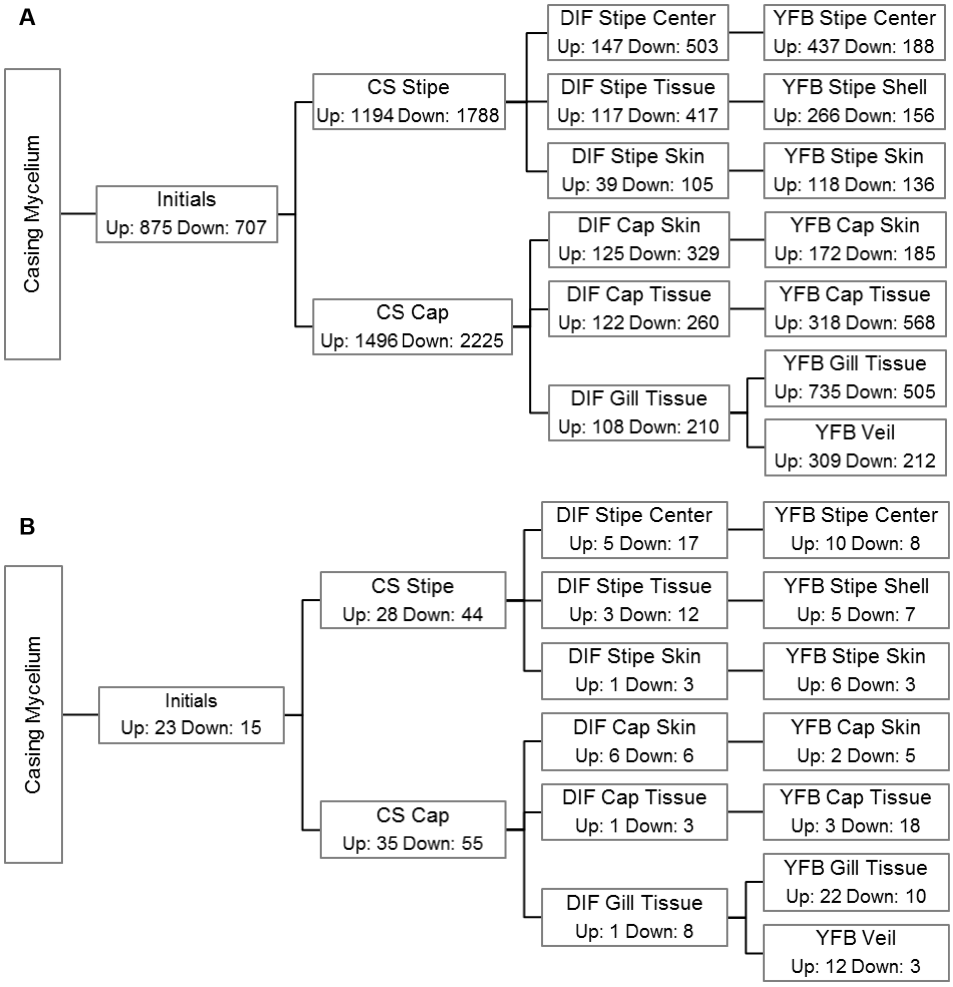

Figure 6.1: Total up- and downregulated genes (A) and up- and downregulated TF genes (B) comparing initials, stage I buttons, stage II buttons, and young fruiting bodies (YFB) with the preceding developmental stage.

expression tests were performed by Cuffdiff using a Benjamini Hochberg false discovery rate of 0.05 (Trapnell et al. 2013). Proteins annotated to contain a DNA-binding or regulatory protein domain in the InterPro annotation predictions provided by JGI DOE were considered TFs.

Statistical analyses

Permutations tests were performed to circumvent non-normal distributions of the data. Within each test 1,000.000 permutations were performed. P-values were corrected with a Benjamini Hochberg procedure using a false discovery rate of 0.05.

Results

Whole genome expression analysis

RNA composition of casing mycelium, initials, stage I and II buttons, and young fruiting bodies of the commercial *A. bisporus* strain A15 were determined. Initials consisted of 1 - 2 mm hyphal knots, while stage I buttons were 4 - 5 mm in diameter. Stage II buttons showed differentiation within the cap and stipe tissue. For instance, gills had developed. Young fruiting bodies were between 15 and 20 mm in diameter and still had their gills covered with veil. Stage I and II buttons and young fruiting bodies were dissected into stipe and cap. Stipes of stage II buttons and young fruiting bodies were subdivided into skin, underlying tissue, and central tissue, while caps were subdivided in skin, underlying tissue, gill tissue, and veil tissue. 875 and 707 genes were up- and downregulated, respectively, in initials when compared to casing mycelium (Figure 6.1A). In stipes and caps of stage I buttons 1194 and 1496 genes were upregulated when compared to initials, while 1788 and 2225 genes were downregulated. The number of genes that were upregulated in tissues of stage II buttons ranged from 39 to 147, while 105 to 503 genes were downregulated when compared to the caps and stipes of stage I buttons. The number of upregulated genes in young fruiting body tissues ranged from 118 to 735 compared to the stage II button tissues, while 136 to 568 genes were downregulated.

The overall number of TF genes that were upregulated ranged from 1 to 35 when consecutive stages were compared, while the number of downregulated regulatory genes ranged from 3 to 55 (Figure 6.1B, Table 6.3 in the Supplementary Material). The most prominent changes were observed when initials and caps of stage I buttons were compared (90 differentially expressed TF genes). Only 4 TF genes were differentially expressed in the transition of stipes of stage I buttons into stipe skin of stage II buttons and from stage I caps to stage II cap tissues (Figure 6.1B).

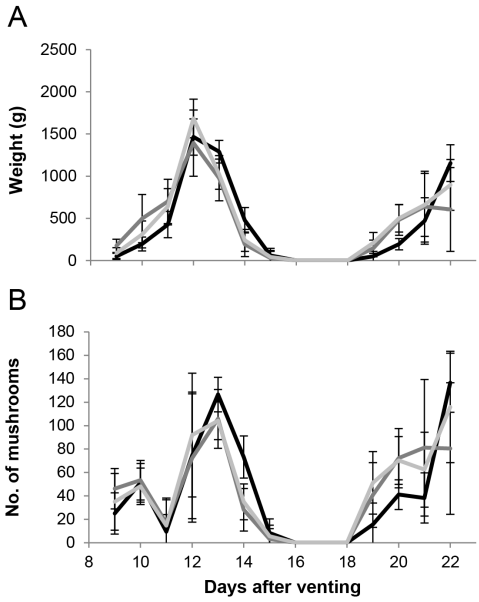

Figure 6.2: Average biomass (A) and number (B) of A15 (black line), AT273-1 (dark grey line), and AT273-5 (light grey line) mushrooms per box (n=10) picked during a 22-day period after venting (t = 0). Bars represent standard deviation.

Expression of the *A. bisporus* orthologues of the blue light sensor gene *wc-1* and the TF genes *wc-2*, *hom2*, *fst4*, *c2h2*, *fst3*, *gat1*, and *hom1* of *S. commune* (Morin et al. 2012) was analyzed. To this end, expression levels at the different stages of development were compared with mycelium in the casing layer. Transcript levels of *wc-2* and *c2h2* increased > 2-fold in initials compared to casing mycelium, while *hom1* levels decreased > 2-fold (Table 6.1; Table 6.4 in the Supplementary Material). Expression of *wc-1* and *wc-2* was in general higher in aerial structures when compared to the casing mycelium, in stipes when compared to caps, and in outer tissues when compared to inner tissues of the aerial structures. Genes *hom2* and *fst4* were ≥ 2-fold upregulated when initials had developed in stage I buttons. Like *wc-1* and *wc-2*, they were more highly expressed in stipes when compared to caps but in this case there was no difference between outer and inner tissues of the stage II buttons and young fruiting bodies. Gene *c2h2* showed high expression at different stages of fruiting body development. Expression levels ≥ 4-fold were observed in initials, caps of stage I buttons, gill tissue of stage II buttons, and veil tissue of young fruiting bodies. Expression of *c2h2* was reduced ≥ 2-fold when compared to casing mycelium in stipe and cap skin and in inner cap tissue of young fruiting bodies. Increased (≥ 2-fold) levels of *fst3* were only observed in stipes of stage I buttons and in stipe skin and tissue of stage II buttons.

Table 6.1: Fold changes in expression during *A. bisporus* development of TF orthologues involved in mushroom formation in *S. commune*.

	wc-1	*wc-2*	*hom2*	*fst4*	*c2h2*	*fst3*	*gat1*	*hom1*
Casing mycelium	1.0	1.0	1.0	1.0	1.0	1.0	1.0	1.0
Initials	1.4	6.0	1.6	1.9	4.4	1.1	0.9	0.4
Stage I buttons								
Stipe	2.3	3.4	5.6	2.3	3.1	2.0	0.4	0.6
Cap	1.1	2.8	1.4	2.1	8.5	0.9	0.4	0.3
Stage II buttons								
Stipe center	1.6	5.5	6.0	2.1	3.2	1.3	0.2	0.7
Stipe tissue	3.4	11.2	6.0	2.1	1.2	2.2	0.2	0.9
Stipe skin	2.7	8.2	4.7	2.0	1.6	2.0	0.4	0.9
Cap skin	2.1	3.2	0.6	1.3	2.1	0.9	0.4	0.6
Cap tissue	1.3	1.5	1.1	1.6	3.8	0.9	0.3	0.5
Gill tissue	0.8	0.8	1.7	1.9	7.6	0.8	0.3	0.4
Young fruiting bodies								
Stipe center	3.1	7.6	8.3	2.1	1.2	1.5	0.5	1.4
Stipe shell	4.6	18.8	8.0	2.0	1.6	1.9	0.3	1.4
Stipe skin	4.1	24.0	4.6	1.7	0.3	1.9	0.3	1.3
Cap skin	3.7	8.2	0.5	0.9	0.4	1.0	0.4	1.1
Cap tissue	2.8	2.3	1.0	0.8	0.1	1.0	0.3	0.8
Gill tissue	3.8	9.1	1.4	1.3	3.0	1.4	0.4	1.1
Veil	2.3	3.3	1.7	1.8	6.7	1.4	0.4	0.7

Expression was related to expression in the casing layer. Dark and light red boxes indicate ≥ 2-fold and ≥ 4-fold reduced expression in the developmental structures, respectively. Light to dark green in the closed boxes indicates ≥ 2-fold, ≥ 4-fold, and ≥ 10-fold increased expression in the aerial structures.

Table 6.2: Total weight and number of mushrooms per box of *A. bisporus* strains A15, AT273-1 and AT273-5 after 2 flushes (n=10).

	Weight (g)		**Number of mushrooms**	
Strain	Average	Standard deviation	Average	Standard deviation
A15	4197.6	200.1	600.1	114.6
AT273-1	4209.8	439.2	573.1	149.1
AT273-5	4324.4	235.5	634.7	90.9

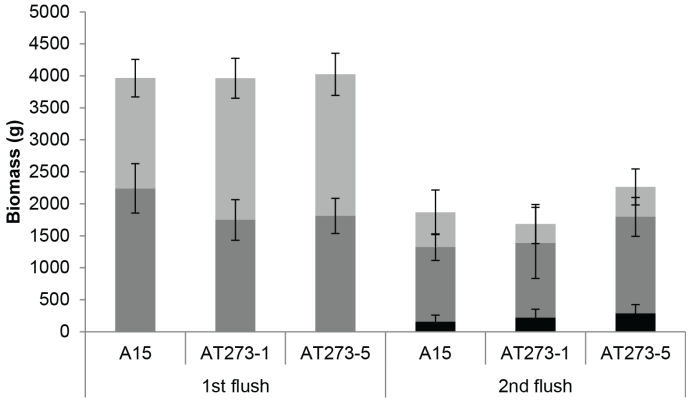

Figure 6.3: Buttons (black bar), mushrooms with 40 mm diameter (dark grey bar), and 60 mm (light grey bar) of A15, AT273-1 and AT273-5 harvested during two flushes. Bars represent standard deviation (n=100).

Gene *hom1*, and in particular *gat1* was in general downregulated when compared to casing mycelium.

FASTER MUSHROOM PRODUCTION BY OVER-EXPRESSION OF *c2h2*

Gene *c2h2* (protein ID 230069) of *A. bisporus* shares 79 % identity with its homologue of *S. commune* (protein ID 1194000; http://genome.jgi.doe.gov/Schco3). Expression construct pKS273 (see Material and methods) encompassing *A. bisporus* gene *c2h2* was introduced into *A. bisporus* A15 using *A. tumefaciens* mediated transformation. This resulted in 10 transformants, 2 of which were picked for further analysis. qPCR showed a 30- and a 2.5-fold increase in *c2h2* expression in *A. bisporus* AT273-1 and AT273-5, respectively, when grown on MEA. Growth of these strains on malt extract medium was similar to the parental strain.

Mushroom production of *A. bisporus* AT273-5 and AT273-1 was assessed in a semi-commercial setting (see Material and methods). The first flush started 9 days after venting and progressed until day 14. The second flush took place between day 19 and day 22 (Figure 6.2). Biomass of mushrooms harvested at day 9 - 11 and at day 19 - 20 was higher for *A. bisporus* AT273-1 when compared to A15 (Figure 6.2A). *A. bisporus* AT273-5 showed higher harvested mushroom biomass at day 11, 19, and 20 when compared to A15. The latter strain produced more biomass at day 13 and 14 compared to both transformants and more biomass compared to *A. bisporus* AT273-1 on day 22. Total production of mushrooms was similar for the 3 strains (Table 6.2). A higher number of A15 mushrooms was harvested at day 13 when compared to *A. bisporus* AT273-5, day 14 compared to both transformants, and day 22 compared to *A. bisporus* AT273-1. A higher number of

A. bisporus AT273-1 and AT273-5 mushrooms were harvested compared to A15 at day 9, 19, and 20 when compared to A15 (Figure 6.2B). Together, these data show that over-expression of *c2h2* accelerates development of mushrooms.

Harvested mushrooms were classified based on size 40 (cap ≤ 40 mm) and size 60 (cap between 40 - 60 mm) (Figure 6.3). During the first flush, A15 produced more size 40 mushrooms (57 %), while the *c2h2* over-expressing strains produced more size 60 mushrooms (56 and 55 %, respectively). The ratio between cap and stem dimensions were similar for all strains. A relative dry weight of 8 % was found for the mushrooms of the 3 strains at day 12 and 13 (Figure 6.4). All strains produced more size 40 mushrooms in the second flush (64 % for A15 versus 73 and 71 % for AT273-1 and AT273-5). Relative dry weight at day 21 amounted between 6.2 and 6.7 % for the three strains (Figure 6.4). Together, these data show that over-expression of *c2h2* promotes size in the first flush.

Mushroom formation was monitored by analyzing photos taken in 24 h intervals. Cap expansion was similar for the 3 strains (Figure 6.5B). The number of buttons emerging from the casing was not significantly different between the three strains but there was a trend that the *c2h2* over-expression strains showed accelerated button emergence (Figure 6.5A).

DISCUSSION

Formation of mushrooms is a highly complex developmental process (Kües 2000). After a submerged mycelium has been formed, hyphae escape the substrate to grow into the air. These hyphae form aggregates with a diameter < 1 mm. They result from a single hypha that branches intensely or arise from branches of neighboring aerial hyphae that grow towards and alongside each other. The dark-grown aggregates of *C. cinerea* can develop into different structures

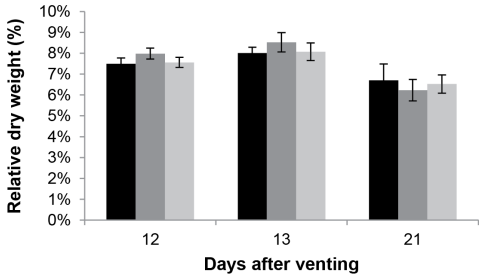

Figure 6.4: Relative dry weight of mushrooms at days 12, 13 and 21 after vent-off for *A. bisporus* strains A15 (black bar), AT273-1 (dark grey bar), and AT273-5 (light grey bar). Bars represent standard deviation (n=10).

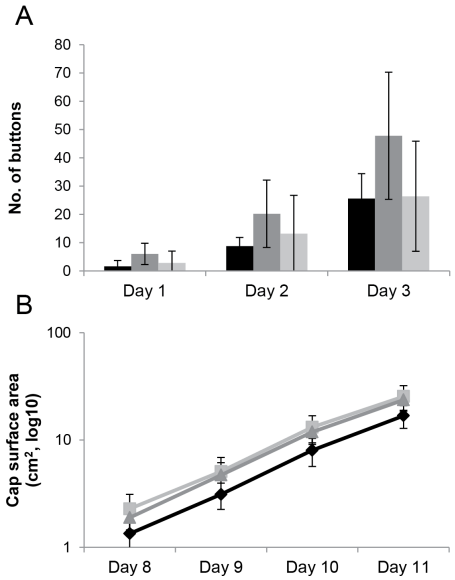

Figure 6.5: Number of A15 (black), AT273-1 (dark grey), and AT273-5 (light grey) buttons that had emerged from the casing soil 1, 2 and 3 days after venting (A) and expansion of mushroom caps of the three strains in time (B). Bars represent standard deviation (n=10).

depending on light conditions. Continuation of growth in the dark results in formation of sclerotia, while a 12 h day-night cycle induces development of initials. Initials, or primordia, are the first fruiting body specific structures and can be selectively stained with Janus green (Sánchez and Moore 1999). The switch from aggregate to primordia can be considered key in development since it determines the structure to develop into a sexual reproductive structure. The fact that *c2h2* of *S. commune* is involved in the switch from aggregates to primordia (Ohm et al. 2011) makes it a gene of high interest for fruiting body development. Here the *c2h2* orthologue of *A. bisporus* was over-expressed resulting in accelerated mushroom formation.

Expression of *c2h2* in different developmental stages was compared to that in casing mycelium. Gene *c2h2* was ≥ 4-fold upregulated in initials of *A. bisporus*. Upregulation was also found in stage I and stage II buttons, in particular in cap tissue. Expression of *c2h2* was reduced or ≤ 2-fold upregulated in the tissues of young fruiting bodies with the exception of veil and gill tissue. These expression data indicate that *c2h2* functions early in fruiting body development, while it also seems to have a role in selective tissues of young mushrooms.

Gene *c2h2* of *A. bisporus* was over-expressed in the commercial *A. bisporus*

strain A15. Two transformants were selected for phenotypic analysis. These strains, called AT273-1 and AT273-5, displayed 30-fold and 2.5-fold increased *c2h2* expression, respectively. Phenotypes of these strains were similar, indicating that a few fold increased expression of *c2h2* is sufficient to obtain a full effect of over-expression. Morphology, cap expansion rate, and total number and biomass of harvested mushrooms were not affected by over-expression of *c2h2*. However, formation of mushrooms with a cap size ≥ 4 cm was accelerated. Biomass of harvested mushrooms was increased on day 9 to 11 (first flush) and 19 to 20 (second flush) in *A. bisporus* AT273-1 and day 11, 19, and 20 in *A. bisporus* AT273-5 when compared to A15. On the other hand, A15 produced more biomass on day 13, 14, and 22. The number of harvested mushrooms also indicated accelerated growth of the *c2h2* over-expressors. The fact that expansion rate of mushrooms was similar between the transformants and A15 implies that accelerated mushroom formation is caused at the level of outgrowth of initials. This is supported by a trend that the transformants had formed more initials when compared to A15 1, 2, and 3 days after venting.

It is difficult to compare our results with other whole genome expression studies of mushroom development (Ohm et al. 2010; 2011; 2013; Morin et al. 2012; Plaza et al. 2014; Muraguchi et al. 2015). In this work RNA from a fertile casing mycelium was used as a reference for differential expression, while Plaza et al. (2014) used fertile vegetative mycelium from complete medium. Ohm et al. (2010, 2011, 2013) compared whole cultures of a sterile monokaryotic vegetative mycelium with whole cultures of the fertile dikaryon at different developmental stages. In contrast, we here used pure developmental structures and tissues. Therefore, we have only focused on expression of genes known to play a role in fruiting body development in *S. commune*. Expression of *c2h2* in *S. commune* is highest in primordia and mature fruiting bodies (Ohm et al. 2011), which is in agreement with the findings in *A. bisporus*. The genes encoding the blue light sensing complex components Wc-1 and Wc-2 are also most highly expressed in primordia and fruiting bodies of *S. commune*. This agrees with the finding that the *A. bisporus* homologues were more highly expressed in aerial structures when compared to casing mycelium, in stipe tissue when compared to cap tissue, and in outer tissues of the aerial structures when compared to inner tissues. *A. bisporus* does not require blue light to produce mushrooms. Yet, blue light sensing is also required to induce UV light-related DNA damage repair (e.g. photolyase) and in conversion of toxic porphyrin intermediates in heme (ferrochelatase) (Ohm et al. 2013). Expression of *hom2* of *S. commune* does not change during development until the stage of mature fruiting bodies when expression drops. Expression of *fst3* and *fst4* is considered constitutive in *S. commune*. Gene *hom2* was ≥ 2-fold

over-expressed when initials had developed into stage I buttons. Like *wc-1* and *wc-2*, expression of *hom2*, *fst4*, and *fst3* were more highly expressed in stipes when compared to caps but only small differences were observed between outer and inner tissues of the stage II buttons and young fruiting bodies. Genes *gat1* and *hom1* of *S. commune* are most highly expressed in late stages of mushroom development, although their upregulation is modest. These genes have a different expression profile in *A. bisporus*. They were generally downregulated in the developmental structures when compared to casing mycelium. This effect was most prominent for *gat1*. It may thus be that their role in *S. commune* and *A. bisporus* is different. Recently, expression profiles of *wc-2*, *hom2*, *fst4*, *c2h2*, *fst3*, *hom1*, and *gat1* were determined in stipe and cap during fruiting body development in *C. cinerea* (Muraguchi et al. 2015). Expression of *wc-2* increased during initial development and was higher in the stipe when compared to cap. Genes *fst4* and *fst3* were also more highly expressed in the stipe. This is similar to the *A. bisporus* expression profiles presented in this study. Expression of *hom2* remained constant during the early development, but in contrast to *A. bisporus*, was higher in the cap during later stages. Transcript levels of *gat1* slightly increased during development in *C. cinerea*, while they diminished in *A. bisporus* at this stage. Expression of *c2h2* was higher in the cap compared to the stipe tissues early in development while this was reversed later in development, a situation similar to *A. bisporus*. Together, these data support the view that mushroom development in the Basidiomycota follows a core regulatory program with species specific variations that may explain differences in morphology and sensitivity to environmental signals.

SUPPLEMENTARY MATERIAL

Table 6.3: ProteinIDs of transcription factor genes differentially expressed in initials, stage I buttons, stage II buttons, and young fruiting bodies (YFB) when compared to the preceding developmental stage. Fc = Fold-change.

Initials					
Upregulated			**Downregulated**		
ProteinID	Annotation	Fc	ProteinID	Annotation	Fc
185241	Fungal transcriptional regulatory protein, N-terminal	1.9	141117	HMG-I and HMG-Y, DNA-binding	0.5
56847	High mobility group box, HMG	INF	71198	Fungal specific transcription factor	0.4
199498	TEA/ATTS	5.6	204681	Fungal transcriptional regulatory protein, N-terminal	0.3
224104	Homeobox	1.9	229742	Zinc finger, C2H2-type	0.5
114694	Zinc finger, C2H2-type	2	206880	Zinc finger, C2H2-type	0.4
117682	Bacterial regulatory protein, MarR	2.5	189981	Zinc finger, C2H2-type	0.4
118034	Homeodomain-like	1.9	179892	High mobility group box, HMG	0.3
116879	Zinc finger, C2H2-type	2.5	180441	Basic helix-loop-helix dimerisation region bHLH	0.5
116860	Homeodomain-like SANT, DNA-binding	1.8	189288	Homeobox	0.5
132586	Basic-leucine zipper (bZIP)	3.8	192433	Homeobox	0.4
199557	Fungal specific transcription factor	2.1	**137362**	Centromere protein B, helix-turn-helix Homeodomain-like	0.2
75421	SANT, glycoside hydrolase	2.5	122840	Zinc finger, C2H2-type	0.4
185465	HMG-I and HMG-Y, DNA-binding	1.8	61584	Basic helix-loop-helix dimerisation region bHLH	0.4
223670	Fungal specific transcription factor	1.9			
192334	Zinc finger, C2H2-type	1.9			
117665	Zinc finger, C2H2-type	2.2			
230069	Zinc finger, C2H2-type	4.4			
120238	High mobility group box, HMG	4.2			
190401	Zinc finger, GATA-type	6			

Stage I buttons stipe					
ProteinID	Annotation	Fc	ProteinID	Annotation	Fc
141117	HMG-I and HMG-Y, DNA-binding	3	113594	Fungal specific transcription factor	0.5
56560	High mobility group box, HMG	2.1	74326	Zinc finger, NF-X1-type	0.5
196071	Basic leucine zipper	2	56847	High mobility group box, HMG	INF
147784	SANT, DNA-binding	2.3	204101	Zinc finger, C2H2-type	INF
147361	Homeobox	2.1	199498	TEA/ATTS	0.5
196103	Zinc finger, C2H2-type	2	116501	Basic helix-loop-helix dimerisation region bHLH	0.4
117837	HMG-I and HMG-Y, DNA-binding	1.8	68386	Homeodomain-like SANT, DNA-binding	0.6
223664	Fungal specific transcription factor	2	78651	Zinc finger, Rad18-type putative	0.4
208468	High mobility group box, HMG	2.2	194792	Basic-leucine zipper (bZIP) transcription factor	0.5

78141	Zinc finger, C2H2-type	2	123182	Fungal specific transcription factor	0.4
197611	Homeodomain-like	1.9	117682	Bacterial regulatory protein, MarR	0.5
215897	Zinc finger, DHHC-type	2	187161	Basic-leucine zipper (bZIP) transcription factor	0.6
138604	Fungal transcriptional regulatory protein, N-terminal	4.1	121841	Zinc finger, GATA-type	0.4
191883	SANT, glycoside hydrolase	2	132586	Basic leucine zipper	0.4
179892	High mobility group box, HMG	2.3	199557	Fungal specific transcription factor	0.3
187697	Fungal specific transcription factor	1.8	**229713**	Homeodomain-like	0.6
136982	Zinc finger, GATA-type	2.6	227329	Zinc finger, TFIIS-type	0.3
189288	Homeobox	2.2	211033	Lambda repressor-like, DNA-binding	0.1
119147	Zinc finger, GATA-type	2.6	192389	p53-like transcription factor, DNA-binding	0.3
212592		1.1	75421	SANT, glycoside hydrolase	0.6
61584	Basic helix-loop-helix dimerisation region bHLH	2.3	183343	Fungal transcriptional regulatory protein, N-terminal	0.4
191328	Fungal specific transcription factor	1.9	190699	Zinc finger, C2H2-type	0.6
192725	Homeobox	3.4	**218115**	DnaJ	0.5
197030	High mobility group box, HMG	2.9	222360	Fungal specific transcription factor	0.6
			187173	Basic helix-loop-helix dimerisation region bHLH	0.5
			116656		0.2
			123539		0.4
			122941	Zinc finger, C2H2-type	0.2
			189365	Zinc finger, C2H2-type	0.4
			192334	Zinc finger, C2H2-type	0.5
			195724	Zinc finger, GATA-type	0.5
			115873	Zinc finger, C2H2-type	0.3
			191564	Homeodomain-like SANT, DNA-binding	0.5
			193132	Zinc finger, C2H2-type	0.4
			193980	Zinc finger, C2H2-type	0.5
			194929		0.5
			177769	Zinc finger, C2H2-type	0.5
			188638	High mobility group box, HMG	0.3
			191136	Fungal transcriptional regulatory protein, N-terminal	0.5

Stage I buttons cap

ProteinID	Annotation	Fc	ProteinID	Annotation	Fc
141117	HMG-I and HMG-Y, DNA-binding	2.7	113594	Fungal specific transcription factor	0.2
56560	High mobility group box, HMG	2.5	74326	Zinc finger, NF-X1-type	0.4
199498	TEA/ATTS	2	56847	High mobility group box, HMG	INF
196071	Basic leucine zipper	2.3	116501	Basic helix-loop-helix dimerisation region bHLH	0.4
147784	SANT, DNA-binding	2.8	68386	Homeodomain-like SANT, DNA-binding	0.6
147361	Homeobox	2.4	78651	Zinc finger, Rad18-type putative	0.5

196103	Zinc finger, C2H2-type	1.8
193519	SANT, DNA-binding	2.1
225055	Homeodomain-like SANT, DNA-binding	1.9
135160	Transcription factor CBF/NF-Y/archaeal histone	2
78141	Zinc finger, C2H2-type	1.9
79223	Zinc finger, C2H2-type	2.8
70431	ssDNA-binding transcriptional regulator	2.2
221859	Basic-leucine zipper (bZIP) transcription factor	1.9
219430	DNA-binding, Ankyrin	2.1
138604	Fungal transcriptional regulatory protein, N-terminal	2.1
191883	SANT, glycoside hydrolase	2.1
71368	DNA-binding, Ankyrin	1.9
179892	High mobility group box, HMG	3.1
189288	Homeobox	3.1
117665	Zinc finger, C2H2-type	4.5
191725	Zinc finger, CCHC-type	2
191645	HMG High mobility group box, HMG1/HMG2	2.6
230069	Zinc finger, C2H2-type	2
190999	High mobility group box, HMG	2.1
193208	Zinc finger, C2H2-type	3.3
175561	Homeodomain-like SANT, DNA-binding	1.8
134080	MBF	2
190684	Homeodomain-like SANT, DNA-binding	2.2
191328	Fungal specific transcription factor	2.1
197030	High mobility group box, HMG	3.7

191917	Basic-leucine zipper (bZIP) transcription factor	0.5
206331	Fungal specific transcription factor	0.4
73014	Fungal transcriptional regulatory protein, N-terminal	0.5
194792	Basic-leucine zipper (bZIP) transcription factor	0.3
182409	Basic-leucine zipper (bZIP) transcription factor	0.4
123182	Fungal specific transcription factor	0.5
117682	Bacterial regulatory protein, MarR	0.4
116508	Zinc finger, C2H2-type	0.2
187161	Basic-leucine zipper (bZIP) transcription factor	0.5
121841	Zinc finger, GATA-type	0.3
132586	Basic leucine zipper	0.4
199557	Fungal specific transcription factor	0.2
219861	Fungal specific transcription factor	0.4
227329	Zinc finger, TFIIS-type	0.2
211033	Lambda repressor-like, DNA-binding	INF
192389	p53-like transcription factor, DNA-binding	0.4
75421	SANT, glycoside hydrolase	0.6
138736	Fungal transcriptional regulatory protein, N-terminal	0.2
183343	Fungal transcriptional regulatory protein, N-terminal	0.4
222360	Fungal specific transcription factor	0.6
187173	Basic helix-loop-helix dimerisation region bHLH	0.3
182895	Basic helix-loop-helix dimerisation region bHLH	0.3
116656		0.1
122941	Zinc finger, C2H2-type	0.1
189365	Zinc finger, C2H2-type	0.3
192334	Zinc finger, C2H2-type	0.5
192345	Basic leucine zipper	0.5
148501	Zinc finger, C2H2-type	0.5
122836	Zinc finger, GATA-type	0.2
195724	Zinc finger, GATA-type	0.5
115873	Zinc finger, C2H2-type	0.2
115875	Zinc finger, C2H2-type	0.5
191490	Zinc finger, C2H2-type	0.3
191564	Homeodomain-like SANT, DNA-binding	0.1

			193132	Zinc finger, C2H2-type	0.4
			193980	Zinc finger, C2H2-type	0.3
			194007	Fungal transcriptional regulatory protein, N-terminal	0.5
			194929		0.4
			122840	Zinc finger, C2H2-type	0.5
			177769	Zinc finger, C2H2-type	0.4
			183616	Fungal transcriptional regulatory protein, N-terminal	0.5
			184201	Zinc finger, C2H2-type	0.2
			188638	High mobility group box, HMG	0.2
			190401	Zinc finger, GATA-type	0.5
			191136	Fungal transcriptional regulatory protein, N-terminal	0.4

Stage II stipe center

ProteinID	Annotation	Fc	ProteinID	Annotation	Fc
208769	Zinc finger, PARP-type	2.9	113594	Fungal specific transcription factor	0.3
117743	Fungal specific transcription factor	3.3	224104	Homeobox	0.1
204206	Fungal transcriptional regulatory protein, N-terminal Zinc finger, C2H2-type	5.3	199557	Fungal specific transcription factor	0.5
224564	Fungal transcriptional regulatory protein, N-terminal Zinc finger, C2H2-type	4.6	178849	Fungal transcriptional regulatory protein, N-terminal	0.5
138736	Fungal transcriptional regulatory protein, N-terminal	3.9	223295	Fungal specific transcription factor	0.5
			122941	Zinc finger, C2H2-type	0.3
			189365	Zinc finger, C2H2-type	0.5
			117665	Zinc finger, C2H2-type	0.1
			195724	Zinc finger, GATA-type	0.4
			115873	Zinc finger, C2H2-type	0.4
			191490	Zinc finger, C2H2-type	0.1
			191564	Homeodomain-like SANT, DNA-binding	0.4
			193208	Zinc finger, C2H2-type	0.1
			184201	Zinc finger, C2H2-type	0.2
			116512		1.8

Stage II stipe tissue

ProteinID	Annotation	Fc	ProteinID	Annotation	Fc
204101	Zinc finger, C2H2-type	1.3	185241	Fungal transcriptional regulatory protein, N-terminal	0.5
177333	Zinc finger, GATA-type	1.7	113594	Fungal specific transcription factor	0.3
190401	Zinc finger, GATA-type	3.3	223451	Zinc finger, C2H2-type	0.4
			224104	Homeobox	0.3
			224564	Fungal transcriptional regulatory protein, N-terminal Zinc finger, C2H2-type	0.5
			192389	p53-like transcription factor, DNA-binding	0.3
			117665	Zinc finger, C2H2-type	0.2

			230069	Zinc finger, C2H2-type	0.4
			191490	Zinc finger, C2H2-type	0.2
			193208	Zinc finger, C2H2-type	0.2
			197030	High mobility group box, HMG	0.5

Stage II stipe skin

ProteinID	Annotation	Fc	ProteinID	Annotation	Fc
190401	Zinc finger, GATA-type	2.4	224564	Fungal transcriptional regulatory protein, N-terminal Zinc finger, C2H2-type	0.5
			138736	Fungal transcriptional regulatory protein, N-terminal	INF
			230069	Zinc finger, C2H2-type	0.5

Stage II cap skin

ProteinID	Annotation	Fc	ProteinID	Annotation	Fc
185241	Fungal transcriptional regulatory protein, N-terminal	2.2	122355	Homeobox	0.6
132586	Basic leucine zipper	2.2	138736	Fungal transcriptional regulatory protein, N-terminal	INF
178849	Fungal transcriptional regulatory protein, N-terminal	2.4	230069	Zinc finger, C2H2-type	0.2
180216	Transcription factor, STE-like	1.8	115875	Zinc finger, C2H2-type	0.5
192433	Homeobox	1.8	192725	Homeobox	0.5
194007	Fungal transcriptional regulatory protein, N-terminal	1.9	116512		0.9

Stage II cap tissue

ProteinID	Annotation	Fc	ProteinID	Annotation	Fc
194007	Fungal transcriptional regulatory protein, N-terminal	1.8	79223	Zinc finger, C2H2-type	0.5
			230069	Zinc finger, C2H2-type	0.4
			116512		0.8

Stage II gill tissue

ProteinID	Annotation	Fc	ProteinID	Annotation	Fc
138736	Fungal transcriptional regulatory protein, N-terminal	3.1	185241	Fungal transcriptional regulatory protein, N-terminal	0.5
			199498	TEA/ATTS	0.4
			79223	Zinc finger, C2H2-type	0.4
			192389	p53-like transcription factor, DNA-binding	0.5
			189365	Zinc finger, C2H2-type	0.6
			191490	Zinc finger, C2H2-type	0.4
			193208	Zinc finger, C2H2-type	0.5
			190401	Zinc finger, GATA-type	0.3

Young fruiting bodies stipe center

ProteinID	Annotation	Fc	ProteinID	Annotation	Fc
185241	Fungal transcriptional regulatory protein, N-terminal	2.3	223451	Zinc finger, C2H2-type	0.3
113594	Fungal specific transcription factor	2.5	147784	SANT, DNA-binding	0.6

116501	Basic helix-loop-helix dimerisation region bHLH	2.4	138604	Fungal transcriptional regulatory protein, N-terminal	0.5
121272	Fungal specific transcription factor	3.1	138736	Fungal transcriptional regulatory protein, N-terminal	0.4
199557	Fungal specific transcription factor	2.6	117665	Zinc finger, C2H2-type	0.3
180441	Basic helix-loop-helix dimerisation region bHLH	1.7	230069	Zinc finger, C2H2-type	0.4
192433	Homeobox	2	197030	High mobility group box, HMG	0.3
195724	Zinc finger, GATA-type	2.7			
191490	Zinc finger, C2H2-type	4.1			
191564	Homeodomain-like SANT, DNA-binding	3.9			

Young fruiting bodies stipe shell

ProteinID	Annotation	Fc	ProteinID	Annotation	Fc
116501	Basic helix-loop-helix dimerisation region bHLH	2.3	224104	Homeobox	0.4
121272	Fungal specific transcription factor	2.6	138604	Fungal transcriptional regulatory protein, N-terminal	0.5
204206	Fungal transcriptional regulatory protein, N-terminal Zinc finger, C2H2-type	5.1	185465	HMG-I and HMG-Y, DNA-binding	0.6
224564	Fungal transcriptional regulatory protein, N-terminal Zinc finger, C2H2-type	3.4	178849	Fungal transcriptional regulatory protein, N-terminal	0.4
180441	Basic helix-loop-helix dimerisation region bHLH	1.7	117665	Zinc finger, C2H2-type	0.2
			193208	Zinc finger, C2H2-type	0.2

Young fruiting bodies stipe skin

ProteinID	Annotation	Fc	ProteinID	Annotation	Fc
189243	Zinc finger, C2H2-type	4.2	178849	Fungal transcriptional regulatory protein, N-terminal	0.4
116501	Basic helix-loop-helix dimerisation region bHLH	2.2	117665	Zinc finger, C2H2-type	0.5
204206	Fungal transcriptional regulatory protein, N-terminal Zinc finger, C2H2-type	1.8	230069	Zinc finger, C2H2-type	0.2
180441	Basic helix-loop-helix dimerisation region bHLH	1.7			
190401	Zinc finger, GATA-type	2.9			

Young fruiting bodies cap skin

ProteinID	Annotation	Fc	ProteinID	Annotation	Fc
189243	Zinc finger, C2H2-type	2.4	132586	Basic leucine zipper	0.5
190401	Zinc finger, GATA-type	2.5	178849	Fungal transcriptional regulatory protein, N-terminal	0.3
			180216	Transcription factor, STE-like	0.5
			191645	HMG High mobility group box, HMG1/HMG2	0.5
			230069	Zinc finger, C2H2-type	0.2

Young fruiting bodies cap tissue

ProteinID	Annotation	Fc	ProteinID	Annotation	Fc
189243	Zinc finger, C2H2-type	2.3	74659	Zinc finger, PARP-type	0.3
192596	Fungal transcriptional regulatory protein, N-terminal	2	199498	TEA/ATTS	0.4
122836	Zinc finger, GATA-type	2.3	78651	Zinc finger, Rad18-type putative	0.5
			224104	Homeobox	0.2
			192389	p53-like transcription factor, DNA-binding	0.3
			185465	HMG-I and HMG-Y, DNA-binding	0.5
			223670	Fungal specific transcription factor	0.5
			178849	Fungal transcriptional regulatory protein, N-terminal	0.4
			223295	Fungal specific transcription factor	0.5
			190080	Zinc finger, TFIIS-type	0.4
			117665	Zinc finger, C2H2-type	0.2
			191645	HMG High mobility group box, HMG1/HMG2	0.4
			230069	Zinc finger, C2H2-type	INF
			191490	Zinc finger, C2H2-type	0.2
			116512		0.8

Young fruiting bodies gill tissue

ProteinID	Annotation	Fc	ProteinID	Annotation	Fc
185241	Fungal transcriptional regulatory protein, N-terminal	4.4	122355	Homeobox	0.5
189243	Zinc finger, C2H2-type	3.4	223451	Zinc finger, C2H2-type	0.4
199498	TEA/ATTS	3.6	196103	Zinc finger, C2H2-type	0.5
116501	Basic helix-loop-helix dimerisation region bHLH	5.8	224564	Fungal transcriptional regulatory protein, N-terminal Zinc finger, C2H2-type	0.5
224104	Homeobox	3	138736	Fungal transcriptional regulatory protein, N-terminal	INF
222207	TEA/ATTS	2.7	189288	Homeobox	0.5
132586	Basic leucine zipper	3	190080	Zinc finger, TFIIS-type	0.4
79223	Zinc finger, C2H2-type	5.9	191645	HMG High mobility group box, HMG1/HMG2	0.4
192389	p53-like transcription factor, DNA-binding	2.5	230069	Zinc finger, C2H2-type	0.4
182895	Basic helix-loop-helix dimerisation region bHLH	2.3			
223295	Fungal specific transcription factor	2			
189365	Zinc finger, C2H2-type	2.7			
192433	Homeobox	2.8			
148501	Zinc finger, C2H2-type	2.4			
115873	Zinc finger, C2H2-type	2.5			
191490	Zinc finger, C2H2-type	2			
193208	Zinc finger, C2H2-type	2.7			
194929		1.7			
188638	High mobility group box, HMG	3.4			
190401	Zinc finger, GATA-type	11.4			

182786	Basic-leucine zipper (bZIP) transcription factor	1.8			

			Young fruiting bodies veil		
ProteinID	Annotation	Fc	ProteinID	Annotation	Fc
185241	Fungal transcriptional regulatory protein, N-terminal	2.1	223451	Zinc finger, C2H2-type	0.5
189243	Zinc finger, C2H2-type	2.9	190080	Zinc finger, TFIIS-type	0.4
224104	Homeobox	2.3			
222207	TEA/ATTS	1.9			
79223	Zinc finger, C2H2-type	3			
182895	Basic helix-loop-helix dimerisation region bHLH	1.8			
189365	Zinc finger, C2H2-type	2.1			
117665	Zinc finger, C2H2-type	1.9			
193208	Zinc finger, C2H2-type	2.4			
188638	High mobility group box, HMG	2.2			
190401	Zinc finger, GATA-type	4.2			

Analysis has been performed in version 3 of the *A. bisporus* genome. Since this improved version is not yet published we use the ProteinIDs and corresponding annotations of version 2 of the genome sequence (v2, http://genome.jgi.doe.gov/Agabi_varbisH97_2). In version 3 some genes, highlighted with dark grey shading, have been newly identified as transcription factor genes. ProteinIDs in bold are present once in the table and light grey shading indicates differential expression. Some genes have been annotated as transcription factors in version 3 that did not exist in version 2. Since these genes do not have a proteinID in version 2, they are not shown in this table.

Table 6.4: Expression levels (FPKM) of orthologues of regulators of mushroom formation in *S. commune* during development of *A. bisporus*.

	wc-1	*wc-2*	*hom2*	*fst4*	*c2h2*	*fst3*	*gat1*	*hom1*
Casing Myc	64	139	50	120	45	74	284	438
Initials	88	827	82	233	196	84	250	166
	Stage I buttons							
Stipe	145	474	281	289	140	155	113	250
Cap	71	382	69	249	384	65	119	150
	Stage II buttons							
Stipe Center	104	772	301	251	143	93	50	312
Stipe Tissue	214	1558	302	251	55	166	69	378
Stipe Skin	174	1145	234	242	70	152	118	386
Cap Skin	137	448	32	155	94	63	123	276
Cap Tissue	86	212	55	192	172	69	95	211
Gill Tissue	51	111	83	234	343	61	86	179
	Young fruiting bodies							
Stipe Center	197	1050	416	286	52	113	135	618
Stipe Shell	297	2620	405	246	73	138	96	627
Stipe Skin	264	3335	232	198	13	139	77	585
Cap Skin	236	1136	25	105	18	75	105	472
Cap Tissue	181	328	51	99	6	75	72	351
Gill Tissue	242	1267	69	161	137	101	116	492
Veil	149	462	86	221	302	98	115	296

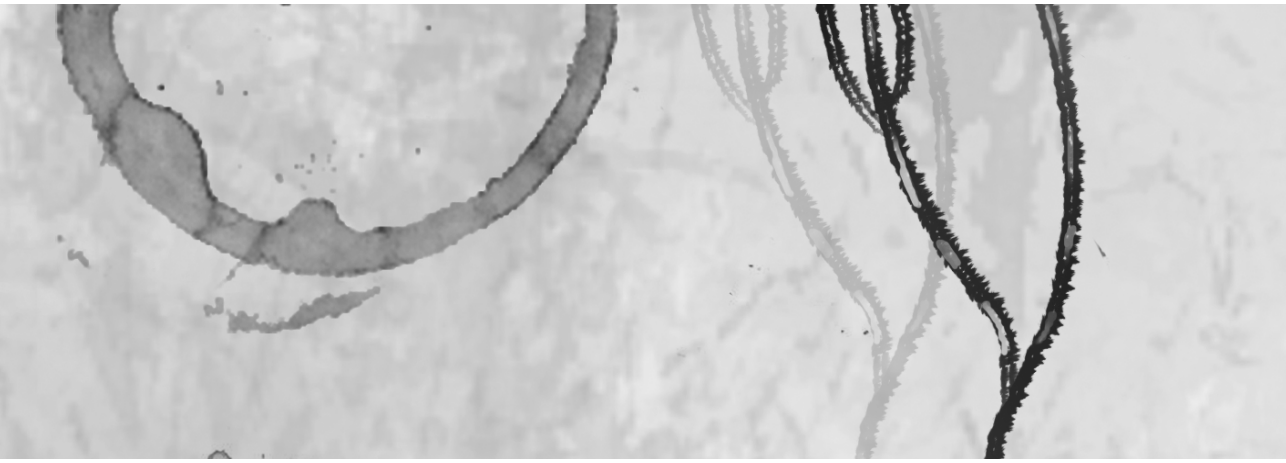

7

RESPIRATORY BURSTS DURING VEGETATIVE GROWTH OF *Agaricus bisporus*

Aurin M. Vos, Luis G. Lugones, Heike Schmitt, Han A. B. Wösten

ABSTRACT

Respiratory rhythms were found during vegetative growth of *Agaricus bisporus* in compost. The respiratory bursts of 3 - 6 h were initially observed every 13 h but the interval increased up to 20 h and became more irregular in time. The bursts were accompanied by an up to 3.5 fold increase in CO_2 production and O_2 consumption and an increase in compost temperature of up to 3 °C. In addition, the respiratory quotient during a respiratory burst was up to 1.2 fold higher when compared to the pre-burst minimum. Respiratory bursts between parts of compost synchronized when they were in physical contact, showing that hyphal interactions and not volatiles or heat are necessary for synchronization. The potential role of the respiratory bursts in lignin degradation is discussed.

INTRODUCTION

Commercially produced mushrooms of the basidiomycete *A. bisporus* are grown on compost. In the Netherlands, this substrate is produced in two phases in large aerated bunkers. Its raw materials comprise of wheat straw, horse manure, gypsum, and water either or not supplemented with chicken manure (Gerrits 1988). Heat produced by microbial activity during the first phase of composting (PI) results in a maximum compost temperature of 80 °C. After 3 - 6 days the compost is transferred to a new bunker to start phase II (PII). During a 2-day period, the temperature is first lowered to 50 °C, then increased to 60 °C, and subsequently decreased to 45 °C. It is kept at this latter temperature for 3 days to allow the development of a thermophilic fungal community (Gerrits 1988). *Scytalidium thermophilum* (also known as *Humicola insolens*; Straatsma and Samson 1993) plays an important role in preparing a compost suitable for colonization by *A. bisporus* (Straatsma et al 1994). It is thought to remove ammonia and to suppress competitors of *A. bisporus* (Ross and Harris 1983). About 60 % and 50 % of xylan and cellulose, respectively, are removed during phase I and II, while lignin remains largely intact (Jurak 2015, Jurak et al. 2015). Mixing spawn of *A. bisporus* through PII-end compost initiates phase III (PIII). The compost is colonized during 16 - 19 days at a substrate temperature of 25 °C. During PIII 50 % of lignin is removed, while only 15 % xylan and 10 % cellulose are removed as compared to PII-end (Jurak 2015). It should be noted that cellulose loss is underestimated due to the contribution of fungal glucan in the glucose assay used to quantify cellulose. PIII-end compost is transferred to mushroom growers. Phase IV (PIV) starts by placing a casing layer consisting of peat and lime on top of the compost. This layer serves as a water reservoir for mushrooms and contains microorganisms thought to be involved in the removal of volatiles that repress mushroom formation (Visscher 1988, Noble et al 2009). High CO_2 levels and a

relative humidity of 85 % ensure efficient colonization of the casing layer during a 7-day-period. Mushroom formation is induced by venting the growth chamber; thereby reducing CO_2 levels and compost temperature to 18 - 22 °C and increasing the relative humidity to 87 - 90 % (Visscher 1988). A yield of 30 kg mushrooms results from a layer of 85 - 95 kg m^{-2} compost. The mushrooms are harvested in 2 - 3 flushes that occur each 7 - 8 days. After PIV, 54 % and 44 % of cellulose and xylan, respectively, have been removed relative to PII-end, while 58 % of lignin has been degraded (Jurak 2015).

Here it is shown that colonization of compost by *A. bisporus* is accompanied by respiratory bursts that are synchronized over large distances (i.e. at least 60 cm) by hyphal interactions. Consumption of O_2 and production of CO_2 increased up to 3.5 fold during a burst, while the respiratory quotient (RQ) increases up to 1.22 fold. These results are discussed in relation to lignin degradation.

MATERIAL AND METHODS

STRAINS AND SUBSTRATE

A. bisporus strains A15 (Sylvan, Netherlands) and MnP1-1 (Chapter 5) were grown at 25 °C on malt extract agar medium (MEA; 20 gr l^{-1} malt extract [BD biosciences, Franklin Lakes, USA], 2.1 gr l^{-1} MOPS, pH 7.0, and 1.5 % agar) or on PII-end compost (CNC Grondstoffen, Milsbeek, the Netherlands). The compost was inoculated with rye based A15 spawn (Sylvan) or with MnP1-1 spawn that was prepared as described (Chapter 3).

Respiration of MnP1-1 (hyg+) was assessed in a 500 ml bottle containing 50 ml MEA supplemented with 40 μg ml^{-1} hygromycin, 50 μg ml^{-1} kanamycin, and 50 μg ml^{-1} ampicillin. Respiration measurements with PII-end compost was done in the presence and absence of strain A15. To this end, 50 g compost was either or not inoculated with 10 spawn grains in a 1 L flask. Temperature was monitored during 21 days in 1 kg (30 x 20 x 22 cm boxes), 8 kg (40 x 60 x 20 cm boxes), or 16 kg (40 x 60 x 22 cm boxes) PII-end compost that was inoculated with 8, 64, or 75 gr of spawn, respectively. The 1 and 8 kg compost boxes were used to monitor temperature during PIII. To this end, they were incubated at 25 °C and covered with plastic film containing 50 holes of 3 mm m^{-2}. The 16 kg compost boxes were used to monitor temperature during PIII and PIV. To this end, they were incubated at 22 °C at a relative humidity of 95 % and 1500 - 2000 ppm CO_2 (Unifarm, Wageningen). After 16 days, the compost of each box was overlaid with 7 kg casing layer (CNC, Milsbeek, The Netherlands), after which growth was prolonged for 14 days. Manually broken casing layer was mixed 4 days prior to venting to create fast regenerative growth and a more equal distribution of *A.*

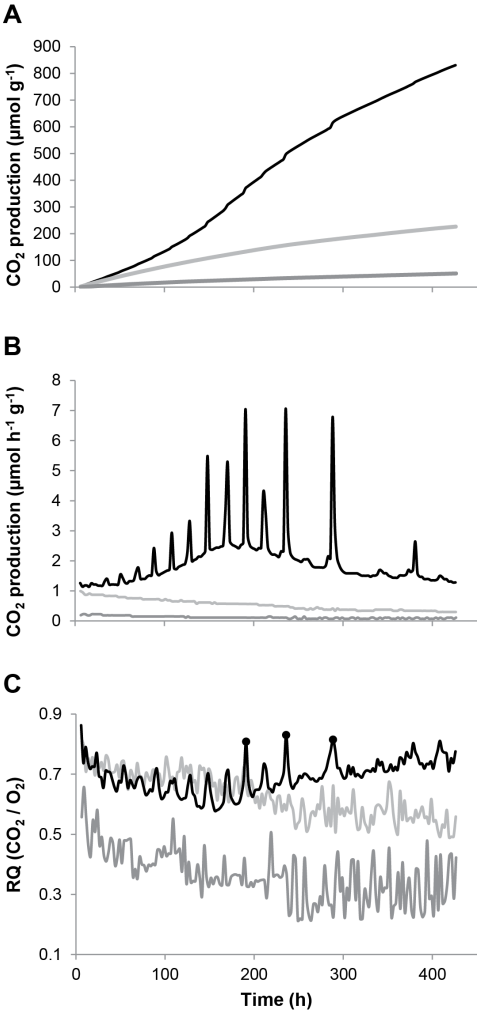

Figure 7.1: Typical patterns of cumulative CO_2 production (A), CO_2 production rate (B), and respiratory quotient (C) by sterile compost (dark-grey), compost without *A. bisporus* (light grey), and compost inoculated with *A. bisporus* (black). At time points indicated with a black dot in (C), O_2 levels were below 17.97 % resulting in an underestimation of the actual O_2 consumption and therefore overestimation of the RQ.

bisporus in the casing. After venting, air temperature was decreased to 18 °C, while relative humidity and CO_2 levels decreased to 85% and 1200 ppm, respectively.

CO_2, O_2, AND TEMPERATURE MEASUREMENTS

Experiments were performed at least in biological triplicates. CO_2 production and O_2 consumption were measured with optical CO_2 and O_2 sensors using a respirometer (Biometric Systems, Germany). In short, CO_2 and O_2 measurements were made at the start of the experiment and 2.5 h later. Air in the flasks was then refreshed allowing a new cycle of measurements at t = 0 and t = 2.5 h. Data were processed with a custom R script (R v3) that calculated molar amounts of produced CO_2 and consumed O_2, correcting for temperature and pressure. Synchronization experiments between parts of compost were analysed using a Mann-Whitney U test ($p < 0.05$).

To correlate temperature changes with changes in CO_2 levels Arduinos (https://www.arduino.cc/) equipped with temperature (DS18B20; Dallas Semiconductor, USA) or CO_2 (MG811; Sandbox Electronics, Finland) sensors were used. To this end, the temperature sensor was placed 2 cm below the compost surface, while the CO_2 sensor was placed 5 cm above the compost.

RESULTS

RESPIRATORY BURSTS IN COMPOST

PII-end compost was sterilized or either or not inoculated with *A. bisporus*. CO_2 production and O_2 consumption were measured every 2.5 h during a 425 h period after 5 days incubation at 25 °C. Total CO_2 produced per gram of sterile compost, compost without *A. bisporus*, and compost with *A. bisporus* was 52, 227, and 831 μmol during the 425 h period, respectively (Figure 7.1A). In compost without *A. bisporus* the CO_2 production rate decreased over time from 1 to 0.3 μmol h^{-1} while $\leq$ 0.23 μmol h^{-1} CO_2 was released from sterile compost (Figure 7.1B). In compost with *A. bisporus* CO_2 production increased from 1.2 to 2.6 μmol h^{-1} during the first 180 h and then decreased to 1.3 μmol h^{-1}. This general course was accompanied by distinct respiratory bursts of 3 - 6 h. The CO_2 production rate during the bursts increased up to 3.5 fold as compared to the intermediate periods. These intermediate periods were initially 13 h in length. They had a length of 20 h and 50 - 90 h after 200 and 240 h, respectively, with an irregular pattern in the latter case. No respiratory bursts were observed in the absence of *A. bisporus* but they were produced in sterilized compost in which this mushroom forming fungus was growing (Figure S1). However, growth of *A. bisporus* in sterilized compost was slow coinciding with low CO_2 production. To verify respiratory burst production

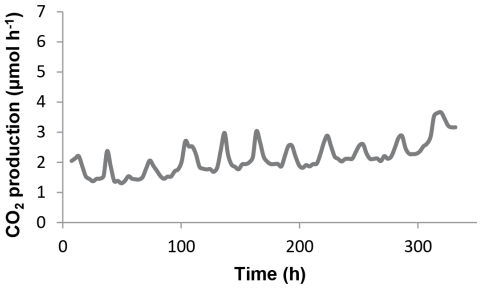

Figure 7.2: Typical CO_2 production profile of *A. bisporus* strain MnP1-1 on malt extract.

of *A. bisporus* in the absence of other microbes, this fungus was also grown on malt extract. Also in this case respiratory burst were observed with a median interval of 30 - 31.5 h (Figure 2). The duration of these bursts was 6 - 15 h reaching a maximum CO_2 production ≤ 2-fold in 3 - 9 h as compared to pre-burst levels, after which CO_2 production normalized in 6 - 9 h.

The respiratory quotient (RQ; mol CO_2 released / mol O_2 consumed) in compost without *A. bisporus* decreased from 0.8 to 0.55 during the 450 h period (Figure 7.1C), while it decreased in sterilized compost from 0.6 to 0.3. During the colonization of *A. bisporus* the maximal RQ decreased from 0.8 to 0.65 during a 150 h period and then increased to 0.8 again in the following 350 h (Figure 7.1C). At three time points the O_2 levels were below 17.9 % resulting in an underestimation of the actual O_2 consumption and overestimation of the RQ (Figure 7.1C, black dots). The RQ was up to 0.13 units higher during a burst as compared to the pre-burst minimum.

CO_2 production correlated with an increase in compost temperature. The increase in temperature was detected 30 min after the start of a respiratory burst, peaked 45 - 90 min later, and took 2 - 8 h to normalize to pre-peak temperature (Figure S2). Monitoring compost temperature can thus also be used to monitor respiratory bursts. Compost temperature was monitored during PIII and PIV of a semi-commercial cultivation of *A. bisporus*. Respiratory bursts were observed between day 10 and 16 of PIII (Figure 7.3) and followed a similar pattern as observed in small scale lab cultivations. They were also observed during colonization of casing and the 1st flush but not during the 2nd flush.

SYNCHRONIZATION OF RESPIRATORY BURSTS

The respiratory bursts during *A. bisporus* colonization of compost were further characterized using 6 temperature sensors that were placed 15 - 20 cm apart in a box of 40 x 60 cm. Respiratory bursts occurred during the first 500 h of a 900

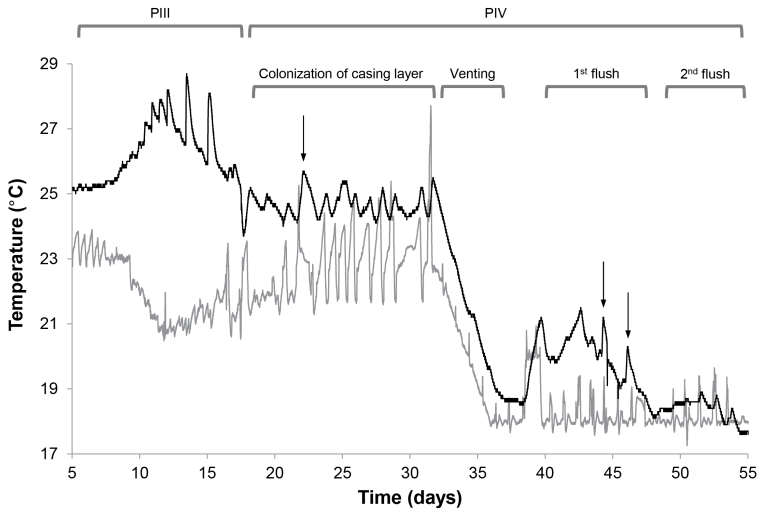

Figure 7.3: Temperature profile of compost (black line) and air in the incubation room (grey line) during vegetative growth (PIII and colonization of casing layer) and mushroom production (Venting, 1st flush, and 2nd flush) of *A. bisporus*. Respiratory bursts occurring in PIV are indicated with an arrow. These temperature peaks cannot be explained by peaks in the temperature of the incubation room.

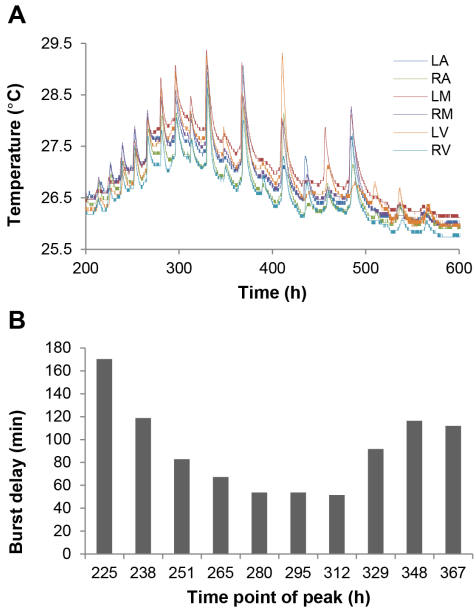

Figure 7.4: Compost temperature measured by 6 sensors spaced 15 - 20 cm apart in a box of 40 x 60 cm (A) and the maximum peak delay between the sensors during a burst (B). LA = left upper corner, RA = right upper corner, LM = left of the middle, RM = right of the middle, LV = left bottom corner, RV = right bottom corner.

h colonization period (Figure 7.4A). They resulted in a temperature increase of up to 2 °C in a 1.5 to 3 h period. Initially, a maximum time difference of 170 min was registered between the different sensors to detect a burst (Figure 7.4B). This decreased to 50 min between 225 and 280 h (Figure 7.4B), showing that the mycelium synchronized its heat production over at least 60 cm (the largest distance between sensors). No clear pattern was observed in the order sensors measured a burst. After 330 h the time between the sensors picking up a burst increased, while after 390 h not all sensors picked up a burst. One more burst was registered by all sensors at 410 h, after which occurrence of bursts became erratic.

Two aliquots of 1 kg PII-end compost were placed next to each other (i.e. physically touching each other), were placed 3 cm apart, or were separated by aluminium foil. In the latter case, transfer of heat did occur but hyphae of the two parts could not interact. The temperature in the center of both parts of compost was monitored for 300 h after 8 days (Figure 7.5). The average time between sensors in the two parts of compost picking up a burst was lower when the parts were in physical contact (38 min) when compared to those placed 3 cm apart or separated by aluminium foil (3 h 50 min and 4 h 33 min, respectively; Mann-Whitney U, $p < 0.05$). These data show that bursts are synchronized during colonization due to physical contact of the mycelium.

DISCUSSION

Here it was shown for the first time that growth and development of *A. bisporus* is accompanied by respiratory bursts with increased O_2 consumption and CO_2 release. These bursts had a 3 - 6 h duration and peaked after 1.5 - 3 hours. The period between bursts increased from 13 h to 20 h within a 14 day growth period after which they became less frequent and irregular. Bursts in compost were more frequent when compared to malt extract that showed a median interval of 30 - 31.5 h. In addition, the increase in CO_2 production during a burst in compost was more pronounced in compost (≤ 3.5 fold) when compared to malt extract (≤ 2 fold). The reasons for the differences in period and intensity of the bursts is not yet clear. The large deviation of the burst period from 24 h excludes a circadian rhythm (Loros and Dunlap 2001). Light independent respiratory patterns with periods varying between 7.5 and 22.5 h were also observed during colonization of malt extract and wood blocks by the mushroom forming fungi *Lentinus lepideus*, *Lenzites trabea*, *Poria monticola*, and *Coniophora* (Damaschke and Becker 1966; Smith 1973). Such ultradian periods (i.e. shorter than a circadian rhythm; Richard 2003) have also been observed in yeast in the case of glycolytic and respiratory oscillations. Temperature profiles of rye colonized by *Pleurotus ostreatus* showed a median infradian interval (i.e. longer than a circadian rhythm)

of 49 h, while *Schizophyllum commune* and *Trametes versicolor* did not produce temperature patterns (our unpublished data, not shown). These data show that respiratory rhythm intervals are highly variable in basidiomycetes and that they may not generally occur in this group of fungi. Bursts of *A. bisporus* became increasingly synchronized with progression of colonization, as was shown by monitoring temperature changes at different positions in the compost. It was hypothesized that this was caused by increasing contact between the mycelia that resulted from different inoculation points (i.e. the spawn grains). Indeed, synchronization was observed when two parts of compost were placed next to each other (i.e. in physical contact) but not when aluminium foil was placed in between the parts or when they were placed 3 cm apart. The latter experiments showed that volatiles or heat transfer are not responsible for synchronization of the bursts. Synchronization of coupled oscillating systems may explain how long distance synchronization arises in fungi (Fricker et al. 2007 and references therein). Notably, near the end of the exponential growth phase the synchronization started to deteriorate, while it disappeared after this phase. This may be caused by a reduction of the connectivity of the hyphal network, which would fit with the observation that a large portion of hyphae in compost is dead after vegetative growth of *A. bisporus* (Chapter 2; Vos et al. 2017).

So far, the cause of the bursts is unknown. It seems not related to oscillations in transport of the amino-acid analogue α-aminoisobutyrate. These oscillations were approximately synchronous in colonies of *Phanerochaete velutina* but were not related to temperature fluctuations (Tlalka et al. 2002; Tlalka et al. 2003; Fricker et al. 2007; Tlalka et al. 2009). The finding that respiratory bursts of *A. bisporus* are accompanied by an increase in RQ indicates that these bursts relate to changes in metabolic activity. For instance, 150 h after the start of the experiment the RQ decreased from 0.7 at the peak of the burst to 0.58 in the following inter-burst period. RQ's of 1 and 0.7 are typical for mineralization of carbohydrates and fats, respectively (Péronnet and Massicotte 1991). A RQ < 0.7 can be explained by mineralization of highly reduced compounds but also by production of highly oxidized compounds. These events may occur at the same time. How could we explain these RQ values in the context of colonization of compost by *A. bisporus*? This basidiomycete converts a relatively high amount of lignin during PIII, while conversion of this polymer is less pronounced during PIV. This correlates with the incidence of the respiratory bursts. Therefore, it is tempting to speculate that lignin is oxidized during the period in between the bursts, which is followed by mineralization during the bursts. This hypothesis could be tested by monitoring the temporal release of ^{13}C- or ^{14}C-labelled CO_2 resulting from mineralization of labelled lignin. An alternative explanation of the

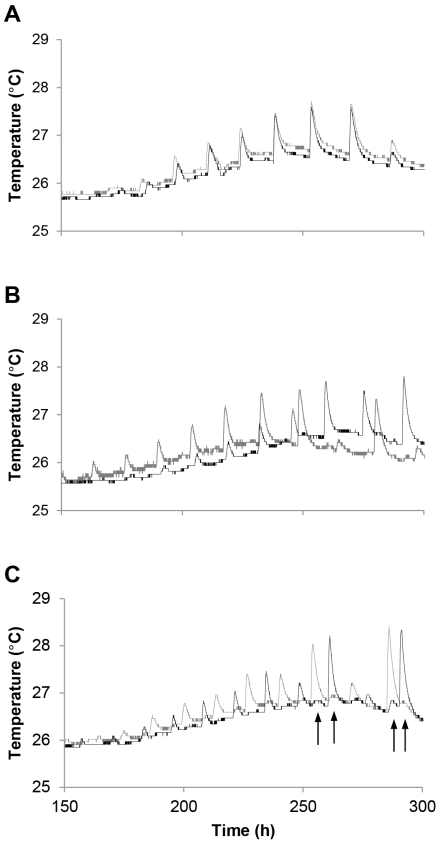

Figure 7.5: Typical temperature profiles of two parts of compost (dark and light grey) pressed together (A), placed 3 cm apart (B), or separated by aluminium foil (C). Arrows indicate where heat transfer through the aluminium foil was detected by the temperature sensor.

burst may be the production of organic acids by *A. bisporus* during the inter-burst periods. These compounds are more oxidized when compared to for instance glucose. However, preliminary evidence shows that bursts and not the inter-burst period is associated with the production of organic acid. Calcium oxalate crystals are associated with the hyphae of *A. bisporus* (Whitney and Arnott 1987). Therefore, the respiratory bursts may be related to oxalic acid secretion during the burst and by its (partial) conversion by secreted oxalate oxidase or oxalate decarboxylase. This would result in CO_2 and H_2O_2 and CO_2 and formic acid, respectively. *A. bisporus* was shown to produce oxalate decarboxylase in malt extract (Kathiara et al. 2000). In addition, laccase and manganese peroxidase can mediate degradation of oxalic acid to CO_2 and a net yield of 1 - 2 or 0 - 1 H_2O_2, respectively, and 0 - 2 Mn^{3+} (Urzúa et al. 1998a; 1998b; Schlosser and Höfer 2002). Notably, H_2O_2 is involved in the Fenton reaction and serves as co-factor of manganese peroxidase (Hofrichter 2002; Arantes et al. 2012). Thus, several mechanisms may link lignin degradation to the respiratory bursts.

SUPPLEMENTARY MATERIAL

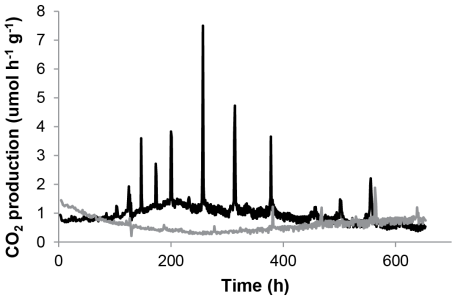

Figure 7.6: CO_2 production rate of 10 g PII-end compost that had (grey line) or had not (black line) been sterilized prior to inoculation with 4 spawn grains of *A. bisporus*. CO_2 production was monitored after pre-growth at 25 °C for 3 days.

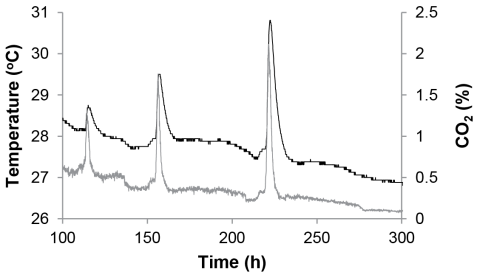

Figure 7.7: Respiratory bursts in 1 kg compost as measured by monitoring changes in temperature (black) and CO_2 (grey).

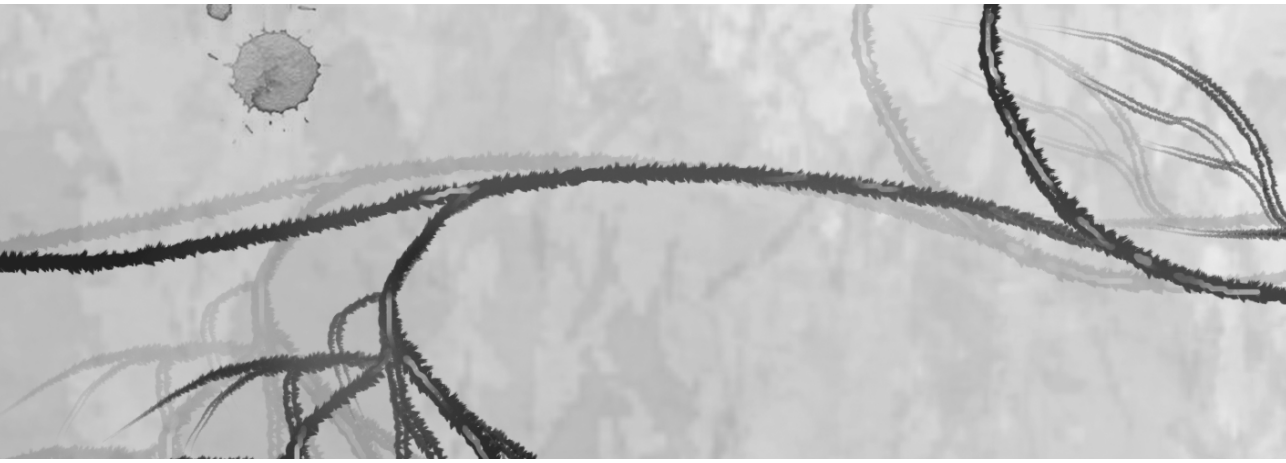

8

SUMMARY AND GENERAL DISCUSSION

Aurin M. Vos

Mushrooms of *Agaricus bisporus*, known as button mushrooms ("champignons"), represent a high quality food. They are rich in protein, fibers, minerals, and contain bioactive compounds such as immune-stimulatory polysaccharides. Button mushroom production can be considered sustainable because of the low amount of pesticides that are used and the use of compost that is based on low quality waste streams. The Dutch mushroom industry produces 270 thousand tons of button mushrooms per annum making the Netherlands one of the main producers worldwide.

Compost used to grow *Agaricus bisporus* is produced in 2 phases. Phase I (PI) starts with mixing horse manure, wheat straw, gypsum, and water, either or not in combination with chicken manure (Gerrits 1988). A thermophilic microbial community develops that increases compost temperature up to 80 °C by metabolizing (simple) sugars. Compost temperature in Phase II (PII) ultimately is reduced to 45 °C allowing the establishment of a thermophilic fungal community. At the end of PII, 8 - 11 days after the start of PI, around 50 % and 60 % of the wheat straw polysaccharides cellulose and xylan have been removed, respectively, while lignin is largely unaffected (Jurak et al. 2014; Jurak 2015; Jurak et al. 2015b). PII-end compost is inoculated with *A. bisporus* spawn to start phase III (PIII). *A. bisporus* colonizes the compost in 16 - 19 days while producing the ligninolytic enzymes laccase (Lcc) and manganese peroxidase (MnP) (Wood and Goodenough 1977; Bonnen et al. 1994). This coincides with degradation of about 50 % of the lignin, while only 15 % and 10 % of xylan and cellulose are degraded relative to PII-end (Jurak 2015). PIII-end compost supplemented with protein (Gerrits 1988) is topped with casing layer at the grower. During Phase IV (PIV) the casing layer is colonized by *A. bisporus* under high CO_2 levels for 7 days. Mushroom formation is induced by venting the atmosphere thereby reducing CO_2 levels, compost temperature, and relative humidity (Visscher 1988). A total of yield of 30 kg m^{-2} is produced in 2 - 3 flushes with a 7 - 8 day interval from 85 - 95 kg compost m^{-2}. Lignin degrading activities like those of Lcc and MnP are downregulated during mushroom formation while (hemi)cellulose acting activities increase (Wood 1977; Claydon et al. 1988; Bonnen et al. 1994). In agreement, about 44 % and 29 % of cellulose and xylan are removed while only 8 % of lignin is degraded during PIV relative to PII (Jurak 2015). As a result, 46 % and 56 % of cellulose and hemicellulose remain unutilized for mushroom production in spent compost (Iiyama et al. 1994; Chen et al. 2000; Jurak 2015). It is important to note that glucose originating from glucan polymers in the *A. bisporus* cell walls contributes to the total glucose that is measured to determine the cellulose content of compost. The left-over of cellulose and xylan at the end of mushroom production led to the project "How mushrooms feed on sugars". The project aimed to understand how the sugar poly-

mers in compost are degraded, which should result in leads to improve digestion of the compost coinciding with higher mushroom yields and lower amounts of spent compost (champost) that is considered an animal waste stream. Within the project I focused on quantification of fungal biomass formation in compost and ways to improve lignocellulose degradation by improving lignin degradation and removal of recalcitrant xylan.

THE MICROBIAL DIET OF *Agaricus bisporus*

It was known that PI - PIV compost is rich in microbes but quantitative information about fungal and bacterial biomass was lacking. I determined microbial biomass at PII-end and during a small scale PIII using laccase activity, and by quantifying chitin and the phospholipid-derived fatty acid (PLFA) marker C18:2ω6 (Chapter 2). PLFA is an indicator of living fungal and bacterial biomass, while chitin is indicative of the total fungal biomass (Frostegård and Bååth 1996; Ekblad et al. 1998). Laccase activity is a marker for *A. bisporus* biomass during PIII but its use during PIV is limited, if useful at all, because it is downregulated during fruiting (Wood and Goodenough 1977; Wood 1979; Ohga et al. 1999). Laccase activity in PIII correlated with C18:2ω6 content but not with chitin content. Based on chitin quantification total fungal biomass at PIII-end was estimated to represent 6.8 % of the dry weight compost while the fraction of living fungal biomass was about 2.9 % at the end of this phase based on PLFA. Notably, chitin content of compost was similar during the small scale PIII in the presence and absence of *A. bisporus* indicating that this fungus consumes the cell walls of the (thermophilic) fungal community that is already present at PII-end. By combining our data with that of others (Chapter 4, Baars et al. 2013, Jurak, 2015, not shown), cellulose loss was underestimated 5 - 10 % implying that still 36 - 41 % of the cellulose remains in the compost after mushroom production.

PLFA indicated that the bacterial biomass decreased 4-fold during PIII, while it remained stable in the absence of *A. bisporus*. This supports the view that bacteria are being consumed by *A. bisporus* while growing in compost. Calculations suggested that < 10 % of *A. bisporus* biomass is provided by feeding on bacteria (Sparling et al. 1982). However, this was based on bacterial cell counts at PII-end not taking into account proliferation of bacteria in PIII and PIV. The actual contribution of bacterial biomass in the diet of *A. bisporus* may therefore be much higher. Based on PLFA it was calculated that bacterial biomass decreased from 17.9 to 4.7 mg g^{-1} compost in a small scale PIII, while fungal biomass increased from 14 to 30 mg g^{-1} in the presence of *A. bisporus* (Chapter 2). This suggests that bacteria may indeed represent the main course of *A. bisporus*. In this scenario, *A. bisporus* secretes enzymes, either or not together with bacteria, to degrade the lig-

nocellulose, bacteria would take up a main part of the degradation products and proliferate, while *A. bisporus* would consume the bacteria that provide essential molecules like vitamins.

PLFA showed that reduction of bacterial biomass during PIII was accompanied by a change in the ratio between Gram-positive and Gram-negative bacteria (Chapter 2). It is tempting to speculate that *A. bisporus* selectively consumes bacteria, resulting in a microbial flora that helps *A. bisporus* degrading compost. This hypothesis is supported by the finding that mineralization of cellulose was higher in non-axenic compost as compared to axenic compost (Wood and Leatham 1983).

IMPROVING SUBSTRATE DEGRADATION

The suboptimal utilization of carbohydrates by *A. bisporus* may be partly explained by the accumulation of recalcitrant arabinoxylan with xylose being double substituted with arabinose (Jurak et al. 2015ac). This was linked to the absence of α-1,3-L-arabinofuranosidase (AXHd3) activity in extract of PIII and PIV compost. Indeed, genes encoding this activity are not widely distributed in the basidiomycete clade. Notably, extract of PII compost does contain AXHd3 activity explained by the presence of the thermophilic fungus *Humicola insolens* (also known as *Scytalidium thermophilium*) at this stage (Straatsma et al. 1989; 1993). Its AXHd3 gene *hgh43* (Sørensen et al 2006) was introduced in *A. bisporus* (Chapter 3). Extract of compost colonized by transformants showed higher activity on doubly substituted arabinoxylan when compared to the parental A15 strain. Yet, oligomers with a backbone of 3 xyloses, doubly substituted with arabinose at its reducing end were (partly) removed by compost extract of A15. This may be explained by xylanase activity acting on the terminal non-substituted xylose of this oligomer. Alternatively, GH51 arabinofuranosidase may act on the double substituted arabinose residues at the non-reducing terminal xylose (Ferré et al. 2000; Lagaert et al. 2010; Borsenberger et al. 2014; Koutaniemi and Tenkanen 2016). The presence of a GH51 in the genome of *A. bisporus* that is highly expressed at PIII-end but lowly expressed during PIV (Patyshakuliyeva et al. 2015) and the accumulation of arabinosyl during PIV but not PIII (Jurak et al. 2015a) support this hypothesis.

More than 40 % of the lignin is not degraded during PIII and PIV. This not only impacts the volume of champost, it is also expected to prevent degradation of (hemi)cellulose. For instance, the failure of *hgh43* transformants to affect compost composition (Chapter 3) could not only be caused by suboptimal AXHd3 production but also by inaccessibility of the double substituted arabinoxylan

caused by covalent interaction to lignin. Hemicellulose can be protected from enzymatic degradation by ferulate crosslinks (Grabber et al. 1998; Grabber et al. 2009). Thus, the ligninolytic system of *A. bisporus* is a target to improve compost degradation. The genome of *A. bisporus* contains the manganese peroxidase genes *mnp1* and *mnp2* (Morin et al. 2012), of which the former is expressed in compost (Lankinen et al. 2001; Patyshakuliyeva et al. 2015). Although it is not expressed, *mnp2* does encode an active peroxidase. Transformants of *Schizophyllum commune* expressing *mnp2* resulted in more active decoloration of the substrate RBBR, while *mnp1* expression resulted in a higher oxidative coupling of MBTH and DMAB (Chapter 5). This indicates that MnP1 and MnP2 have different roles in lignin degradation.

Transformants of *A. bisporus* overexpressing *mnp1* produced a 0.3- and 3-fold higher MnP activity at casing and after the 2nd flush, respectively, in a semi commercial cultivation relative to the parental A15 strain (Chapter 4). However, effects on lignin degradation were only minor, if present at all. In contrast, mineralization of lignin and carbohydrate digestibility of cotton stalk was increased by over-expressing the ligninolytic gene encoding versatile peroxidase in *Pleurotus ostreatus* (Salame et al. 2012). Limited availability of the MnP co-factors H_2O_2 and Mn^{2+} may explain the absence of an increase in ligninolytic activity in the case of the *A. bisporus* transformants. Yet, Mn^{2+} is not considered a limiting micronutrient in Dutch compost (CNC Grondstoffen and Walkro Compost, personal communication; Burton 2015) and modification of lignin by MnP1-1 and A15 was not affected when compost had been supplemented with Mn^{2+} (Chapter 4). In contrast, H_2O_2 production was 4 - 8 fold lower than its consumption, suggesting that this co-factor indeed limits MnP activity. Similarly, H_2O_2 was limiting the ligninolytic activity of *Phanerochaete chrysosporium* (Buswell et al. 1984; Kirk et al. 1986). It is tempting to speculate that H_2O_2 was also the limiting factor for lignin degradation of MnP producers of *S. commune* on birch wood (Chapter 5). Together, this makes H_2O_2 production a target for optimizing lignin removal from compost and, consequently, increased carbohydrate consumption by *A. bisporus*. Supplementation of CaO_2 to compost could provide a source of H_2O_2 for the ligninolytic machinery of *A. bisporus*. It's supplementation to PIII-end compost increased compost temperatures in the first 24 - 48 h after supplementation but fungal biomass as quantified by chitin did not change, while laccase activity was lower in supplemented compost (not shown).

IMPROVING MUSHROOM DEVELOPMENT

Compost degradation was not improved by introduction and over-expression of α-1,3-L-arabinofuranosidase and MnP, respectively (Chapter 3 and Chap-

ter 4). Moreover, supplementing compost after PIII with cellulose and hemicellulose did not increase mushroom yield (Baars et al. 2013). Together, this points to other factors than carbohydrate utilization that limit mushroom production. Developmental processes may be such a factor. Transcription factors (TFs) involved in mushroom development have recently been shown also to impact vegetative growth in *S. commune*. TFs BriI and Hom1 of this model fungus that are involved in late stages of mushroom development stimulate vegetative growth, while Wc-2, Hom2, Tea1, and Fst4 that function early in development repress vegetative growth (Pelkmans, 2016). It is tempting to speculate that modulation of vegetative growth impacts enzyme release and thereby substrate degradation. This is supported by the fact that ligninolytic activity is downregulated during mushroom formation, while (hemi)cellulose acting activities increase (Wood 1977; Claydon et al. 1988; Bonnen et al. 1994). The Cys2His2 zinc finger TF C2H2 was over-expressed in *A. bisporus* to assess whether results obtained in *S. commune* can be extrapolated to other mushroom forming fungi (Chapter 6). C2H2 is involved in the switch from aggregates to primordia in *S. commune* (Ohm et al. 2011). Transcriptome analysis suggests that the orthologue of *c2h2* in *A. bisporus* is also involved in early development of mushroom development but also in selective tissues of young fruiting bodies (Chapter 6). Morphology, cap expansion rate, and number and biomass of mushroom was unaffected by over-expression of *c2h2*. However, formation of mature mushrooms was accelerated by one day. This is likely the result of accelerated outgrowth of initials since *c2h2* over-expression did not affect the expansion rate of mushrooms. Clearly, *c2h2* is a target for breeding of *A. bisporus* and this could also hold for the *A. bisporus* orthologues of the other TFs involved in vegetative growth and development of *S. commune*.

SYNCHRONIZED RESPIRATORY BURSTS IN COMPOST

Agaricus bisporus showed respiratory bursts during its vegetative growth in compost (Chapter 7). These bursts had a 3 - 6 h duration. Peak levels were reached in 1.5 - 3 h coinciding with up to 3.5 fold higher CO_2 production and O_2 consumption when compared to the inter-burst levels. Respiratory bursts produced on malt extract differed in their interval, duration, and intensity when compared to compost. The reason for these differences are not clear but both burst types deviated greatly from a 24 h period excluding a circadian rhythm (Loros and Dunlap 2001). Respiratory rhythms have also been observed in *Lentinus lepideus*, *Lenzites trabea*, *Poria monticola*, and *Coniophora* with interval periods varying between 7.5 and 22.5 h (Damaschke and Becker 1966; Smith 1973), while *Pleurotus ostreatus* showed even an interval period of 49 h (Chapter 7). The fact that *S. commune* and *Trametes versicolor* did not show respiratory bursts (Chapter 7) indicates that not all mushroom forming fungi produce respiratory rhythms.

Bursts of *A. bisporus* progressively synchronized over a minimum distance of 60 cm during vegetative growth (Chapter 7). Compost separated by air (allowing exchange of volatiles) or aluminium foil (allowing exchange of heat) did not synchronize, while compost in physical contact did. Notably, synchrony was reduced at the end of the exponential growth phase. This may be due to a reduction in the connectivity of the hyphal network. This would fit with the observation that a significant part of hyphae are dead after vegetative growth of *A. bisporus* (Chapter 2). Synchronization of oscillations in transport of the amino-acid analogue α-aminoisobutyrate in *Phanerochaete velutina* and *Coniophora puteana* was proposed to occur through coupled oscillating systems (Fricker et al. 2007 and references therein). Colony wide oscillations in α-aminoisobutyrate transport was not related to temperature fluctuations. Moreover, synchronization of different colonies upon anastomosis occurred with a phase shift while synchronization of bursts in compost was in-phase (Tlalka et al. 2002; Tlalka et al. 2003; Fricker et al. 2007; Tlalka et al. 2009).

The respiratory quotient (RQ) of bursts was higher as compared to the inter-burst period (e.g. 0.7 and 0.58, respectively). RQs of 1 and 0.7 are typical for mineralization of glucose and fat, respectively (Péronnet and Massicotte 1991). RQs lower than 0.7 are indicative of mineralization of highly reduced compounds, production of highly oxidized compounds, or a combination of both. Respiratory bursts occurred primarily in PIII, correlating with the mineralization of lignin by *A. bisporus*. Preliminary data suggests that respiratory bursts in PIII are associated with acid production but also with its neutralization (possibly by mineralization). At the same time laccase seems to be produced but also damaged during bursts. It is tempting to speculate that the respiratory bursts and the ligninolytic activity of *A. bisporus* are linked. Calcium oxalate crystals are associated with hyphae of *A. bisporus* (Whitney and Arnott 1987). The extracellular oxalic acid may be converted into CO_2 and formic acid or CO_2 and H_2O_2 by the action of oxalate decarboxylase and oxalate oxidase, respectively. The former activity has been found in *A. bisporus* (Kathiara et al. 2000). Oxalic acid may also be degraded by Lcc and MnP coinciding with a net increase in H_2O_2 and Mn^{2+} (Urzúa et al. 1998a; 1998b; Schlosser et al. 2002). Together, these activities may increase ligninolytic activity and heat production during respiratory bursts.

REFERENCES

Addleman K, Dumonceaux T, Paice MG, Bourbonnais R, Archibald FS (1995) Production and characterization of *Trametes versicolor* mutants unable to bleach hardwood kraft pulp. Appl Environ Microbiol 61:3687-3694.

Agger JW, Isaksen T, Várnai A, Vidal-Melgosa S, Willats WG, Ludwig R, Horn SJ, Eijsink VGH, Westereng B (2014) Discovery of LPMO activity on hemicelluloses shows the importance of oxidative processes in plant cell wall degradation. Proc Nat Acad Sci USA 111:6287-6292.

Arantes V, Jellison J, Goodell B (2012) Peculiarities of brown-rot fungi and biochemical Fenton reaction with regard to their potential as a model for bioprocessing biomass. Appl Microbiol Biotechnol 94:323-338.

Baars JJP, Sonnenberg ASM, de Visser JAGM, Blok C (2013) Input-output Fase III. http://edepot.wur.nl/294997.

Baldrian P (2008) Enzymes of saprotrophic basidiomycetes. Br Mycol Soc Symp Ser [ZDB] 28:19-41.

Baldrian P, Valášková V (2008) Degradation of cellulose by basidiomycetous fungi. FEMS Microbiol Rev 32:501-521.

Béguin P, Aubert JP (1994) The biological degradation of cellulose. FEMS Microbiol Rev 13:25-58.

Bels-Koning H (1950) Experiments with casing soils, water supply and climate. Mushroom Sci 1:78-84.

Bligh EG, Dyer WJ (1959) A rapid method of total lipid extraction and purification. Can J Biochem Phys 37:911-917.

Boerjan W, Ralph J, Baucher M (2003) Lignin biosynthesis. Annu Rev Plant Biol 54:519-546.

Bolger AM, Lohse M, Usadel B (2014) Trimmomatic: a flexible trimmer for Illumina sequence data. Bioinformatics 30:2114-2120.

Bonnen AM, Anton LH, Orth AB (1994) Lignin-degrading enzymes of the commercial button mushroom, *Agaricus bisporus*. Appl Environ Microbiol 60:960-965.

Boominathan K, Dass SB, Randall TA, Kelley RL, Reddy CA (1990) Lignin peroxidase-negative mutant of the white-rot basidiomycete *Phanerochaete chrysosporium*. J Bacteriol 172:260-265.

Borsenberger V, Dornez E, Desrousseaux M-L, Massou S, Tenkanen M, Courtin CM, Dumon C, O'Donohue MJ, Fauré R (2014) A ^{1}H NMR study of the specificity of α-L-arabinofuranosidases on natural and unnatural substrates. Biochim Biophys Acta 1840:3106–3114.

Bratbak G, Dundas I (1984) Bacterial dry matter content and biomass estimations. Appl

Environ Microbiol 48:755-757.

Burton K (2015) Understanding Mushroom Nutrition: Project aimed at improving yield, substrate efficiency and utilisation and flavour. M056 Final Report September 2015.

Buswell JA, Mollet B, Odier E (1984) Ligninolytic enzyme production by *Phanerochaete chrysosporium* under conditions of nitrogen sufficiency. FEMS Microbiol Lett 25:295-299.

Camarero S, Bocchini P, Galletti GC, Martınez MJ, Martınez AT (2001) Compositional changes of wheat lignin by a fungal peroxidase analyzed by pyrolysis-GC-MS. J Anal Appl Pyrol 58:413-423.

Castillo MD, Stenstrom J, Ander P (1994) Determination of manganese peroxidase activity with 3-methyl-2-benzothiazolinone hydrazone and 3-(dimethylamino) benzoic acid. Anal Biochem 218:399-404.

Chen Y, Chefetz B, Rosario R, van Heemst JDH, Romaine PC, Hatcher PG (2000a) Chemical nature and composition of compost during mushroom growth. Compost Sci Util 8:347-359.

Chen X, Stone M, Schlagnhaufer C, Romaine CP (2000b) A fruiting body tissue method for efficient *Agrobacterium*-mediated transformation of *Agaricus bisporus*. Appl Environ Microbiol 66:4510–4513.

Chomczynski P, Sacchi N (1987) Single-step method of RNA isolation by acid guanidinium thiocyanate-phenol-chloroform extraction. Anal Biochem 162:156–159.

Claydon N, Allan M, Wood DA (1988) Fruit body biomass regulated production of extracellular endocellulase during periodic fruiting by *Agaricus bisporus*. Trans Br Mycol Soc 90:85-90.

Conesa A, Jeenes D, Archer DB, van den Hondel CA, Punt PJ (2002) Calnexin overexpression increases manganese peroxidase production in *Aspergillus niger*. Appl Environ Microbiol 68:846-851.

Daba AS (2006) Mushroom cultivation in Egypt: Food of the Gods Down the Nile Valley. ISMS newsletter 105:4-7.

Davin LB, Jourdes M, Patten AM, Kim KW, Vassao DG, Lewis NG (2008) Dissection of lignin macromolecular configuration and assembly: comparison to related biochemical processes in allyl/propenyl phenol and lignan biosynthesis. Nat Prod Rep 25 :1015-1090.

del Río JC, Rencoret J, Prinsen P, Martínez ÁT, Ralph J, Gutiérrez A (2012) Structural characterization of wheat straw lignin as revealed by analytical pyrolysis, 2D-NMR, and reductive cleavage methods. J Agric Food Chem 60:5922–5935.

Damaschke K, Becker G (1966) Rhythmen des Sauerstoffverbrauchs von Basidiomyceten. Mater Org (Berlin) 1:275-290.

Díaz JL (1977) Ethnopharmacology of sacred psychoactive plants used by the Indians of Mexico. Annu Rev Pharmacol Toxicol 17:647-675.

Dobin A, Davis CA, Schlesinger F, Drenkow J, Zaleski C, Jha S, Batut P, Chaisson M, Gingeras

TR (2013) STAR: ultrafast universal RNA-seq aligner. Bioinformatics 29:15-21.

Dodd D, Cann IK (2009) Enzymatic deconstruction of xylan for biofuel production. Glob Change Biol Bioenergy 1:2-17.

Eastwood DC, Herman B, Noble R, Dobrovin-Pennington A, Sreenivasaprasad S, Burton KS (2013) Environmental regulation of reproductive phase change in *Agaricus bisporus* by 1-octen-3-ol, temperature and CO_2. Fungal Genet Biol 55:54-66.

Eggert C, Temp U, Dean JF, Eriksson KEL (1996) A fungal metabolite mediates degradation of non-phenolic lignin structures and synthetic lignin by laccase. FEBS Lett 391:144-148.

Eggert C, Temp U, Eriksson KEL (1997) Laccase is essential for lignin degradation by the white-rot fungus *Pycnoporus cinnabarinus*. FEBS Lett 407:89-92.

Ekblad ALF, Wallander H, Näsholm T (1998) Chitin and ergosterol combined to measure total and living fungal biomass in ectomycorrhizas. New Phytol 138:143-149.

Englyst H, Wiggins HS, Cummings JH (1982) Determination of the non-starch polysaccharides in plant foods by gas-liquid chromatography of constituent sugars as alditol acetates. Analyst 107:307-318.

Englyst HN, Cummings JH (1984) Simplified method for the measurement of total non-starch polysaccharides by gas-liquid chromatography of constituent sugars as alditol acetates. Analyst 109:937-942.

Fabing HD (1956) On going berserk: A neurochemical inquiry. Am J Psychiatry 113:409-415.

Ferré H, Broberg A, Duus JØ, Thomsen KK (2000) A novel type of arabinoxylan arabinofuranohydrolase isolated from germinated barley. Eur J Biochem 267:6633–6641.

Filley TR, Cody GD, Goodell B, Jellison J, Noser C, Ostrofsky A (2002) Lignin demethylation and polysaccharide decomposition in spruce sapwood degraded by brown rot fungi. Org Geochem 33:111-124.

Fincher GB (2009) Revolutionary times in our understanding of cell wall biosynthesis and remodeling in the grasses. Plant Physiol 149:27-37.

Flegg P (1956) The casing layer in the cultivation of the mushroom (*Psalliota hortensis*). J Soil Sci 7:168-176.

Floudas D, Binder M, Riley R, Barry K, Blanchette RA, Henrissat B, Martínez AT, Otillar R, Spatafora JW, Yadav JS, Aerts A, Benoit I, Boyd A, Carlson A, Copeland A, Coutinho PM, de Vries RP, Ferreira P, Findley K, Foster B, Gaskell J, Glotzer D, Górecki P, Heitman J, Hesse C, Hori C, Igarashi K, Jurgens JA, Kallen N, Kersten P, Kohler A, Kües U, Kumar TKA, Kuo A, LaButti K, Larrondo LF, Lindquist E, Ling A, Lombard V, Lucas S, Lundell T, Martin R, McLaughlin DJ, Morgenstern I, Morin E, Murat C, Nagy LG, Nolan M, Ohm RA, Patyshakuliyeva A, Rokas A, Ruiz-Dueñas FJ, Sabat G, Salamov A, Samejima M, Schmutz J, Slot JC, John FS, Stenlid F, Sun H, Sun S, Syed K, Tsang A, Wiebenga A, Young D, Pisabarro A, Eastwood DC, Martin F, Cullen D, Grigoriev IV, Hibbett1 DS (2012) The Paleozoic origin of enzymatic lignin decomposition reconstructed from 31 fungal genomes. Science 336:1715-1719.

Floudas D, Held BW, , Riley R, Nagy LG, Koehler G, Ransdell AS, Younus H, Chow J,

Chiniquy F, Lipzen A, Tritt A, Sun H, Haridas S, LaButti K, Ohm RA, Kües U, Blanchette RA, Grigoriev IV, Minto RE, Hibbett DS (2015) Evolution of novel wood decay mechanisms in Agaricales revealed by the genome sequences of *Fistulina hepatica* and *Cylindrobasidium torrendii*. Fungal Genet Biol 76:78-92.

François JM (2006) A simple method for quantitative determination of polysaccharides in fungal cell walls. Nat Protoc 1:2995-3000.

Fricker MD, Tlalka M, Bebber D, Tagaki S, Watkinson SC, Darrah PR (2007) Fourier-based spatial mapping of oscillatory phenomena in fungi. Fungal Genet Biol 44:1077-1084.

Frostegård Å, Tunlid A, Bååth E (1991) Microbial biomass measured as total lipid phosphate in soils of different organic content. J Microbiol Meth 14:151-163.

Frostegård Å, Bååth E, Tunlid A (1993) Shifts in the structure of soil microbial communities in limed forests as revealed by phospholipid fatty acid analysis. Soil Biol Biochem 25:723-730.

Frostegård Å, Bååth E (1996) The use of phospholipid fatty acid analysis to estimate bacterial and fungal biomass in soil. Biol Fertility Soils 22:59-65.

Frostegård Å, Tunlid A, Bååth E (2011) Use and misuse of PLFA measurements in soils. Soil Biol Biochem 43:1621-1625.

Geib SM, Filley TR, Hatcher PG, Hoover K, Carlson JE, del Mar Jimenez-Gasco M, Nakagawa-Izumill A, Sleighter RL, Tien M (2008) Lignin degradation in wood-feeding insects. Proc Natl Acad Sci USA 105:12932-12937.

Gerrits JPG (1988) Nutrition and compost. In: Griensven LJLD (ed) The cultivation of mushrooms, 1st edn. Darlington Mushroom Laboratories Ltd, pp 29–72.

Gilbert HJ, Knox JP, Boraston AB (2013) Advances in understanding the molecular basis of plant cell wall polysaccharide recognition by carbohydrate-binding modules. Curr Opin Struct Biol 23:669-677.

Glass NL, Schmoll M, Cate JH, Coradetti S (2013) Plant cell wall deconstruction by ascomycete fungi. Annu Rev Microbiol 67:477-498.

Gómez-Toribio V, García-Martín AB, Martínez MJ, Martínez ÁT, Guillén F (2009) Induction of extracellular hydroxyl radical production by white-rot fungi through quinone redox cycling. Appl Environ Microbiol 75:3944-3953.

Grabber JH, Hatfield RD, Ralph J (1998) Diferulate cross-links impede the enzymatic degradation of non-lignified maize walls. J Sci Food Agric 77:193–200.

Grabber JH, Mertens DR, Kim H, Funk C, Lu F, Ralph J (2009) Cell wall fermentation kinetics are impacted more by lignin content and ferulate cross-linking than by lignin composition. J Sci Food Agric 89:122–129.

Griensven LJLD (1988) Geschiedenis en ontwikkeling. In: Griensven LJLD (ed) The cultivation of mushrooms, 1st edn. Darlington Mushroom Laboratories Ltd, pp 11-27.

de Groot PW, Basten DE, Sonnenberg AS, Van Griensven LJ, Visser J, Schaap PJ (1998) An endo-1,4-β-xylanase-encoding gene from Agaricus bisporus is regulated by

compost-specific factors. J Mol Biol 277:273-284.

Guillén F, Martínez MJ, Muñoz C, Martínez AT (1997) Quinone redox cycling in the ligninolytic fungus *Pleurotus eryngii* leading to extracellular production of superoxide anion radical. Arch Biochem Bioph 339:190-199.

Guillén F, Muñoz C, Gómez-Toribio V, Martínez AT, Martínez MJ (2000) Oxygen activation during oxidation of methoxyhydroquinones by laccase from *Pleurotus eryngii*. Appl Environ Microbiol 66:170-175.

Guillén F, Martínez MJ, Gutiérrez A, del Rio JC (2005) Biodegradation of lignocellulosics: microbial, chemical, and enzymatic aspects of the fungal attack of lignin. Int Microbiol 8:195-204.

Hammel KE, Kapich AN, Jensen KA, Ryan ZC (2002) Reactive oxygen species as agents of wood decay by fungi. Enzyme Microb Technol 30:445-453.

Hammel KE, Cullen D (2008) Role of fungal peroxidases in biological ligninolysis. Curr Opin Plant Biol 11:349-355.

Harris PV, Welner D, McFarland KC, Re E, Poulsen JCN, Brown K, Salbo R, Ding H, Vlasenko E, Merino S, Xu F, Cherry J, Larsen S, Leggio LL (2010) Stimulation of lignocellulosic biomass hydrolysis by proteins of glycoside hydrolase family 61: structure and function of a large, enigmatic family. Biochem 49:3305-3316.

Hatakka A (1994) Lignin-modifying enzymes from selected white-rot fungi: production and role from in lignin degradation. FEMS microbiol rev 13:125-135.

ten Have R, Teunissen PJ (2001) Oxidative mechanisms involved in lignin degradation by white-rot fungi. Chem Rev 101:3397-3414.

ten Have R, Wijngaard H, Ariës-Kronenburg NA, Straatsma G, Schaap PJ (2003) Lignin degradation by *Agaricus bisporus* accounts for a 30% increase in bioavailable holocellulose during cultivation on compost. J Agric Food Chem 51:2242-2245.

Hedlund K (2002) Soil microbial community structure in relation to vegetation management on former agricultural land. Soil Biol Biochem 34:1299-1307.

Heijboer A, ten Berge HF, de Ruiter PC, Jørgensen HB, Kowalchuk GA, Bloem J (2016) Plant biomass, soil microbial community structure and nitrogen cycling under different organic amendment regimes; a ^{15}N tracer-based approach. Appl Soil Ecol 107:251-260.

Hiscox J, Baldrian P, Rogers HJ, Boddy L (2010) Changes in oxidative enzyme activity during interspecific mycelial interactions involving the white-rot fungus Trametes versicolor. Fungal Genet Biol 47:562-571.

Hofrichter M (2002) Review: lignin conversion by manganese peroxidase (MnP). Enzyme Microb Technol, 30:454-466.

Iiyama K, Stone BA, Macauley BJ (1994) Compositional changes in compost during composting and growth of *Agaricus bisporus*. Appl Environ Microbiol 60:1538-1546.

Jurak E, Kabel MA, Gruppen H (2014) Carbohydrate composition of compost during composting and mycelium growth of *Agaricus bisporus*. Carbohydr Polym 101:281-288.

Jurak E (2015) How mushrooms feed on compost: conversion of carbohydrates and lignin in industrial wheat straw based compost enabling the growth of *Agaricus bisporus*. Dissertation, Wageningen University.

Jurak E, Patyshakuliyeva A, De Vries RP, Gruppen H, Kabel MA (2015a) Compost grown *Agaricus bisporus* lacks the ability to degrade and consume highly substituted xylan fragments. PLoS One. doi: 10.1371/journal.pone.0134169

Jurak E, Punt AM, Arts W, Kabel MA, Gruppen H (2015b) Fate of carbohydrates and lignin during composting and mycelium growth of *Agaricus bisporus* on wheat straw based compost. PLoS One 10:1-16.

Jurak E, Patyshakuliyeva A, Kapsokalyvas D, Xing L, van Zandvoort MAMJ, de Vries RP, Gruppen H, Kabel MA (2015c) Accumulation of recalcitrant xylan in mushroom-compost is due to a lack of xylan substituent removing enzyme activities of *Agaricus bisporus*. Carbohydr Polym 132:359-368.

Kalberer PP (1987) Water potentials of casing and substrate and osmotic potentials of fruit bodies of *Agaricus bisporus*. Sc Horticulturae 32:175-182.

Kersten PJ, Kirk TK (1987) Involvement of a new enzyme, glyoxal oxidase, in extracellular H_2O_2 production by *Phanerochaete chrysosporium*. J Bacteriol 169:2195-2201.

Kathiara M, Wood DA, Evans CS (2000) Detection and partial characterization of oxalate decarboxylase from *Agaricus bisporus*. Mycol Res 104:345-350.

Klamer M, Bååth E (2004) Estimation of conversion factors for fungal biomass determination in compost using ergosterol and PLFA 18:2ω6,9. Soil Biol Biochem 36:57-65.

Kirk TK, Tien M, Johnsrud SC, Eriksson KE (1986) Lignin degrading activity of *Phanerochaete chrysosporium* Burds.: comparison of cellulase-negative and other strains. Enzyme Microb Technol 8:75-80.

Kirk TK, Farrell RL (1987) Enzymatic "combustion": the microbial degradation of lignin. Annu Rev Microbiol 41:465-501.

Kormelink FJM, Searle-Van Leeuwen MJF, Wood TM, Voragen AGJ (1993) Purification and characterization of three endo-(1,4)-β-xylanases and one β-xylosidase from *Aspergillus awamori*. J Biotechnol 27:249–265.

Koutaniemi S, Tenkanen M (2016) Action of three GH51 and one GH54 α-arabinofuranosidases on internally and terminally located arabinofuranosyl branches. J Biotechnol 229:22–30.

Kristensen JB, Thygesen LG, Felby C, Jørgensen H, Elder T (2008) Cell-wall structural changes in wheat straw pretreated for bioethanol production. Biotechnol Biofuels 1:5.

Kües U (2000) Life history and developmental processes in the basidiomycete *Coprinus cinereus*. Microbiol Mol Biol Rev 64:316-353.

Kües U, Navarro-González M (2015) How do Agaricomycetes shape their fruiting bodies? 1. Morphological aspects of development. Fungal Biol Rev 29:63-97.

van Laere KMJ, Voragen CHL, Kroef T, Van den Broek LAM, Beldman G, Voragen AGJ (1999) Purification and mode of action of two different arabinoxylan arabinofu-

ranohydrolases from *Bifidobacterium adolescentis* DSM 20083. Appl Microbiol Biotechnol 51:606–613.

Lagaert S, Pollet A, Delcour JA, Lavigne R, Courtin CM, Volckaert G (2010) Substrate specificity of three recombinant α-L-arabinofuranosidases from *Bifidobacterium adolescentis* and their divergent action on arabinoxylan and arabinoxylan oligosaccharides. Biochem Biophys Res Commun 402:644–650.

Lankinen PV, Bonnen AM, Anton LH, Wood DA, Kalkkinen N, Hatakka A, Thurston CF (2001) Characteristics and N-terminal amino acid sequence of manganese peroxidase from solid substrate cultures of *Agaricus bisporus*. Appl Microbiol Biotechnol 55:170-176.

Lawther JM, Sun R, Banks WB (1995) Extraction, fractionation, and characterization of structural polysaccharides from wheat straw. J Agric Food Chem 43:667-675.

Levasseur A, Drula E, Lombard V, Coutinho PM, Henrissat B (2013) Expansion of the enzymatic repertoire of the CAZy database to integrate auxiliary redox enzymes. Biotechnol Biofuels 6:41.

Li K, Horanyi PS, Collins R, Phillips RS, Eriksson KEL (2001) Investigation of the role of 3-hydroxyanthranilic acid in the degradation of lignin by white-rot fungus *Pycnoporus cinnabarinus*. Enzyme Microb Technol 28:301-307.

Li M, Foster C, Kelkar S, Pu Y, Holmes D, Ragauskas A, Saffron CM, Hodge DB (2012) Structural characterization of alkaline hydrogen peroxide pretreated grasses exhibiting diverse lignin phenotypes. Biotechnol Biofuels 5:38.

Liu R, Yu H, Huang Y (2005) Structure and morphology of cellulose in wheat straw. Cellulose 12:25-34.

Livak KJ, Schmittgen TD (2001) Analysis of relative gene expression data using real-time quantitative PCR and the $2^{-\Delta\Delta CT}$ method. Methods 25:402-408.

Logatcheva K, Smit PX, van der Meulen HAB (2014) Market intelligence champignons: productie en handel van Nederlandse champignons in context. Brochure LEI Wageningen UR.

Lombard V, Ramulu HG, Drula E, Coutinho PM, Henrissat B (2014) The carbohydrate-active enzymes database (CAZy) in 2013. Nucleic Acids Res 42:D490-D495.

Loros JJ, Dunlap JC (2001) Genetic and molecular analysis of circadian rhythms in *Neurospora*. Annu Rev Physiol 63:757-794.

Lugones L, Scholtmeijer K, Klootwijk R, Wessels JGH (1999) Introns are necessary for mRNA accumulation in *Schizophyllum commune*. Mol Microbiol 32:681–689.

Martınez AT, Camarero S, Gutiérrez A, Bocchini P, Galletti GC (2001) Studies on wheat lignin degradation by *Pleurotus* species using analytical pyrolysis. J Anal Appl Pyrolysis 58:401-411.

Martínez PM, Appeldoorn MM, Gruppen H, Kabel MA (2016) The two *Rasamsonia emersonii* α-glucuronidases, Re GH67 and Re GH115, show a different mode-of-action towards glucuronoxylan and glucuronoxylo-oligosaccharides. Biotechn biofuels 9:1.

Matcham SE, Jordan BR, Wood DA (1985) Estimation of fungal biomass in a solid substrate by three independent methods. Appl Microbiol Biotechnol 21:108-112.

Mewis K, Lenfant N, Lombard V, Henrissat B (2016) Dividing the large glycoside hydrolase family 43 into subfamilies: a motivation for detailed enzyme characterization. Appl Environ Microbiol 82:1686–1692.

Morin E, Kohler A, Baker AR, Foulongne-Oriol M, Lombard V, Nagye LG, Ohm RA, Patyshakuliyeva A, Brun A, Aerts AL, Bailey AM, Billette C, Coutinho PM, Deakin G, Doddapaneni H, Floudas D, Grimwood J, Hildén K, Kües U, LaButti KM, Lapidus A, Lindquist EA, Lucas SM, Murat C, Riley RW, Salamov AA, Schmutz J, Subramanian V, Wösten HAB, Xu J, Eastwood DC, Foster GD, Sonnenberg ASM, Cullen D, Vries RP de, Lundell T, Hibbett DS, Henrissat B, Burton KS, Kerrigan RW, Challen MP, Grigoriev IV, Martin F (2012) Genome sequence of the button mushroom *Agaricus bisporus* reveals mechanisms governing adaptation to a humic-rich ecological niche. Proc Natl Acad Sci 109:17501–17506.

Muraguchi H, Umezawa K, Niikura M, Yoshida M, Kozaki T, Ishii K, Sakai K, Shimizu M, Nakahori K, Sakamoto Y, Choi C, Ngan CY, Lindquist E, Lipzen A, Tritt A, Haridas S, Barry K, Grigoriev IV, Pukkila PJ (2015) Strand-specific RNA-Seq analyses of fruiting body development in *Coprinopsis cinerea*. PLoS One 10:e0141586.

Niederpruem DJ (1963) Role of carbon dioxide in the control of fruiting of *Schizophyllum commune*. J Bacteriol 85:1300-1308.

Noble R, Fermor TR, Lincoln S, Dobrovin-Pennington A, Evered C, Mead A, Li R (2003) Primordia initiation of mushroom (*Agaricus bisporus*) strains on axenic casing materials. Mycologia 95:620-629.

Noble R, Dobrovin-Pennington A, Hobbs PJ, Pederby J, Rodger A (2009) Volatile C8 compounds and pseudomonads influence primordium formation of *Agaricus bisporus*. Mycologia 101:583-591.

Ohga S, Smith M, Thurston CF, Wood DA (1999) Transcriptional regulation of laccase and cellulase genes in the mycelium of *Agaricus bisporus* during fruit body development on a solid substrate. Mycol Res 103:1557-1560.

Ohm RA, De Jong JF, Lugones LG, Aerts A, Kothe E, Stajich JE, de Vries RP, Record E, Levasseur A, Baker SE, Bartholomew KA, Coutinho PM, Erdmann S, Fowler TJ, Gathman AC, Lombard V, Henrissat B, Knabe N, Kües U, Lilly WW, Lindquist E, Lucas S, Magnuson JK, Piumi F, Raudaskoski M, Salamov A, Schmutz J, Schwarze FWMR, vanKuyk FA, Horton JS, Grigoriev IV, Wösten HAB (2010) Genome sequence of the model mushroom *Schizophyllum commune*. Nature biotechnol 28:957-963.

Ohm RA, de Jong JF, de Bekker C, Wösten HA, Lugones LG (2011) Transcription factor genes of *Schizophyllum commune* involved in regulation of mushroom formation. Mol Microbiol 81:1433-1445.

Ohm RA, Aerts D, Wösten HAB, Lugones LG (2013) The blue light receptor complex WC-1/2 of *Schizophyllum commune* is involved in mushroom formation and protection against phototoxicity. Environ Microbiol 15:943-955.

Patyshakuliyeva A, Post H, Zhou M, Jurak E, Heck AJR, Hildén KS, Kabel MA, Mäkelä

MR, Altelaar MAF, Vries RP (2015) Uncovering the abilities of *Agaricus bisporus* to degrade plant biomass throughout its life cycle. Environ Microbiol 17:3098-3109.

van Peer AF, de Bekker C, Vinck A, Wösten HAB, Lugones LG (2009) Phleomycin increases transformation efficiency and promotes single integrations in *Schizophyllum commune*. Appl Environ Microbiol 75:1243-1247.

Pelkmans JF, Vos AM, Scholtmeijer K, Hendrix E, Baars JJP, Gehrmann T, Reinders MJT, Lugones LG, Wösten HAB (2016) The transcriptional regulator *c2h2* accelerates mushroom formation in *Agaricus bisporus*. Appl Microbiol Biotechnol 100:7151–7159.

Peintner U, Pöder R, Pümpel T (1998) The iceman's fungi. Mycol Res 102:1153-1162.

Perkins JH, Gordon SA (1969) Morphogenesis in *Schizophyllum commune*. II. Effects of monochromatic light. Plant Physiol 44:1712-1716.

Péronnet F, Massicotte D (1991) Table of nonprotein respiratory quotient: an update. Can J Sport Sci 16:23-29.

Plaza DF, Lin CW, van der Velden NSJ, Aebi M, Künzler M (2014) Comparative transcriptomics of the model mushroom *Coprinopsis cinerea* reveals tissue-specific armories and a conserved circuitry for sexual development. BMC Genomics 15:492.

Puls J, Schmidt O, Granzow C (1987) α-Glucuronidase in two microbial xylanolytic systems. Enzyme Microb. Technol 9:83-88.

Quinlan RJ, Sweeney MD, Leggio LL, Otten H, Poulsen JCN, Johansen KS, Kroghc KBMR, Jørgensenc CI, Tovborgc M, Anthonsenc A, Tryfonad T, Walterc CP, Dupreed P, Xua F, Daviese GJ, Waltone PH (2011) Insights into the oxidative degradation of cellulose by a copper metalloenzyme that exploits biomass components. Proc Natl Acad Sci USA 108:15079-15084.

Raudaskoski M, Viitanen H (1982) Effect of aeration and light on fruit body induction in *Schizophyllum commune*. Tr British Mycol Soc 78:89-96.

Reissig JL, Strominger JL, Leloir LF (1955) A modified colorimetric method for the estimation of N-acetylamino sugars. J Biol Chem 217:959-966.

Richard P (2003) The rhythm of yeast. FEMS Microbiol Rev 27:547-557.

Riley R, Salamova AA, Brown DW, Nagy LG, Floudas D, Held BW, Levasseur A, Lombard V, Moring E, Otillara R, Lindquist, Sun H, LaButti KM, Schmutz J, Jabbour D, Luo H, Baker SE, Pisabarro AG, Walton JD, Blanchette RA, Henrissat B, Martin F, Cullen D, Hibbett DS, Grigoriev IV (2014) Extensive sampling of basidiomycete genomes demonstrates inadequacy of the white-rot/brown-rot paradigm for wood decay fungi. Proc Natl Acad Sci USA 111:9923-9928.

del Rio JC, Gutiérrez A, Martınez MJ, Martınez AT (2001) Py–GC/MS study of *Eucalyptus globulus* wood treated with different fungi. J Anal Appl Pyrol 58:441-452.

del Rio JC, Speranza M, Gutiérrez A, Martınez MJ, Martınez AT (2002) Lignin attack during eucalypt wood decay by selected basidiomycetes: a Py-GC/MS study. J Anal Appl Pyrol 64:421-431.

Romaine CP, Chen X (2005) Methods and compositions for highly efficient transformation of filamentous fungi. U.S. Patent No. 6,964,866. 15 Nov. 2005.

Ross RC, Harris PJ (1983) The significance of thermophilic fungi in mushroom compost preparation. Sci Hort, 20:61-70.

Ruess L, Chamberlain PM (2010) The fat that matters: soil food web analysis using fatty acids and their carbon stable isotope signature. Soil Biol Biochem 42:1898-1910.

Sabotič J, Ohm RA, Künzler M (2016) Entomotoxic and nematotoxic lectins and protease inhibitors from fungal fruiting bodies. Appl Microbiol Biotechnol 100:91–111.

Salame TM, Knop D, Levinson D, Mabjeesh SJ, Yarden O, Hadar Y (2012) Release of *Pleurotus ostreatus* versatile-peroxidase from Mn^{2+} repression enhances anthropogenic and natural substrate degradation. PLOS ONE 7:e52446.

Salame TM, Knop D, Levinson D, Mabjeesh SJ, Yarden O, Hadar Y (2014) Inactivation of a *Pleurotus ostreatus* versatile peroxidase-encoding gene (*mnp2*) results in reduced lignin degradation. Environ microbiol 16:265-277.

Sánchez C, Moore D (1999) Conventional histological stains selectively stain fruit body initials of basidiomycetes. Mycol Res 103:315-318.

Savoie JM (1998) Changes in enzyme activities during early growth of the edible mushroom, *Agaricus bisporus*, in compost. Mycol Res 102:1113-1118.

Schlosser D, Höfer C (2002) Laccase-catalyzed oxidation of Mn^{2+} in the presence of natural Mn^{3+} chelators as a novel source of extracellular H_2O_2 production and its impact on manganese peroxidase. Appl Environ Microbiol 68:3514-3521.

Schmidt O, Liese W (1980) Variability of wood degrading enzymes of *Schizophyllum commune*. Holzforschung [ZDB] 34:67-72.

Schmittgen TD, Livak KJ (2008) Analyzing real-time PCR data by the comparative CT method. Nat Protoc 3:1101–1108.

Scholtmeijer K, Cankar K, Beekwilder J, Wösten HAB, Lugones LG, Bosch D (2014) Production of (+)-valencene in the mushroom-forming fungus *S. commune*. Appl microbiol biotechnol 98:5059-5068.

Schuren FH, Wessels JG (1994) Highly-efficient transformation of the homobasidiomycete *Schizophyllum commune* to phleomycin resistance. Curr Genet 26:179-183.

Sharma PD, Fisher PJ, Webster J (1977) Critique of the chitin assay technique for estimation of fungal biomass. Trans Brit Mycol Soc 69:479-483.

Sjaarda CP, Abubaker KS, Castle AJ (2015) Induction of *lcc2* expression and activity by *Agaricus bisporus* provides defence against *Trichoderma aggressivum* toxic extracts. Microbial biotech 8:918-929.

Smith RS (1973) Continuous automatic measurement of rhythms in fungal respiration using a gas chromatograph. Can J Bot 51:701-710.

Sørensen HR, Jørgensen CT, Hansen CH, Jørgensen CI, Pedersen S, Meyer AS (2006) A novel GH43 α-L-arabinofuranosidase from *Humicola insolens*: mode of action and synergy with GH51 α-L-arabinofuranosidases on wheat arabinoxylan. Appl Microbiol Biotechnol 73:850–861.

Špániková S, Biely P (2006) Glucuronoyl esterase–novel carbohydrate esterase produced by *Schizophyllum commune*. FEBS Lett 580:4597-4601.

Sparling GP, Fermor TR, Wood DA (1982) Measurement of the microbial biomass in composted wheat straw, and the possible contribution of the biomass to the nutrition of *Agaricus bisporus*. Soil Biol Biochem 14:609-611.

Stewart P, Whitwam RE, Kersten PJ, Cullen D, Tien M (1996) Efficient expression of a *Phanerochaete chrysosporium* manganese peroxidase gene in *Aspergillus oryzae*. Appl Environ Microbiol 62:860-864.

Straatsma G, Gerrits JP, Augustijn MP, Den Camp HJO, Vogels GD, Van Griensven LJ (1989) Population dynamics of *Scytalidium thermophilum* in mushroom compost and stimulatory effects on growth rate and yield of *Agaricus bisporus*. Microbiology 135:751-759.

Straatsma G, Samson RA (1993) Taxonomy of *Scytalidium thermophilum*, an important thermophilic fungus in mushroom compost. Mycol Res 97:321-328.

Straatsma G, Olijnsma TW, Gerrits JP, Amsing JG, Den Camp HJO, Van Griensven LJ (1994) Inoculation of *Scytalidium thermophilum* in button mushroom compost and its effect on yield. Appl Environ Microbiol 60:3049-3054.

Straatsma G, Sonnenberg AS, van Griensven LJ (2013) Development and growth of fruit bodies and crops of the button mushroom, *Agaricus bisporus*. Fungal Biol 117:697-707.

Sun R, Lawther JM, Banks WB (1995) Influence of alkaline pre-treatments on the cell wall components of wheat straw. Ind Crops Prod 4:127-145.

Sun R, Lawther JM, Banks WB (1996) Fractional and structural characterization of wheat straw hemicelluloses. Carbohydr Polym 29:325-331.

Sun R, Fang JM, Rowlands P, Bolton J (1998) Physicochemical and thermal characterization of wheat straw hemicelluloses and cellulose. J Agric Food Chem 46:2804-2809.

Sun R, Sun XF, Wang SQ, Zhu W, Wang XY (2002) Ester and ether linkages between hydroxycinnamic acids and lignins from wheat, rice, rye, and barley straws, maize stems, and fast-growing poplar wood. Ind Crops Prod 15:179-188.

Sun XF, Sun R, Fowler P, Baird MS (2005) Extraction and characterization of original lignin and hemicelluloses from wheat straw. J Agric Food Chem 53:860-870.

Thibault JF (1979) Automatisation du dosage des substances pectiques par la methode au meta-hydroxydiphenyl. Lebensm-Wiss Technol 12:247-251.

Tlalka M, Watkinson SC, Darrah PR, Fricker MD (2002) Continuous imaging of amino-acid translocation in intact mycelia of *Phanerochaete velutina* reveals rapid, pulsatile fluxes. New Phytol 153:173-184.

Tlalka M, Hensman D, Darrah PR, Watkinson SC, Fricker MD (2003) Noncircadian oscillations in amino acid transport have complementary profiles in assimilatory and foraging hyphae of *Phanerochaete velutina*. New Phytol 158:325-335.

Tlalka M, Bebber DP, Darrah PR, Watkinson SC, Fricker MD (2007) Emergence of self-organised oscillatory domains in fungal mycelia. Fungal Genet Biol 44:1085-1095.

Trapnell C, Roberts A, Goff L, Pertea G, Kim D, Kelley DR, Pimentel H, Salzberg SL, Rinn JL, Pachter L (2012) Differential gene and transcript expression analysis of RNA-seq

experiments with TopHat and Cufflinks. Nat protoc 7:562-578.

Trapnell C, Hendrickson DG, Sauvageau M, Goff L, Rinn JL, Pachter L (2013) Differential analysis of gene regulation at transcript resolution with RNA-seq. Nature Biotechnol 31:46-53.

Tsiafouli MA, Thébault E, Sgardelis SP, de Ruiter PC, van der Putten WH, Birkhofer K, Hemerik L, de Vries FT, Bardgett RD, Brady MV, Bjornlund L, Jørgensen HB, Christensen S, Hertefeldt TD, Hotes S, Gera Hol WH, Frouz J, Liiri M, Mortimer SR, Setälä H, Tzanopoulos J, Uteseny K, Pižl V, Stary J, Wolters V, Hedlund K (2015) Intensive agriculture reduces soil biodiversity across Europe. Global Change Biol 21:973-985.

Umar MH, van Griensven LJ (1997) Morphological studies on the life span, developmental stages, senescence and death of fruit bodies of *Agaricus bisporus*. Mycol Res 101:1409-1422.

Urzúa U, Kersten PJ, Vicuña R (1998a) Manganese peroxidase-dependent oxidation of glyoxylic and oxalic acids synthesized by *Ceriporiopsis subvermispora* produces extracellular hydrogen peroxide. Appl Environ Microbiol 64:68-73.

Urzúa U, Kersten PJ, Vicuña R (1998b) Kinetics of Mn^{3+}-oxalate formation and decay in reactions catalyzed by manganese peroxidase of *Ceriporiopsis subvermispora*. Arch Biochem Biophys 360:215-222.

Vaaje-Kolstad G, Westereng B, Horn SJ, Liu Z, Zhai H, Sørlie M, Eijsink VG (2010) An oxidative enzyme boosting the enzymatic conversion of recalcitrant polysaccharides. Science, 330:219-222.

Visscher HR (1988) Functions of casing soil. In: Griensven LJLD (ed) The cultivation of mushrooms. Darlington Mushroom Laboratories Ltd, p 75-89.

Vanholme R, Demedts B, Morreel K, Ralph J, Boerjan W (2010) Lignin biosynthesis and structure. Plant Physiol 153:895-905.

Vogel J (2008) Unique aspects of the grass cell wall. Curr Opin Plant Biol, 11:301-307.

Wariishi H, Akileswaran L, Gold MH (1988) Manganese peroxidase from the basidiomycete *Phanerochaete chrysosporium*: spectral characterization of the oxidized states and the catalytic cycle. Biochem 27:5365-5370.

Weil DA, Beelman RB, Beyer DM (2006) Manganese and other micronutrient additions to improve yield of *Agaricus bisporus*. Bioresour Technol 97:1012-1017.

White DC, Davis WM, Nickels JS, King JD, Bobbie RJ (1979) Determination of the sedimentary microbial biomass by extractible lipid phosphate. Oecologia 40:51-62.

Whiteford JR, Wood DA, Thurston CF (2000) Characterisation of xylanases produced in liquid and compost cultures of the cultivated mushroom *Agaricus bisporus*. Mycol Res, 104:810-819.

Whitney KD, Arnott HJ (1987) Calcium oxalate crystal morphology and development in *Agaricus bisporus*. Mycologia 79:180-187.

Wientjes FB, Woldringh CL, Nanninga N (1991) Amount of peptidoglycan in cell walls of gram-negative bacteria. J Bacteriol 173:7684-7691.

Wood DA, Goodenough PW (1977) Fruiting of *Agaricus bisporus*. Arch Microbiol 114:161-

165.

Wood DA (1979) A method for estimating biomass of *Agaricus bisporus* in a solid substrate, composted wheat straw. Biotechnol Lett 1:255-260.

Wood DA (1980a) Inactivation of extracellular laccase during fruiting of *Agaricus bisporus*. Microbiology 117:339-345.

Wood DA (1980b) Production, purification and properties of extracellular laccase of *Agaricus bisporus*. Microbiology 117:327-338.

Wood DA, Leatham GF (1983) Lignocellulose degradation during the life cycle of *Agaricus bisporus*. FEMS Microbiol Lett 20:421-424.

Vane CH, Abbott GD, Head IM (2001a) The effect of fungal decay (*Agaricus bisporus*) on wheat straw lignin using pyrolysis–GC–MS in the presence of tetramethylammonium hydroxide (TMAH). J Anal Appl Pyrol 60:69-78.

Vane CH, Martin SC, Snape CE, Abbott GD (2001b) Degradation of lignin in wheat straw during growth of the oyster mushroom (*Pleurotus ostreatus*) using off-line thermochemolysis with tetramethylammonium hydroxide and solid-state ^{13}C NMR. J Agric Food Chem 49:2709-2716.

Vos AM, Heijboer A, Boschker HTS, Bonnet B, Lugones LG, Wösten HAB (2017) Microbial biomass in compost during colonization of *Agaricus bisporus*. AMB Express 7:12.

Yagüe E, Mehak-Zunic M, Morgan L, Wood DA, Thurston CF (1997). Expression of CEL2 and CEL4, two proteins from *Agaricus bisporus* with similarity to fungal cellobiohydrolase I and β-mannanase, respectively, is regulated by the carbon source. Microbiology 143:239-244.

Yelle DJ, Ralph J, Lu F, Hammel KE (2008) Evidence for cleavage of lignin by a brown rot basidiomycete. Environ microbiol 10:1844-1849.

Yelle DJ, Wei D, Ralph J, Hammel KE (2011) Multidimensional NMR analysis reveals truncated lignin structures in wood decayed by the brown rot basidiomycete *Postia placenta*. Environ Microbiol 13:1091-1100.

Zelles L (1999) Fatty acid patterns of phospholipids and lipopolysaccharides in the characterisation of microbial communities in soil: a review. Biol Fertil Soils 29:111-129.

Zeng J, Singh D, Chen S (2011) Thermal decomposition kinetics of wheat straw treated by *Phanerochaete chrysosporium*. Int Biodeter Biodegr 65:410-414.

NEDERLANDSE SAMENVATTING

Paddenstoelen van de schimmel *Agaricus bisporus*, beter bekend als de champignon, zijn een hoogwaardige voedingsbron. Ze zijn rijk in eiwit, vezels en mineralen en bevatten bioactieve componenten zoals suikers die het afweersysteem stimuleren. Champignons worden geteeld zonder pesticiden op compost dat onder andere bestaat uit afvalmateriaal van maneges en de agro-industrie. Dit maakt de champignon een duurzaam product. De Nederlandse champignonindustrie is één van de grootste in de wereld met een productie van 270 duizend ton champignons per jaar. Na de productie van de champignon blijft er champost over. Deze bevat dan nog 46 % cellulose en 56 % hemicellulose relatief tot de compost voordat de champignon geïntroduceerd wordt. De overgebleven cellulose en hemicellulose aan het eind van de champignonproductie leidde tot het project "How mushrooms feed on sugars" (Hoe de champignon van suikers eet). Dit project had als doel het begrijpen van de afbraak van suikerpolymeren in compost waardoor champignon productie zou kunnen worden verhoogd en de productie van champost verminderd. Binnen het project lag mijn focus op het kwantificeren van schimmelbiomassa in compost en manieren om de afbraak van suikers in compost te verbeteren door het stimuleren van lignine afbraak en het verwijderen van moeilijk afbreekbaar hemicellulose.

HET MICROBIOLOGISCH DIEET VAN DE CHAMPIGNON

Voorafgaand aan mijn onderzoek was er weinig informatie beschikbaar over schimmel en bacteriële biomassa tijdens de groei van de champignon in de compost. In mijn onderzoek heb ik gebruik gemaakt van laccase activiteit, chitine bepalingen en fosfolipide afgeleide vetzuur (PLFA) bepalingen om de microbiële biomassa in de compost te bepalen (Hoofdstuk 2). De laccase activiteit in compost correleerde met de PLFA schimmelmerker C18:2ω6 maar niet met chitine. Gebaseerd op het chitine gehalte was de schimmelbiomassa 5.8 % van de totale droge stof in compost voor de introductie van de champignon en 6.8 % in compost na volledige kolonisatie. Dit was echter 1.4 % wanneer uitgegaan werd van de PLFA waardes. Dit suggereert dat een significant gedeelte van de schimmelbiomassa dood is. PLFA geeft namelijk informatie over de levende schimmelfractie terwijl chitine informatie over de totale schimmelfractie geeft. Na incuberen van compost zonder champignonmycelium en het incuberen van compost met champignonmycelium was het chitinegehalte vergelijkbaar. Dit suggereert dat de

champignon zich voedt met de schimmelpopulatie die aanwezig is in de compost voordat de champignon geïntroduceerd wordt.

Met behulp van bacteriële PLFA merkers werd aangetoond dat de bacteriebiomassa viervoudig af nam tijdens de vegetatieve groei van de champignon terwijl er geen afname was indien er geen champignonmycelium in de compost geïntroduceerd werd. Dit ondersteunt het beeld dat de champignon bacteriën in compost als voedselbron gebruikt. Gebaseerd op de PLFA data werd berekend dat de bacteriële biomassa afnam van 17.9 mg g^{-1} naar 4.7 mg g^{-1} droge stof compost terwijl de schimmelbiomassa toe nam van 14 mg tot 30 mg g^{-1}. Dit suggereert dat bacteriën de belangrijkste voedselbron vormen voor champignonmycelium. Vanuit dit perspectief zou de champignon, al dan niet samen met bacteriën, enzymen produceren om plantenmateriaal af te breken waarna de bacteriën de afbraakproducten als voedselbron gebruiken. Vervolgens gebruikt de champignon bacteriën als voedselbron om zo essentiële bouwstoffen als vitamines te verkrijgen.

HET VERBETEREN VAN COMPOSTAFBRAAK

De suboptimale afbraak van compost door de champignon zou gedeeltelijk verklaard kunnen worden door de accumulatie van moeilijk afbreekbaar hemicellulose (xylan met xyloses die dubbel gesubstitueerd zijn met arabinose). Er is geen α-1,3-L-arabinofuranosidase (AXHd3) activiteit, dat betrokken is bij de afbraak van dit xylan, in compostextract aanwezig wanneer *Agaricus bisporus* de compost koloniseert. Inderdaad heeft de champignon geen genen die voor dit enzym coderen. Het *hgh43* gen van *Humicola insolens*, dat codeert voor het AXHd3 eiwit werd geïntroduceerd in de champignon om de afbraak van het arabinoxylan te verbeteren. Compost extract van *hgh43* transformanten was actiever op dubbel gesubstitueerd arabinoxylan oligomeren dan dat van de ouderstam. Desondanks waren de *hgh43* transformanten niet in staat de suikersamenstelling van de compost te beïnvloeden tijdens de groei op compost.

Meer dan 40 % van de lignine in compost wordt niet afgebroken tijdens de kweek van de champignon. Lignine is niet alleen van invloed op de hoeveelheid champost maar kan ook afbraak van (hemi)cellulose verhinderen. Zo zou de afwezigheid van een effect van introductie van het *hgh43* gen kunnen komen doordat lignine de toegang tot het moeilijk afbreekbare hemicellulose belemmert. Daarom zou het verbeteren van het lignine afbraak systeem van de champignon kunnen lijden tot een betere compostafbraak. Het genoom van de champignon bevat de mangaanperoxidase (MnP) genen *mnp1* en *mnp2*. Transformanten die *mnp1* tot overexpressie brachten produceerde tijdens een semi-commerciële cultivatie tot 3 keer meer MnP activiteit ten opzichte van de ouderstam (Hoofdstuk

4). Afbraak van lignine en (hemi)cellulose werd echter niet beïnvloed door MnP overexpressie. Dit is mogelijk te verklaren door een gebrek aan de MnP cofactor H_2H_2. H_2H_2 productie bleek namelijk tot 8 keer lager dan zijn consumptie. Dit maakt H_2H_2 productie een kandidaat om lignine afbraak in compost, en daarmee de beschikbaarheid van suikers, te verhogen.

HET VERBETEREN VAN PADDENSTOELVORMING

Zoals hierboven is beschreven, werd compostafbraak niet verbeterd door de introductie van enzymen die betrokken zijn bij de afbraak van het substraat. Mogelijk zijn niet enzymen maar andere factoren limiterend voor de productie van champignons. Regulatie van paddenstoelvorming blijkt één van deze factoren te zijn (Hoofdstuk 6). Over-expressie van het regulatie eiwit C2H2 van de champignon versnelde paddenstoelvorming met een dag, terwijl de vorm van de paddenstoel, hun aantal en hun biomassa niet beïnvloed werd. Transcriptoom analyse liet zien dat *c2h2* in de champignon betrokken is in de beginfase van paddenstoelvorming maar ook in bepaalde weefsels van jonge paddenstoelen (Hoofdstuk 6). Deze bevindingen maken *c2h2* een kandidaat gen in de veredeling van de champignon.

GESYNCHRONISEERDE ERUPTIES VAN RESPIRATIE IN COMPOST

De champignon produceert erupties van metabole activiteit tijdens zijn vegetatieve groei in compost (Hoofdstuk 7). Deze erupties duurden 3 tot 6 uur en maximale respiratie werd na 1.5 - 3 uur gevonden met een 3.5-voudige verhoging van CO_2 productie en O_2 consumptie in vergelijking met de periodes tussen de erupties. De respiratie quotiënt (RQ), de geproduceerde CO_2 gedeeld door de geconsumeerde O_2, was tijdens erupties hoger (0.7) dan de periode tussen erupties (0.58). RQs lager dan 0.7 wijzen op mineralisatie van sterk gereduceerde stoffen, de productie van sterk geoxideerde stoffen of een combinatie van beide. De erupties synchroniseerden gedurende de vegetatieve groei van de champignon over een minimale afstand van 60 cm. Het is waarschijnlijk dat fysieke interactie van mycelium noodzakelijk is om deze synchronisatie tot stand te brengen omdat deze synchronisaties niet optraden tussen compost dat gescheiden was door lucht of aluminium folie. Aan het einde van de exponentiele groei fase nam de synchroniciteit van de erupties af. Dit lijkt overeen te komen met de observatie dat een significant gedeelte van het mycelium in compost dood is aan het einde van de vegetatieve groei van de champignon (Hoofdstuk 2). Aangezien de erupties plaatsvinden tijdens de periode van lignine afbraak, zouden deze processen gekoppeld kunnen zijn.

LIST OF PUBLICATIONS

JOURNAL ARTICLES

Vos AM, Heijboer A, Boschker HT, Bonnet B, Lugones LG, Wösten HAB (2017) Microbial biomass in compost during colonization of *Agaricus bisporus*. AMB Express 7:12.

Pelkmans JF, **Vos AM**, Scholtmeijer K, Hendrix E, Baars JJP, Gehrmann T, Reinders MJT, Lugones LG, Wösten HAB (2016) The transcriptional regulator *c2h2* accelerates mushroom formation in *Agaricus bisporus*. Appl Microbiol Biotechnol 100:7151–7159.

Celis AM, **Vos AM**, Triana S, Medina CA, Escobar N, Restrepo S, Wösten HAB, de Cock H (2017) Highly efficient transformation system for *Malassezia furfur* and *Malassezia pachydermatis* using *Agrobacterium tumefaciens*-mediated transformation. J Microbiol Methods 134:1-6.

Vos AM, Jurak E, Gijsel P, Ohm RA, Henrissat B, Lugones LG, Kabel M, Wösten HAB (2016) *Agaricus bisporus* production of α-1,3-L-arabinofuranosidase (AXHd3) active on double substituted xylan does not improve compost degradation. (In preparation).

Vos AM, Jurak E, Pelkmans JF, Herman K, Pels G, Baars JJ, Hendrikx E, Kabel MA, Lugones LG, Wösten HAB (2016) H_2O_2 as a candidate bottleneck for MnP action during cultivation of *Agaricus bisporus* in compost. (In preparation).

BOOK CHAPTERS

Vos AM, Lugones LG, Wösten HAB (2014) REMI in Molecular Fungal Biology. In: van den Berg MA , Maruthachalam K (Ed) Genetic Transformation Systems in Fungi, 1st edn., pp 273-287.

Knaus H, Blab GA, Agronskaia AV, **Vos AM**, Gerritsen HC, Wösten HAB (2014) Monitoring melanin and the metabolic state during development of *Agaricus bisporus* by nonlinear spectral microscopy. In: Nonlinear Spectral Imaging of Fungi. Dissertation, Utrecht University.

DANKWOORD

Om bij het begin te beginnen: lieve ouders, Johan en Ineke, jullie waren en zijn er altijd onvoorwaardelijk voor mij. Daarmee staan jullie aan de basis van alles wat ik in dit leven bereikt heb en ga bereiken. Het is niet in woorden te vatten hoe dankbaar ik ben voor de stabiele springplank die jullie geboden hebben. Jedide, ik ben blij jou mijn broer te kunnen noemen. Ik waardeer onze gesprekken, de rondjes hardlopen, skivakantie en (jeugd)herinneringen inclusief de ruzies om wie waar mag tandenpoetsen. Johan, Ineke en Jedide ik hou van jullie!

Han en Luis, mijn promotor en copromotor of ook wel academische ouders (bepaal zelf maar wie de moederrol heeft), hebben sterk bijgedragen aan de totstandkoming van dit boekje en mijn academische vorming. De wat chaotische en onwijs creatieve Luis werd gecomplementeerd door de georganiseerde en wat meer gestructureerde Han. Luis, ik heb genoten van je enthousiasme, onze discussies over werk en alles daarnaast. Bedankt voor de goede en creatieve oplossingen voor problemen waarvan ik al dan niet doorhad dat ik ze had. Han, jouw rust, overzicht, enthousiasme en pragmatische blik waren onmisbaar. Ik ben je dankbaar voor alle kansen die je geboden hebt!

De mannen van Fungal Pleasure: Jordi, de enige die wel op tijd zijn boekje af had, Brand, die nog altijd aan zijn boekje werkt (ahum), Thies, f*** your mother, en Freek, mooiste jongen van de UBV en op nationale TV. Door jullie was werken niet alleen een genot maar ook vaak hilarisch.

De collega's van microbiologie die elk op hun eigen manier hebben bijgedragen aan de goede sfeer van de vakgroep en gezorgd hebben voor fantastische jaren. Op volgorde van kantoor: Robin, Wieke, Ria K, Inge (Koffie!), Ioana, Peter-Jan, Jesus (and his spanish gang), Martin, Hans, Margot, Pauline, Natalia (Chiquita!), Ivan, Adriana, Esther, David, Ria T, Florian, Jan en alle master en bachelor studenten. Oudcollega's: Jerre (wat waren we toch bang van boekakees), Karin, Elsa, Florian. De master studenten die ik begeleid heb: Charlotte, Lama, Marwa, Thomaz, Maarten, Koen, Tom en Brigit. Bedankt voor jullie inzet!

All co-authors! Especially Amber and Edita, who helped out sooooo much with the PLFA and pyrolysis stuff, respectively.

The project partners: Alexa, Ronald, Edita en Mirjam. All the best to you and hope to work with you in the future! The industrial partners in my project that provided critical knowledge, materials and feedback: Caroline (CNC), Thed and Hennie (Walkro), Mark and Barbara (Sylvan), and Marco (DSM).

De meest Bruuske mannen: Sander, Brand, Jaap, Jeroen, Johan, Michiel, Ralf, Rogier en Simon. Ruim 10 jaar hebben wij op dinsdagen gegeten en spelletjes gespeeld terwijl ik laf een biertje minder dronk. Dit had ik voor geen goud willen missen! En niet te vergeten, de weekenden en vakanties. Ik kijk uit naar nog heel veel meer van hetzelfde!

Alle vrienden uit het zuiden: Cantal, Sep, Irene, Michiel, Elbrich, Ben, Daniëlle, Onno, Pascal, Toad, Judith, Peter, Becca, Danny en alle anderen, bedankt voor de geweldige vakanties, volleybalweekenden (iets met een Baard!), Slabakken (met 4^{de} ronde natuurlijk).

Om met een begin te eindigen: lieve Kyra, apie, na heel wat jaren verras je nog steeds. Ik ben ontzettend blij met de manier waarop we praten, lopen, chillen en apen. Je hebt en zal nog vaak moeten tolereren dat ik door gedoe met experimenten laat thuis ben en af wil halen. Ik heb heel veel zin om met jou alle uitdagingen die onze kant op worden geslingerd aan te gaan. Oeh Oeh Oeh !!!

CURRICULUM VITAE

Aurin M. VOS

Aurin Vos was born on the 9th of August, 1986 in 's Hertogenbosch, the Netherlands. He followed his secondary education at the Onze Lieve Vrouwe Lyceum in Breda in the Netherlands and graduated in 2005. In September of 2005 he started the Bachelor Biology at Utrecht University followed by the master Molecular and Cellular Life Sciences at Utrecht University that he combined with a minor on the Fundamentals of Business and Economics.

As part of his studies, Aurin completed two research internships, the first of which at Utrecht University. In this project Aurin worked with Dr. Karin Scholtmeijer on the production of therapeutic proteins in mushrooms at the Molecular Microbiology group of the Department of Biology at Utrecht University. In his second internship he worked with Prof. Dr. Ian Stansfield on determinants of translational efficiency and noise at the Institute of Medical Sciences at the University of Aberdeen in Scotland. Aurin obtained his MSc degree in August 2011. In the same month he started his PhD with the Molecular Microbiology group of the Department of Biology at Utrecht University under the supervision of Dr. L.G. Lugones and Prof. Dr. H.A.B. Wösten. The research on compost degradation and growth of *A. bisporus* was financially supported by Technologiestichting STW and is described in this thesis.

After his PhD, Aurin started as a postdoctoral researcher in the group of Prof. Dr. J.T. Pronk at the TU Delft where he works on the anaerobic physiology of fungi.